HYPERVERZWEIGTE LACTON-COPOLYMERE: ENZYMATISCHE SYNTHESE, CHARAKTERISIERUNG UND DARSTELLUNG STRUKTURIERTER POLYMERNETZWERKE

(HYPERBRANCHED LACTONE COPOLYMERS BY ENZYME CATALYSIS: SYNTHESIS, CHARACTERIZATION AND PREPARATION OF STRUCTURED POLYMER NETWORKS)

Dissertation
zur Erlangung des Grades
"Doktor der Naturwissenschaften"

am Fachbereich 09
Chemie, Pharmazie und Geowissenschaften
der Johannes Gutenberg-Universität
in Mainz

Ingo Th. Neuner
geboren in
Heidenheim an der Brenz

Mainz, 2005

Dekan: N.N.

1. Berichterstatter: N.N.

2. Berichterstatter: N.N.

Tag der mündlichen Prüfung: 21. November 2005

meinen Eltern

Die experimentellen Untersuchungen zu dieser Arbeit wurden im Januar 2002 am Institut für Makromolekulare Chemie der Albert-Ludwigs-Universität zu Freiburg, begonnen, ab September 2002 am Institut für Organische Chemie der Johannes Gutenberg-Universität zu Mainz fortgeführt und im Juni 2005 vollendet.

TABLE OF CONTENTS

ABBREVIATIONS, SYMBOLS AND ACRONYMS

e.g.	exempli gratia
i.e.	id est
ca.	circa
cf.	confer
hb	hyperbranched
l	linear
AB_2 (monomer)	Monomer carrying one functional group of type A and two of type B
BHB	2, 2'-Bis(hydroxymethyl) butyric acid
CALB	Candida Antarctica Lipase B
CL	ε-Caprolactone, repeating unit
DCC	1, 3-Dicyclohexylcarbodiimide
DMA	Dynamic Mechanical Analysis
DPTS	4-(Dimethylamino)pyridinium 4-toluenesulfonate
DSC	Dynamic Scanning Calorimetry
GPC	Gel Permeation Chromatography (also abbreviated as SEC)
HEMA	2-Hydroxyethyl methacrylate
HPLC	High Performance Liquid Chromatography
MALDI-TOF MS	Matrix Assisted Laser Desorption Ionization – Time of Flight Mass Spectroscopy
bis-MPA	2, 2'-Bis(hydroxymethyl) propionic acid
NMR	Nuclear magnetic resonance
PCL	Poly(ε-caprolactone)
PS	Polystyrene
SDS-PAGE	Sodium Dodecylsulfate Polyacrylamide Gel Electrophoresis
TCM	Trichloromethane (chloroform)
THF	Tetrahydrofurane
TMC	Trimethylene carbonate, trimethylene carbonate repeating unit
VL	δ-Valerolactone, δ-valerolactone repeating unit
VOC	Volatile Organic Compounds
VPO	Vapor Pressure Osmometry
WLF	William-Landel-Ferry
MW	Molecular weight

VARIABLES, PARAMETERS, UNITS AND TRADEMARKS

DB	Degree of branching
$<DP_s>$	Average length of linear segment between two branching points
E_a	Arrhenius Energy
ΔH_f	Heat of fusion
<E>, E', E''	Young modulus, real term, imaginary term
<G>, G', G''	Shear modulus, real term, imaginary term
$<M_n>$	Number average molecular weight
$<M_w>$	Weight average molecular weight
PDI	Polydispersity
T_c	Temperature of crystallization
T_g	Glass transition temperature
T_m	Melting temperature
X_c	Degree of crystallization
σ, σ_y	Stress
ε, ε_y	Strain
λ, λ_B	Elongation, Elongation at break
$[\eta]$	Intrinsic viscosity
η_{sp}	Specific viscosity
c	Concentration
α	Mark-Houwink α
K	Huggins coefficient
amu	Atomic mass unit
Da, kDa	Dalton, kilo Dalton
hrs	Hours
L	Liter

Trademarks	CALB L, CAPA 6100, CAPA 6500, CAPA 6503, Capronol, Dexon, Lewatit, Novozyme 435.

1 GENERAL INTRODUCTION

1.1 Branched Polymers

The interest in globular, cascade-branched polymers developed in the late 1980s (Figure 1-1). Since then, the fascination with their structural and chemical peculiarities has led to more than 1500 relevant publications annually. Depending on the degree of regularity of branching on a molecular scale, such materials are usually categorized as *dendrimers* and *hyperbranched polymers*.[6] These *branch-on-branch*, or *cascade-branched* polymers invariably lack a connecting line between any two end-groups that passes all branching points. This feature translates to a structure that contains one closed cycle per molecule at maximum, leading to unique physico-chemical properties, such as the non-occurrence of gelation.[7]

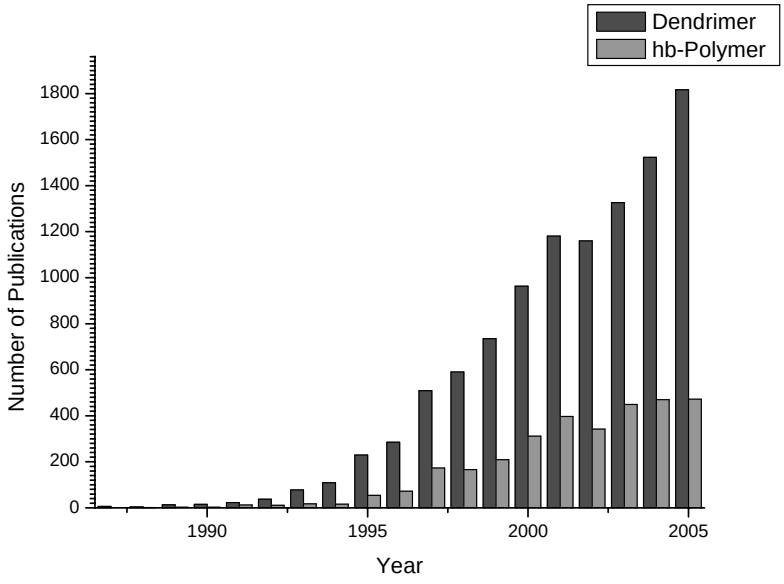

Figure 1-1: Number of publications concerning dendrimers and hyperbranched polymers since 1984.

The perfect branch-on-branch structures of dendrimers are synthesized by multi-step protocols including alternating build-up reactions of the shell and purification steps. The advantage of this "organic" synthesis is a perfectly symmetrical and absolutely monodisperse polymer of unprecedented structural precision.

Hyperbranched polymers are usually produced by a one-pot one-step synthesis. In opposition to dendrimers preparation is straight-forward and fast, but they are randomly branched, e.g. some branching points are connected in a linear manner, the pendent branch carrying a functional group (Figure 1-2). This synthetic simplicity and the reported

similarities of the physical and mechanical properties of both hyperbranched polymers and dendrimers that possess the same repeating units led to the development of tailored materials[8] where high performance and/or novel functionality are needed.

The natural occurrence of "hyperbranching," which is a topological feature, was reported as early as the 1930s by Staudinger.[9] Meyer and Bernfeld proposed the first hyperbranched structure for polysaccharides in 1940.[10] Glycogen, amylopectin and dextran are the most prominent of the abundant natural energy storage polymers in which branching is the key concept to fast release of large quantities of glucose.[1] It is interesting to note that none of these materials possesses a perfectly branched dendrimer structure.

Nevertheless, the first published examples of synthetic hyperbranched polymers possibly came up as early as the late 19th century. In 1854, Cannizzaro discovered what he described as "amorphous carbon" $(C_7H_6)_n$.[11] In 1885, Friedel and Crafts reported the reaction of benzyl chloride and Al_2Cl_6,[12] which was the first confirmed branched macromolecular structure.

More than 60 years later, in 1950, Flory published his visionary theoretical work on "random AB_m polycondensates."[13] Such polymers are prepared by the step-growth

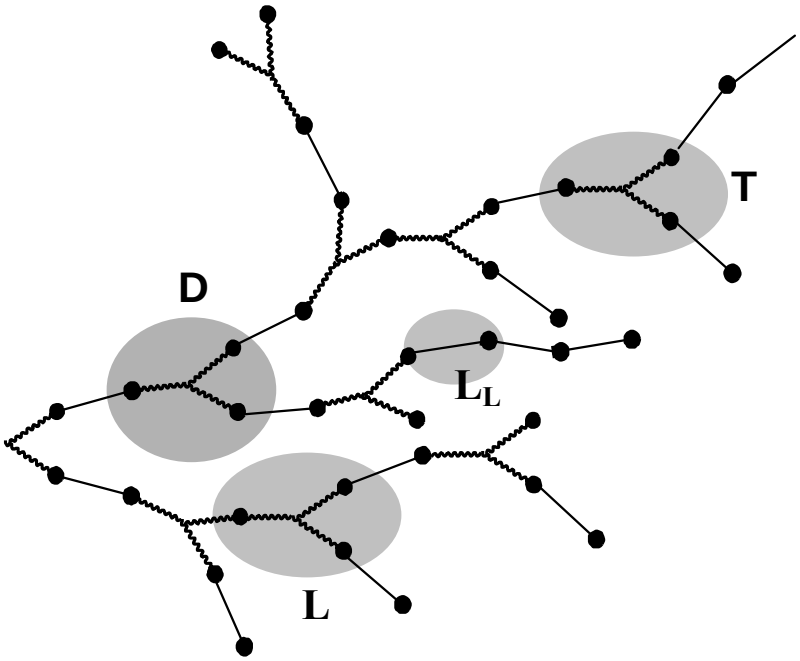

Figure 1-2: Schematic structure of a hyperbranched polymer based on AB_2 and AB monomer units. Four different incorporation modes (Dendritic (D), Linear (L_L), Linear-dendritic (L) and Terminal (T) are highlighted.

[1] production by nature: 10^9 metric tons/year.

polymerization of AB_m monomers, in which one monomer possesses complementary A and B functionalities (e.g. hydroxyl and carboxyl groups) and the only reaction in the system is the coupling of A and B-groups.

In the 1980s, hyperbranched polymers were rediscovered due to the fascination with the structurally perfect dendrimers. Characteristic properties, such as low viscosity in bulk and solution or the amorphous solid state are consequences of i) a globular, dense structure, ii) an absence of entanglements, and iii) a high number of functional end-groups in pronounced contrast to linear polymer chains.

Most hyperbranched polymers published so far are based on AB_2 monomers; more than 150 have been created since 1980, leading, e.g., to polycarbosilanes,[14,15] polyesters,[16] polyamides,[17] polyethers,[18] poly(ether ketones),[19,20] and polyphenylenes[6,21] (Figure 1-3).

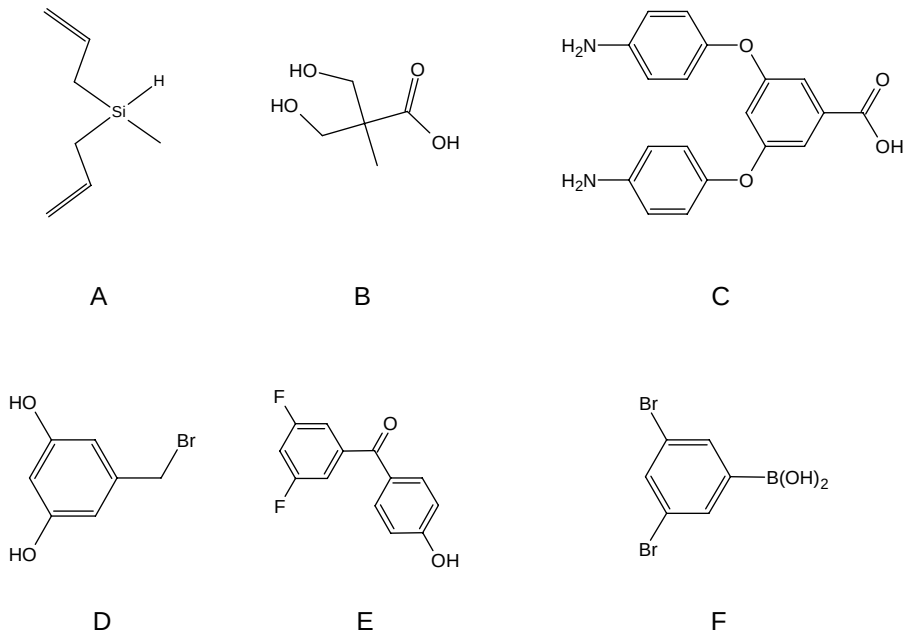

Figure 1-3: AB_2-monomers leading to hyperbranched (A) polycarbosilanes, (B) polyesters, (C) polyamides, (D) polyethers, (E) poly(ether ketones) and (F) polyphenylenes.

1.2 Characteristic Properties of Hyperbranched Polymers

Linear polymer chains form random coils in both dilute solution and melt. If a critical concentration is exceeded, chains interpenetrate. This phenomenon is called chain entanglement which leads to increased viscosity in contrast to non-entangled structures. However, it is generally assumed that dendrimers and hyperbranched polymers are intrinsically incapable of forming entanglements due to their compact, highly branched structure.[22]

In addition, hyperbranched polymers are usually amorphous materials in solid state, since crystallization is impeded by the hyperbranched structure. The compact globular shape causes lower viscosity in the melt as well as in solution compared to the linear analogue (Figure 1-4).[5] Plotting the logarithm of the intrinsic viscosity log [η] against the logarithm of the average molecular weight log [<M>] results in a straight line the slope of which corresponds to the exponent α of the Mark-Houwink-Sakurada Equation (Eq. 1-1).

$$\eta = K \cdot M^{\alpha} = K \cdot \frac{V_h}{M} \qquad \textbf{(1-1)}$$

α is determined by the shape of the polymer chain in solution, varying between 0 in the case of ideal hard spheres and 2 for rigid rods. [η] also describes the ratio of the hydrodynamic volume V_h to the molar mass M. Thus, it is a function of the reciprocal density. In theta state, the unperturbed coil α equals 0.5. Hyperbranched macromolecules induce significantly lower α values than linear polymers. This strongly indicates the more compact structure of hyperbranched polymers in solution.

Since they cannot entangle, hyperbranched matter forms rather weak materials of low toughness in solid state. The appearance is highly dependent on the glass transition temperature T_g. Low T_g materials are viscous fluids in contrast to brittle solids with high T_g. Another interesting feature is based on the high number of functional groups. Macromolecular substitution reactions open routes for numerous modifications, e.g. reactive functionalization or alkylation to fine-tune solubility.[23,24]

In summary, hyperbranched polymers have three key characteristics: i) a lack of entanglements, ii) relatively low viscosity in solution as well as in melt and iii) a high number of functional end-groups per molecule that are part of a condensed structure. In addition, they offer the convenience of a one-pot synthesis leading to a large number of potential applications. However, broad inherent molecular weight distribution and limited control of important structural parameters restrict potential application.

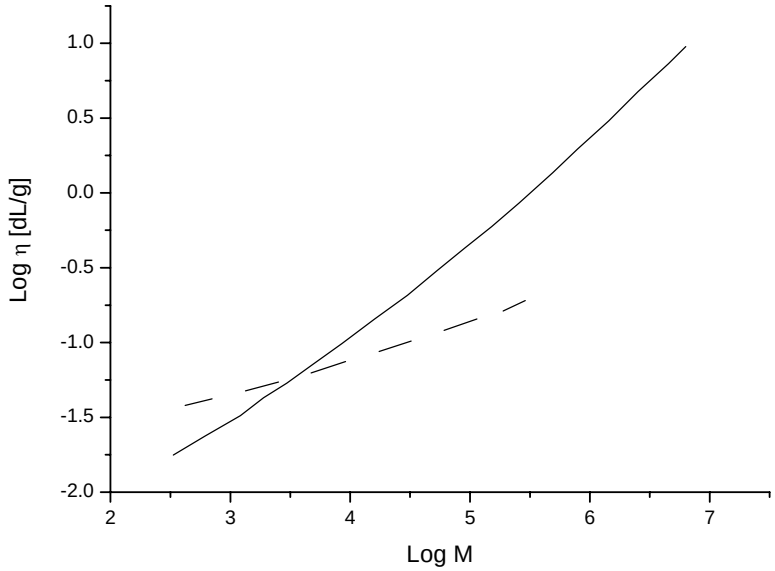

Figure 1-4: The intrinsic viscosity [η] of linear and hyperbranched polymers; straight line - linear polystyrene, dashed line - *hb* polymer.[5]

1.3 Applications of Hyperbranched Polymers

The novel physical properties of hyperbranched macromolecules make these polymers ideal candidates for use in a wide range of applications. A schematic diagram of the most common applications in which hyperbranched polymers have been used is shown in Figure 1-5. These are often bulk applications.

The production process of resins involves the addition of reactive diluents to reduce the pre-polymer's viscosity. Reactive functionalization of hyperbranched polymers with groups that are cross-linked later, e.g. methacrylation, opens their use as multi-functional precursors. Since these compounds do possess low viscosity, diluents become obsolete.[16,25]

Shrinkage is also a crucial issue when resins are cured, e.g., in dental chemistry. One of the current concepts to overcome shrinkage is based on the use of oligomeric macromonomers in order to reduce the number of new bindings. Since good processing properties are required for the precursor, hyperbranched materials are the matter of choice.[26]

Further potential evolves from polymer blends. Blends of polystyrene with hyperbranched polyphenylenes improve thermal stability and melt viscosity of the final material.[27]

Massa et al. observed increased tensile and compressive moduli in cases of immiscible polymer blends of linear polycarbonate and hyperbranched aromatic polyesters. Compared

to unmodified polycarbonate, decreased toughness and strain-to-break were revealed, and higher T_g was observed.[28] Some more work on rheological modification of commodities by the use of hyperbranched polymers was published lately.[29-34]

Other concepts on the use of hyperbranched polymers were directed towards use in photo refractive materials in the field of non-linear optics[35,36] or introducing liquid crystalline properties by covalent attachment of mesogens. In this case, thermotropic and lyotropic properties were observed.[24,27,37,38] In contrast to structurally related dendrimers that carry mesogenic end-groups, broad nematic phases with low viscosities were observed.[39,40] Specific properties of hyperbranched molecules, e.g. the absence of entanglements and the high concentration of end groups, are promising for the preparation of liquid crystalline materials with low viscosity and possibly short switching times.

In a recent work of our group, build-up of structured hydrogels with hyperbranched polyglycerol was studied.[41] Using multi-functional polyglycerols, hydrogels with high content of free functional groups were created.

Nanotechnology is a further promising field for hyperbranched materials. Hyperbranched polymers could serve as templates in the production of nanoporous materials with low dielectric constants[42] or in the fabrication of defined hybrid particles (e.g. biomineralization techniques).

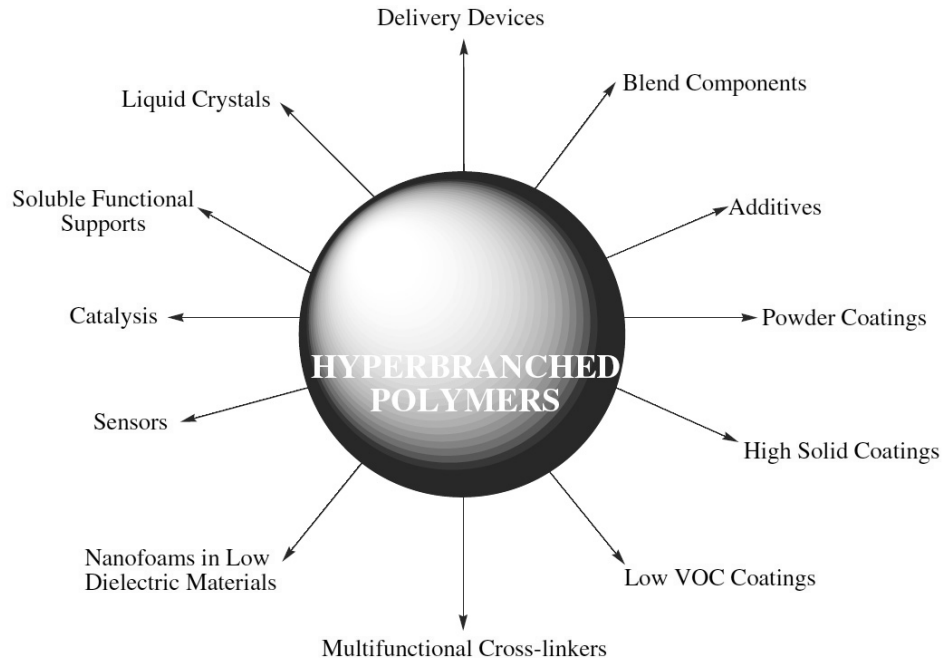

Figure 1-5: Applications of hyperbranched polymers.

Lastly, high functionality is an appreciated asset in biomedical and pharmaceutical research. In this area, mostly dendrimers were studied, but highly defined hyperbranched polymers may equally serve as high-loaded contrast agents[43] or host compartments for controlled drug-release.[44-48] Homogenous supports in catalysis[49,50] and biochemical solid phase synthesis[51] are promising topics as well.

1.4 Degree of Branching

The experimental parameter commonly employed to express the extent of branching in cascade-branched macromolecules is the so-called degree of branching (DB). It describes the relative amount of branching points versus the maximum number of branching points in the molecule implied by feed. By definition, perfect dendrimers have a DB equal to 1 (100 %), linear structures meet DB = 0.[52,53] In an ideal random bulk polymerization of an AB_2-monomer, the ratio of dendritic (D), linear (L) and terminal (T) building blocks is expected to be 1 :2 :1, corresponding to a DB = 0.5 (50 %)[52] (Eq. 1–2).

$$DB = \frac{2 \cdot D}{2 \cdot D + L} \qquad \textbf{(1-2)}$$

In general, the degree of branching is calculated from NMR spectra based on signals that are distinctively assigned either to linear (L_L), branched (D) or linear-dendritic (L) segments. Linear-dendritic segments refer to AB_2 units, in which only one B group is connected to another building block. Since DB is a purely statistical parameter resulting from a macroscopic point of view, no information on microstructures or topological isomers is obtained.[54]

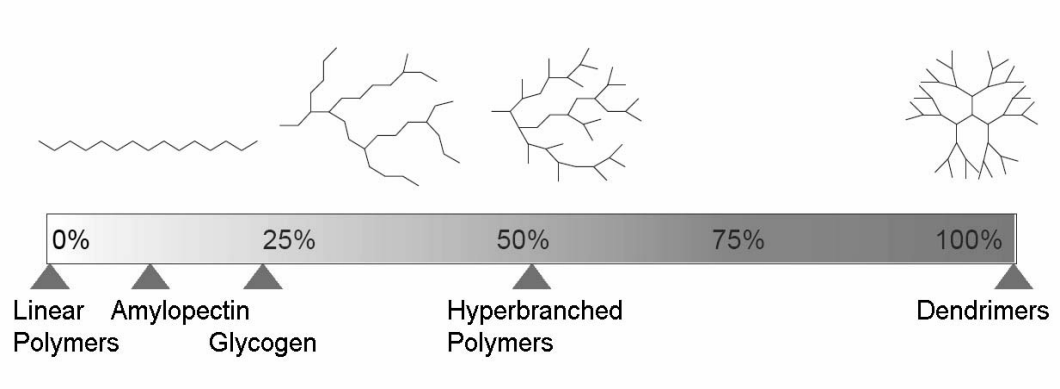

Figure 1-6: Topological classification of branched polymers by the degree of branching (DB).

1.5 Concurrent AB/AB_2 Polymerization

Based on the seminal work of Flory,[13] the common synthetic approach to hyperbranched polymers is a polycondensation of AB_2 monomers where A and B functionalities are complementary. It is a typical feature of step-growth reactions of this type that each AB_2-monomer in the reaction mixture can react with any other species, i.e. monomers and present oligomers, in the absence of cross-linking. High degree of polymerization (<DP_n>) is only achieved at high conversion, which is accompanied by a drastic increase in polydispersity (PDI ≈ <DP_n>/2). It is hence obvious that no control over the polymerization reaction is achieved.

In a theoretical paper in 1999, Frey et al. discussed whether control of DB is achieved by variation of the ratio of two co-monomers, AB and AB_2, as building blocks.[55] Similar to the theory for AB_m monomers,[52] only purely statistical aspects were considered.

The central step, which determines the DB in a statistical AB/AB_2 copolymerization, is the condensation of two, one or no further building unit(s) onto an AB_2 unit at the terminus of a growing branch of the molecule. This AB_2 unit is then called dendritic (D), linear (L) or terminal (T). AB units, however, are always added linearly (L_L) and do not affect the formation of branching points. If the growing branch is terminated by a linear segment, it is referred to as terminal unit (T_L). Figure 1-7 illustrates likely combinations.

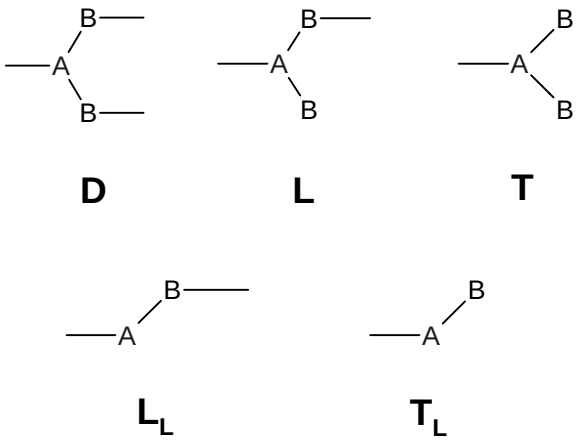

Figure 1-7: Building combinations of AB_2 and AB monomer units.

In the discussion of copolymers made from AB$_2$- and AB-monomers, linear AB building blocks (L$_L$) are treated like linear-dendritic AB$_2$ units (L). Linear, but terminal units (T$_L$) were not considered since they are already correlated to the terminal units (T).
As consequence, for AB/AB$_2$ copolymerizations, DB is defined as:

$$DB = \frac{2 \cdot D}{2 \cdot D + L + L_L} \tag{1-3}$$

Regarding the probability of a linear or dendritic insertion respectively, and assuming full conversion, DB^{stat}_{AB/AB_2}, which depends solely on x$_{AB}$, is obtained:

$$DB^{stat}_{AB/AB_2} = 2 \cdot \frac{1 - x_{AB}}{\left(2 - x_{AB}\right)^2} \tag{1-4}$$

in which

$$x_{AB} = \frac{[AB]}{[AB] + [AB_2]} \tag{1-5}$$

The transformation of equation (1-5) yields x$_{AB}$ as function of DB:

$$x^{stat}_{AB/AB_2} = 2 + \frac{\sqrt{1 - 2 \cdot DB} - 1}{DB} \tag{1-6}$$

Employing Eq.1–6, one can adjust the desired DB between 0 and 0.5 by means of the ratio of the two co-monomers AB and AB$_2$.

1.6 Hyperbranched Poly(ε-caprolactone)

Poly(ε-caprolactone) has been used in medical care for more than 30 years. Biological and physical properties are tailored in polymer blends or block copolyesters of ε-caprolactone, glycolide, and L-lactide amongst others. Tunable biodegradability is especially appreciated for sutures and drug delivery devices.
However, almost all syntheses published for hyperbranched polyesters to date require harsh conditions, such as temperatures exceeding 150 °C and catalysts like sulfuric acid.[56]
Hedrick et al. first reported the synthesis of hyperbranched poly(ε-caprolactone) (*hb*-PCL) in 1998 (Figure 1-8)[4]. They employed a four-step protocol, first preparing exactly defined

macromonomers of bis-MPA with linear poly(ε-caprolactone) arms of defined length. After deprotection through hydrogenolysis, hyperbranching polycondensation of the macromonomers led to *hb*-PCLs of $<M_n>$ = 40–90 kDa and PDI values of 1.6 to 2.2. Relatively mild conditions, but long reaction times of 92 hours in total and temperatures up to 100 °C were necessary.

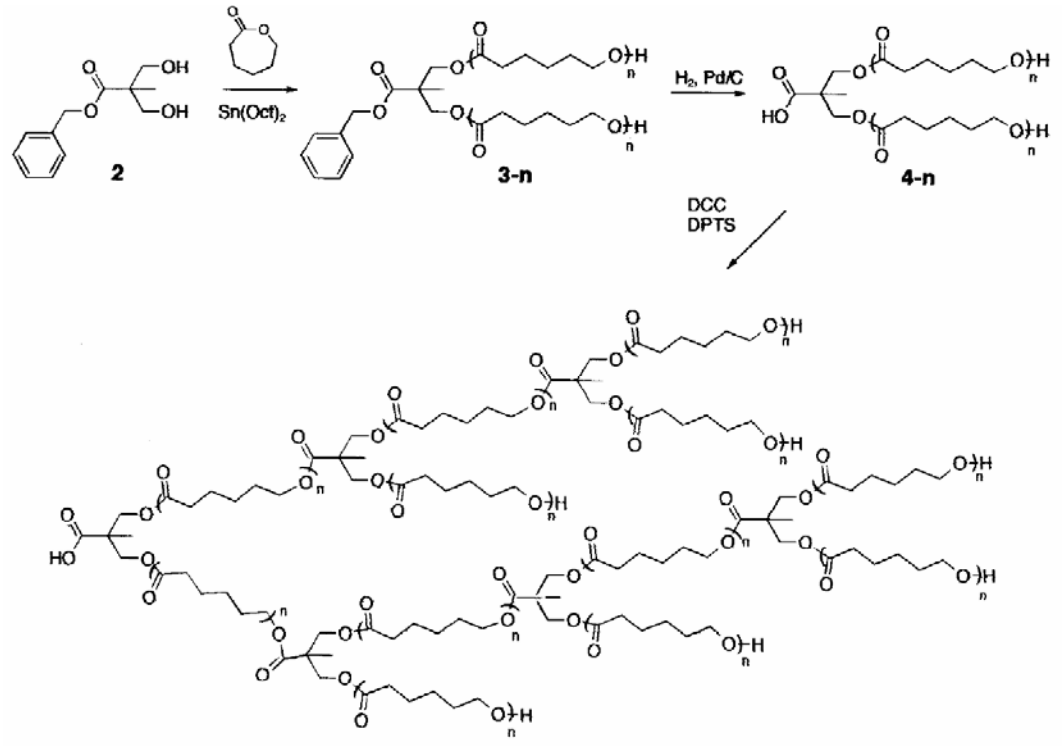

Figure 1-8: Hyperbranched poly(ε-caprolcatone) by a four step approach using defined macromonomers (Choi & Kwak). [2]

In 2003, Choi & Kwak reported a similar protocol avoiding the use of DCC/DPTS in the final hyperbranching step (Figure 1-9).[2] They extensively investigated the influence of the length of the linear segments on thermal,[2] mechanical and rheological properties.[57,58] The net reaction time was 66 hours, the highest temperature employed was 110 °C for 5 hours.

Enzyme catalysis in organic media has seen enormous progress during the last 20 years promoting a variety of small molecule transformations under mild reaction conditions.[59] In the 1990s, the early enzyme-catalyzed polymerizations using, e.g. ε-caprolactone,[60] δ-valerolactone[61] and γ-butyrolactone[62] as monomers, required long reaction times and only low molecular weight polyesters were obtained (M_n < 5.0 kDa). A first success was

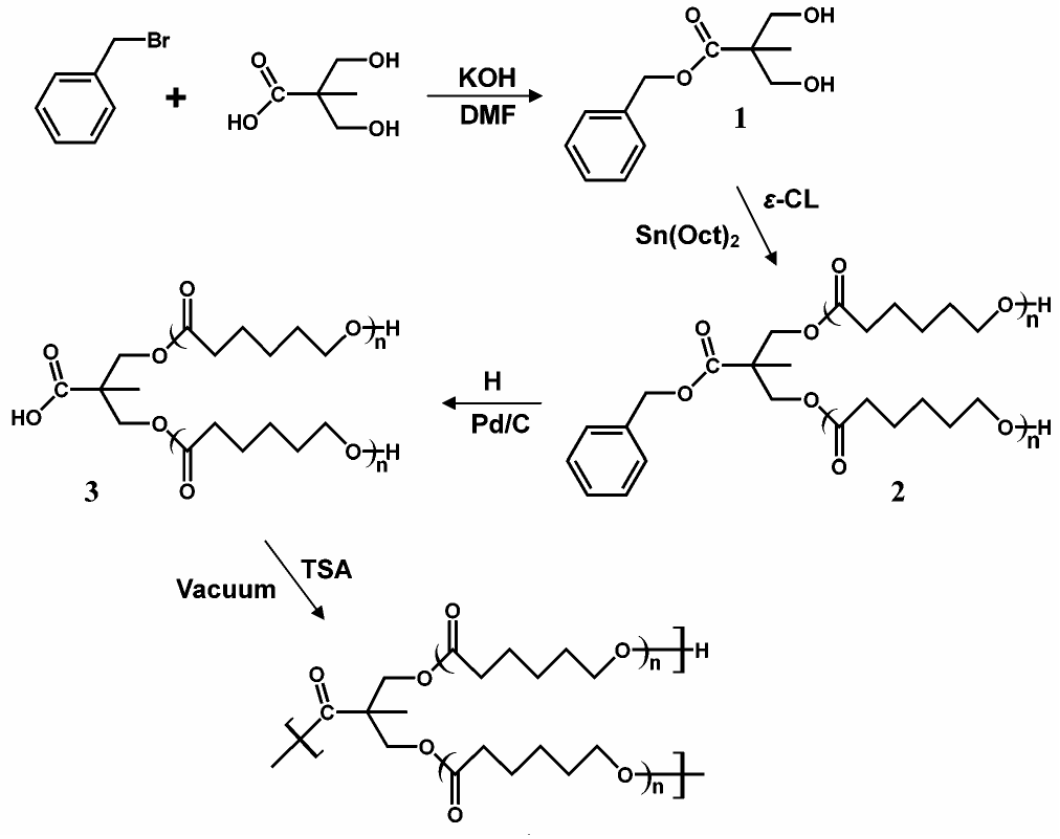

Figure 1-9: Hyperbranched poly(ε-caprolcatone) by a four-step approach using defined macromonomers (Tollsås et al.). [4]

achieved with the use of immobilized Lipase B from Candida Antarctica (Novozyme 435, CALB) for the polymerization of ε-caprolactone as well as ω-pentadecalactone in toluene or other apolar solvents.[63] The state of the art in the field has been summarized in some comprehensive reviews.[64-66]

To date, there is only one communication published by Frey et al. in 2002 employing enzymatic methods for the preparation of hyperbranched polymers.[67] This concept implies the concurrent ring-opening polymerization / branching polycondensation giving control of DB by the comonomer ratio in the feed (Figure 1-10).[55] However, this procedure yields random copolyesters, i.e. the length of the linear segments is not defined and molecular weights were found to depend strongly on the extent of branching (DB).

Since Novozyme 435 was used as catalyst, post-reaction purification was simply realized by filtration of the Novozyme beads. Inspired by this promising initial work, two major projects on *hb*-PCL were initiated in our group:

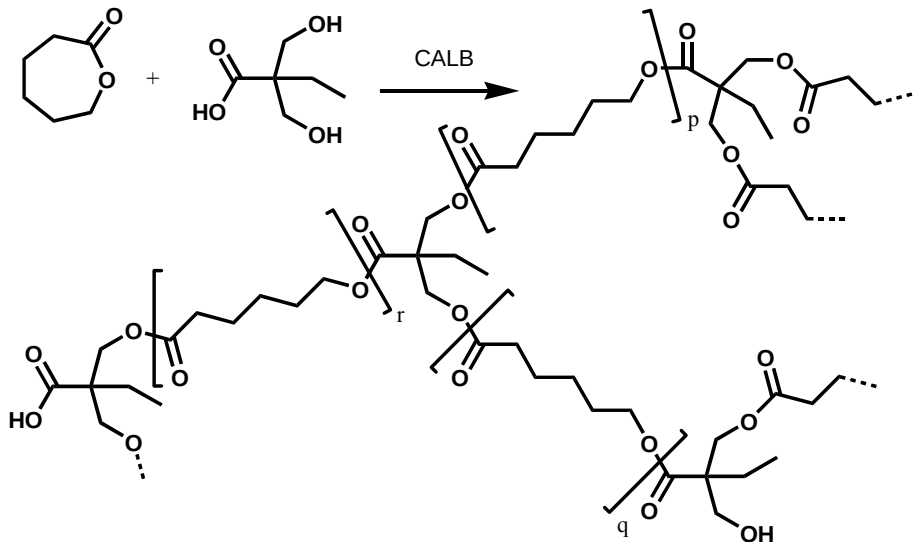

Figure 1-10: Copolymerization of ε-caprolactone and 2,2'-bis(hydroxymethyl)butyric acid. [67]

I) Dr. Mihaela Ursu, at the time a PhD student from Romania, was eager to extensively investigate the mechanical and rheological properties[68] of hyperbranched poly(ε-caprolactone), blends hereof with PVC,[69] and its biodegradability as part of her thesis.

II) At the same time, the objective of the present thesis led to a procedure for hyper-branching bulk polymerization of ε-caprolactone and some similar structures. Since com-parable

materials were received by both protocols, scale-up synthesis in bulk was defined as a key objective for future work. Lately, polymer analogous functionalization of the pendent free hydroxyl groups and formation of networks by UV-curing has been demonstrated. Finally, the influence of the quantity of hyperbranched methacrylated poly(ε-caprolactone) in 2-hydroxy-ethyl methacrylic acid (HEMA) networks on the mechanical properties was studied.

It should be emphasized that this concept implies mild reaction temperatures and a short reaction time (24 hours, 75–85 °C). Moreover, by the use of Novozyme 435, toxic catalysts, heavy metals as reducing agents, and organic solvents were avoided as far as possible. Therefore, an economic route that is a major contribution to waste reduction is introduced.

2 OBJECTIVE

2.1 Introduction

Hyperbranched polymers have received considerable attention in the field of polymeric materials in recent years, as reviewed in Chapter 1.

While the rapidly developing field of dendrimer research has disclosed unique features of globular, multifunctional structures based on branch-on-branch topologies, restrictions apply if applications are considered, because these compounds suffer from their cost-intensive, tedious preparation.

Ten years ago, Wooley et al. as well as other authors suggested that the structurally related hyperbranched polymers could compete with dendrimers with respect to their structure-property profiles in most applications. [8]

Syntheses of hyperbranched polymers were achieved by bulk polymerization of various AB_m-monomers. This has been known since the seminal work of Flory in the 1950s,[13] although control of these reactions still remains a major challenge.

In the late 1990s, some basic theoretical works reflecting on the importance of the degree of branching (DB) were published. Hölter et al. derived a definition of DB for AB_m-monomers and discussed to what extent one can overcome the statistical maximum of DB under special reaction conditions.[52] In a subsequent contribution, copolymerization of AB_2 and AB monomers as a way to gain control of DB was suggested,[55] and first results supporting these concepts have been published in recent years.[70-73]

Besides conventional polycondensation of AB_2-monomers, hyperbranched polymers have also been synthesized employing alternative concepts. Enzyme catalysis represents an innovative approach in this field. While in the 1990s efforts to polymerize ε-caprolactone (ε-CL) in solution implied long reaction times and low molecular weights of the final polymers[61,62,74] due to concurrent cyclization,[75-77] enormous progress has been seen most recently.[65,66]

In 2002, Skaria et al. first reported the synthesis of hyperbranched polymers employing enzyme catalysis in organic media.[67] The concept of concurrent ring-opening polymerization and polycondensation of BHB and CL made proper control of the final polymer's DB possible. Although higher molecular weights (M_n > 10 kDa) were obtained, molecular weights were found to depend strongly on the comonomer ratio in feed.

The objectives of this thesis are based on the concept of the above mentioned paper.[67] The concept of concurrent polycondensation/ROP will be further investigated with respect

to scope and limitations. Moreover, the scale-up of the polyester synthesis and the development of transesterification routes towards hyperbranched polymeric cross-linkers are central issues of the present work.

Aliphatic polyesters have been known as biodegradable materials for many decades. While the potential of poly-L-lactide in medical care was recognized in the early 1960s (Dexon^{TM}), poly(ε-caprolactone) initially attracted attention as a soil-degradable container material in 1982.[78] To date, it is widely used in drug delivery devices (Capronol^{TM}) due to its excellent biocompatibility, low glass transition (T_g) and high permeability.[79]

2.2 Hyperbranched Poly(ε-caprolactone)s

Highly branched polymers exhibit unique properties compared to their linear analogues. Because of their high and tunable number of functional groups per molecule, they possess advantageous physical properties that can be adjusted over a broad range, e.g. viscosity, leading to purpose-specific tailored materials. On the other hand, these materials are suitable for blending with common linear polymers to enhance their mechanical properties to the specific need of the desired application.[69]

To date, three routes to hyperbranched poly(ε-caprolactone) are reported (*cf.* section 1.6). Hedrick et al.[4] and Choi et al.[2] both elaborated multi-step protocols, involving long reaction times to produce highly defined materials. The main benefit of these efforts was the control of the length of the linear segments that allowed detailed studies on the influence of the size of crystallizable, ordered segments on the physical and mechanical properties.

In contrast, Skaria introduced a protocol to prepare hyperbranched poly(ε-caprolactone) in organic media by enzymatic catalysis within short production cycles under mild reaction conditions.[67] The degree of branching of the final product is defined by the comonomer ratio in feed, and the distribution of branching points is statistical. While Ursu employed Skaria`s protocol and extensively investigated the biological as well as the mechanical and physical properties of these hyperbranched poly(ε-caprolactone)s, [68,69,80] the aim of the present work is to develop an optimized protocol to produce these materials in bulk. Characterization should reveal similarities and discrepancies compared to the materials prepared by the original protocol.

Since ready availability of hyperbranched poly(ε-caprolactone)s is a prerequisite for application testing, the reaction parameters – e.g. the catalyst quantity required and a valid procedure for its regeneration – should be assessed, leading to cost-effective and ecologic production on the kg-scale.

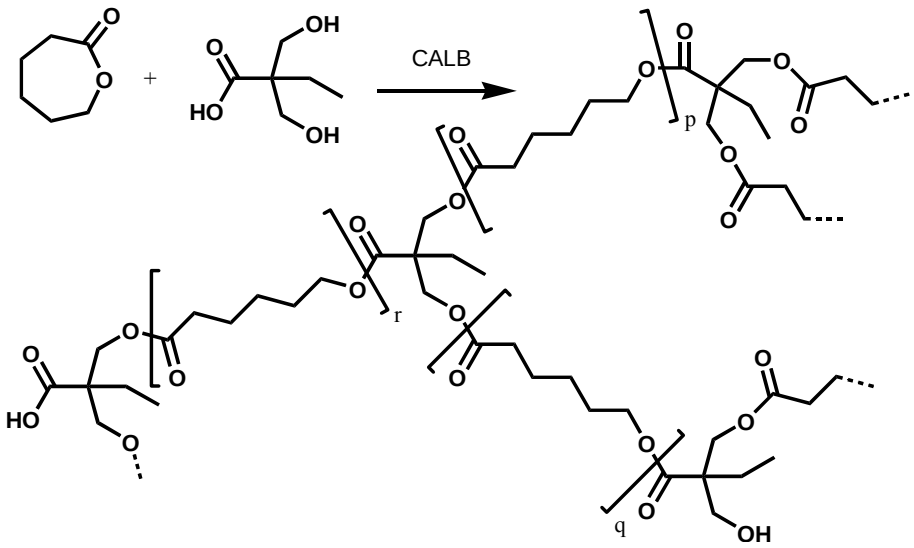

Figure 2-1: Copolymerization of ε-caprolactone and 2,2'-bis(hydroxymethyl)butyric acid.

2.3 Reknitting as a New Method of Synthesizing Hyperbranched Poly(ε-caprolactone)s

Nowadays, polymer production requires intensive research in material recycling in order to reduce the cost of waste disposal. To preserve primary resources, this research usually deals either with the combustion of plastics and composites or with the monomer / oligomer regeneration as secondary feedstock for a new production cycle. Lately, even recycling of synthetic biodegradable materials has been addressed because of future limited carbon resources.[81-83]

In chapter 4, a new concept of polymer recycling that we termed "reknitting" is investigated. The aim is to "recycle" a sample of commercial linear poly(ε-caprolactone) (*l*-PCL) by modification into hyperbranched PCL (*hb*-PCL) using the transesterification capability of Novozyme 435. The insertion of BHB into the linear chain generates branching points. Employing this technique, isolation and purification of monomers or oligomers, which often requires the use of toxic solvents, thus generating waste, shall be avoided.

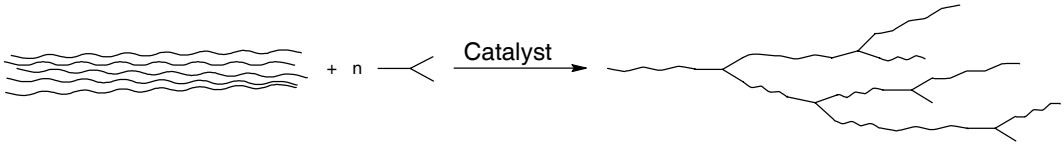

Figure 2-2: Schematic of reknitting.

2.4 Methacrylated Hyperbranched Poly(ε-caprolactone)s as Multi-functional Crosslinkers

Versatile applications of multi-functional molecules extending into three dimensions motivate researchers specializing in methods for chemical modification of (hyper-) branched polymers, e.g. towards unimolecular micelles[84] or as homogenous support in peptide synthesis[85,86] and organic catalysis.[86-88] Although methods of controlling the degree of branching and the molecular weight of hyperbranched polymers have been established recently,[67] structured networks have not been created so far. Lately, some work on amphiphilic model networks was reported,[89-91] but defined hyperbranched structures disclose a wide variety of opportunities.

Truly new features are brought into polymeric drug delivery devices by functionalized hyperbranched polymers. Unlike unimolecular nanocapsules, drugs are covalently attached, and only a small portion of the hyperbranched carrier's available methacrylated groups might be cross-linked, e.g. with HEMA. This leads to drug carriers with extended release rates whose parameters are highly tunable.

To date, only little work has been reported on the use of hyperbranched polyesters as compounds for cross-linking.[16,92] The research on these networks originated in the area of coatings and deals mainly with processing; thus the materials have not been investigated in detail.

A number of macromolecular substitution reactions of polymeric aliphatic polyols were realized in our group. The formation of nanocapsules as containers for dyes or as fluid phase extraction devices[84,93] have been reported recently. The aim of this part of the present thesis is to provide a route to methacrylate *hb*-PCL as a precursor for cross-linking reactions.

In the second part, work on UV curing of mixtures of these multi-methacrylated hyperbranched materials and 2-hydroxyethyl methacrylic acid (HEMA) to form networks is described. Finally, the mechanical and physical properties of these complex networks are elaborated upon.

2.5 Hyperbranching Polymerization of Other Lactones or Carbonates

Concurrent ring-opening polymerization and polycondensation of ε-caprolactone and an AB_2 monomer by enzyme catalysis in bulk, in which both reactions exhibit similar kinetics, has been proven to be a powerful method of preparing hyperbranched aliphatic

polyesters. It even facilitates large-scale, low-cost production, if monomers are chosen that are readily available on the market.

In chapter 6, screening experiments of several lactones are laid out, the only prerequisite being commercial availability. In addition, trimethylene carbonate was investigated representing a six-membered cyclic carbonic ester, which was prepared in a one-step reaction. The copolymerization of the latter should lead to high-loading materials with high biodegradation rates, given that linear poly(trimethylene carbonate) is completely amorphous[94] and can thus be degraded by bacteria[83] and *in vivo*.[95]

Since copolymerization of δ-valerolactone and trimethylene carbonate was successful in the initial screening experiments, these two novel classes of hyperbranched polymers shall be investigated in further testing. Detailed characterization and comparison with hyperbranched poly(ε-caprolactone) shall be achieved.

3 HYPERBRANCHED POLY(ε-CAPROLACTONE)S

Highly branched polymers exhibit unique properties compared to their linear analogues. Because of their high and tunable number of functional groups per molecule they have preferable physical properties that can be adjusted over a broad range, e.g. viscosity, leading to purpose-specific, tailored materials.

For medical and pharmaceutical application, biocompatibility is a precondition. Moreover, for some applications, such as drug delivery systems in subcutaneous implants or as film former in ointment formulations, controlled degradability, by UV radiation or *in vivo*, is highly desirable, too. Another prerequisite for this segment of application is the complete absence of heavy-metal catalysts and other potentially toxic organic residues, such as solvents or residual monomer.

Poly(ε-caprolactone) (*l*-PCL) is known for its excellent biocompatibility, low glass transition and high permeability.[79,96,97] The biocompatibility of 2,2'-bis(hydroxylmethyl) butyric acid (BHB) is not approved so far. Since poly(2-hydroxy butyrate), a structural derivative, is a highly crystalline, biological energy storage product in algae and bacteria,[98,99] P(BHB) is probably tolerated by living organisms. As a consequence, it is expected that copolyesters of PCL and BHB are bioresorbable and –degradable. Therefore, such *hb*-PCLs could be employed as carriers, either highly loaded for diagnostic purposes (e.g., for magnetic resonance imaging (MRI) of blood vessels)[43,100] or as host compartments for controlled drug release.[48] The low viscosity index [η] that comes along with high DB, and thus high functionality, may open up further use as rheological modifier.[101]

3.1 Synthesis

Hyperbranched polymers are commonly prepared from AB_2-monomers or compounds that possess a hidden or latent AB_2 functionality, which is set free in the course of the reaction, i.e. a lactone-ring is cleaved and a α-hydroxy-ω-carboxylic acid is generated. Due to this synthetic principle, the degree of branching and related properties are usually subjected to reaction kinetics, but cannot be adjusted to a specific value.

Routes to *hb*-PCL previously reported either employed self condensing ring-opening polymerization (SCROP)[102,103] or macro-monomers that were prepared via controlled synthesis of the linear segments by protection of the carboxylic group of the branching point[2,4] and subsequent hyperbranching polycondensation. While the branching density is

exactly defined in SCROP, it can be adjusted in the latter method by the length of the CL arms. The precise control of molecular geometry comes along with certain synthetic effort in monomer synthesis.

In 2002, Skaria et al. introduced "a general enzymatic route towards hyperbranched aliphatic copolyesters that is based on the combination of ring-opening polymerization (ROP) and polycondensation of suitable bis(hydroxy) carboxylic acids as branching AB_2 comonomer units."[104] This concept was first confirmed by the copolymerization of BHB and CL.[67] The reaction was catalyzed by Novozyme 435 – immobilized *Candida Antarctica* lipase B (CALB) – in toluene solution at 85 °C. Argon was used as inert gas to prevent side reactions. In contrast to the previously described methods, both monomers are commercially available at moderate cost and the reaction is a true one-pot, one-step synthesis making preparation straightforward. The degree of branching is controlled by the comonomer ratio in the feed, the distribution of the branching points is random and final molecular weights are somewhat limited, depending on the degree of branching.

However, polymerization in solution comprises a number of drawbacks: Volatile organic compounds (VOCs) are usually a hazard to environment and expensive on waste disposal. Furthermore, most organic solvents that are tolerated by Novozyme 435 have a boiling point around or beneath 100 °C on the one hand, on the other the active enzyme of the Novozyme 435 preparation becomes inefficient at temperatures exceeding 100 °C. This turns the removal of water, which is formed by the condensation process *in-situ* into a challenge. Since the boiling point of CL is 96 °C at 20 hPa, water is removed under reduced pressure without evaporation of the monomer. For that reason, it is assumed that polymerization under bulk conditions will yield higher molecular weights and lower the cost of production.

Transfer of this protocol to bulk polymerization includes some work on optimization of reaction parameters that is described in detail in section 3.5. In general, the following reaction conditions were employed: CL was distilled over CaH_2 and stored over molecular sieves prior to use. The reaction vessels (carousel reactor tubes, round bottom flasks) were oven-dried and flushed with argon. BHB and CL were heated to 85 °C under vacuum. Above 76 °C, BHB dissolves in CL, thus the feed is a homogenous liquid. Next, the reaction vessel was purged with argon, the enzyme beads were added and vacuum was applied over the whole reaction period to remove water formed in the condensation process. Post-reaction work-up comprised dissolution in chloroform, catalyst removal by filtration of the enzyme beads, washing and drying steps.

A schematic structure of the *hb*-PCL macromolecules prepared by this method is shown in Figure 1-2. Since all hydroxyl groups remain potentially active in the course of the polymerization, the resulting structure is hyperbranched and consists of perfect dendritic (D), linear (L_L), linear-dendritic (L) and terminal (T) units. Linear units (L_L) are produced by ring-opening of CL, while linear-dendritic (L) units represent BHB units in which only one of both hydroxyl groups was subject to further condensation.

3.2 Characterization

3.2.1 NMR Experiments

NMR is an important method to characterize hyperbranched polymers since detailed analysis of the spectra permits to extract information on both the degree of polymerization ($<DP_s>$) and the degree of branching (*DB*). Furthermore, information on the insertion pattern, i.e. statistical or block copolymerization, is obtained. Therefore the results of this method are discussed in detail.

^{1}H-NMR signal assignments for *hb*-PCLs in which 2,2-bis-(hydroxymethyl) propionic acid (bis-MPA) served as AB_2 component, have first been reported by Hedrick et al.[4] A distinct chemical shift for the methyl group of bis-MPA was observed depending on the type of ester formed by its carboxyl function. These observations are supported by studies on model compounds.[103]

In Figure 3-1, a typical spectrum of *hb*-PCL, discussed in this thesis, is depicted. In contrast to the polymers, in which bis-MPA was employed as AB_2 monomer, no distinction between different ester groups caused by neighboring segments was observed. However, careful analysis facilitates distinction between terminal (*e*) and linear-dendritic (*f*) methylol groups. Furthermore, the chemical shift of alkoxy groups participating in the ester linkage depends on the substitution scheme. A distinction in CL-O-CO-CL (*g*), BHB-O-CO-CL (*h*), and CL-O-CO-CL-OH (g'), the last being a second to terminal unit, was assessed. The integral of signal *d* was set to unity in order to directly compare spectra of *hb*-PCL of different DB.

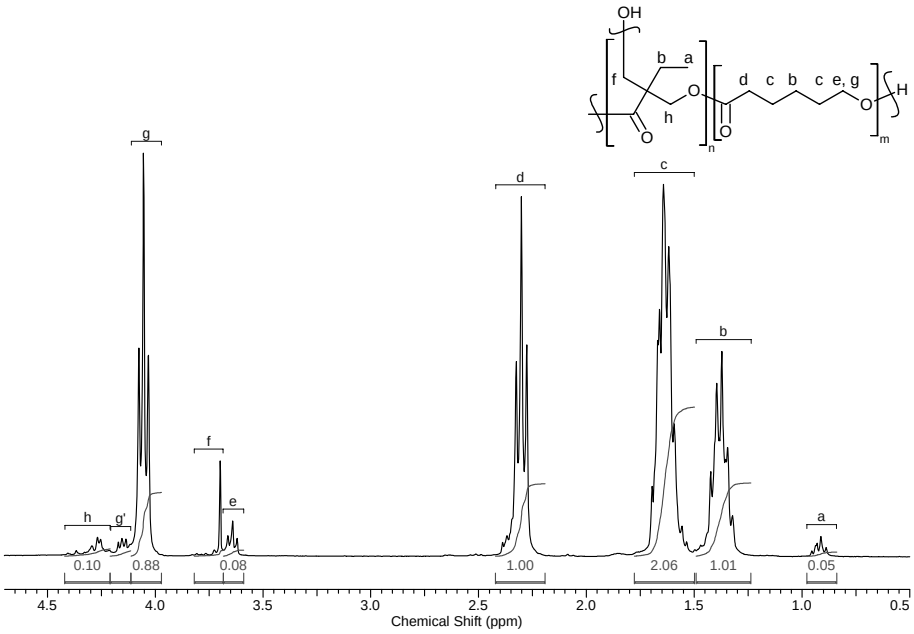

Figure 3-1: ^{1}H-NMR spectrum of a copolymer of CL and BHB containing 3.7 mol% of BHB.

Since standard ^{13}C-NMR spectra are not integrable and information on DB is extracted from ^{1}H-NMR correlation, only qualitative interpretation was done. An exemplified spectrum is shown in Figure 3-2. By comparison of spectra, in which DB of the samples is different and with the help of computer-assisted prediction, all signals were assigned. With increasing DB new signals 4', 5', Ct' and E_{LD} appear, shifted by 1-4 ppm. These represent C-atoms of the backbone of terminal CL-units, which become visible because their signal intensity is a function proportional to DB and thus, hidden in the noise of linear to moderately branched samples. The signal near E_D originates from BHB units that are inserted in a linear-dendritic fashion.

The degree of branching (DB) can be calculated on the basis of the intensities of ^{1}H-NMR-signals from the fraction of structural units using a previously derived equation (*cf*. section 1.4).

$$DB = \frac{2 \cdot D}{2 \cdot D + L} \qquad \textbf{(3-1)}$$

In Eq. 3-1, *DB* represents the degree of branching, *D* and *L* the fractions of dendritic and linear units. The *DB* values (Table 3-3) were calculated by the ratio of signal *A* and *D*, but according to the theory, any pair of two signals can be chosen, that correspond to unique, structural features of each of the two building blocks.. For sure, more accurate results are obtained if high intensity signals are preferred.

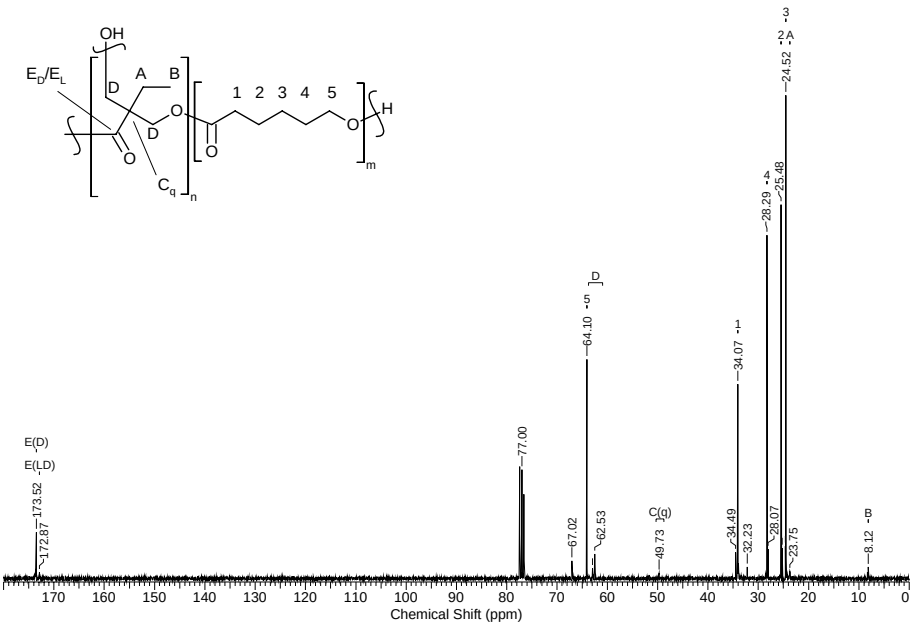

Figure 3-2: ^{13}C-NMR spectrum of a copolymer of CL and BHB containing 3.7 mol% of BHB.

Another value that is obtained from NMR-analysis is the number-average length of linear segments between two branching points (<DP_s>). It reveals information concerning the global topology of hyperbranched polymers and is calculated according to expression 3-2.[55] Orlicki et al.[72] have shown that for AB/AB_2 copolymers the average segment length is correlated to the rheological properties of the hyperbranched polymers.

$$<DP_s> = \frac{L_{co}}{D + T_{co}} = \frac{1}{2} \cdot \frac{\left(r^2 + 2r + 2\right)}{r+1} \qquad \textbf{(3-2)}$$

In which D – dendritic units; L_{co} – total number of linear units in the AB/AB_2 copolymer; T_{co} – total number of terminal units; r defines the monomer ratio AB/AB_2.

3.2.2 VPO, GPC, GPC-Online Viscometry and Solution Viscometry

Molecular weights and polydispersity are fundamental parameters in macromolecular characterization. Whereas NMR-analysis usually supplies reliable data for core initiated polymers, it fails, if random macromolecules with no core are investigated.

Vapor pressure Osmometry (VPO) is a technique that is inherently independent of the polymer's solution properties. Since it depends only on the number of molecules in solution, careful sample preparation is mandatory and often, number average molecular weights (<M_n>) are underestimated. In Figure 3-3, the data obtained by vapor pressure osmometry for a series of *hb*-PCLs is visualized. In case of aggregation due to hydrogen bonding the slope of this concentration-dependent plot is expected to decrease with

increasing concentration. This behavior was not observed in TCM solution containing up to 4 wt% of *hb*-PCL, evidencing the absence of aggregation in this concentration range. Molecular weights were calculated by dividing the product of the slope of the benzil curve and the molar mass of benzil by the slope of the respective *hb*-PCL curve. However, the values obtained by VPO measurements are generally low compared to GPC and MALDI-TOF analysis (*cf*. section 3.2.3).

In Figure 3-4 the results of viscosity measurements of some *hb*-PCLs in TCM solution are depicted. This analytical technique is based on the increase of a liquid's viscosity, which is direct proportional to the amount, the shape and the molecular weight of a herein dissolved (macromolecular) solid. The linear relationship between η_{sp} and concentration demonstrates that no aggregation occurred in the investigated concentration range, which is supported by similar observations in VPO measurements. Concentrations used in viscometry were in the same range as in VPO measurements.

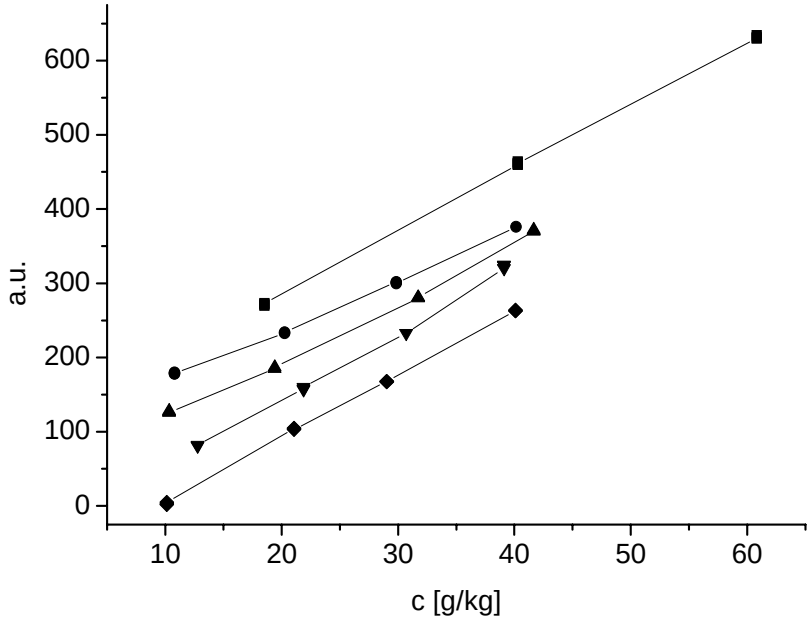

Figure 3-3: Results of vapor pressure osmometry of ● *hb*-PCL-97 (M_n= 1250 g/mol), ▲ *hb*-PCL-93 (M_n= 1100 g/mol), ▼*hb*-PCL-84 (M_n= 950 g/mol) and ◆ *hb*-PCL-76 (M_n= 950g/mol) in TCM at 30°C, calibrated with ■ benzil (M= 210.23 g/mol).

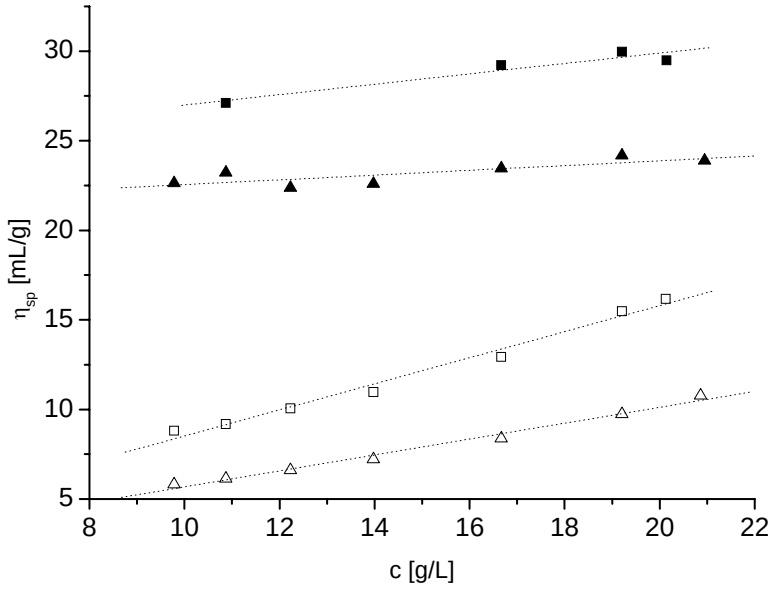

Figure 3-4: Specific viscosity (η_{sp}) of *hb*-PCLs as a function of concentration in TCM at 30 °C. Intrinsic viscosities [η] are 24.1 mL/g for ■ *hb*-PCL-97, 21.2 mL/g for ▲ *hb*-PCL-95, 1.2 mL/g for □ *hb*-PCL-93, and 1.2 mL/g for Δ *hb*-PCL-84.

GPC calibration is a difficult task, given that the hydrodynamic volume of hyperbranched polymers is a function of the degree of polymerization, the degree of branching and polymer/solvent interactions. In particular, absolute molecular weight measurements of hyperbranched macromolecules having a variable degree of functionality are a tough challenge.

Relative molecular weight determination is based on a calibration curve, for which polystyrene samples are used. Such data may serve as comparison to that previously published by other authors. Mostly neglected, this calibration generates reliable molecular weight estimates only for samples that are similar to the calibration standard in chemical structure and polarity, and therefore in their physical polymer/solvent interactions.

Absolute molecular weights (<M_w>) are obtained by light scattering or membrane osmosis (<M_n>). Although independent of the hydrodynamic volume in solution some limitations apply, e.g. the refractive index increment has to be determined, which depends on the polymer, its molecular weight and the DB. Since dn/dc appears squared in the scattering equation, inaccuracy leads to large deviations in molecular weight. In opposition, membrane osmometry permits fast molecular weight determination, but works only in the range of $M_r = 10^4–10^6$ Da.

Due to the nature of hyperbranched polymers, additional difficulties arise using these techniques: As dn/dc strongly depends on molecular weight up to 20 kDa[105] and on DB, light scattering is not a routine method for high throughput analysis. Whether or not light scattering detectors can be used depends decisively on the refractive index increment of the polymer solvent combination. Where values are high, as in the case of polystyrene in THF (dn/dc = 0.185), usable signals are obtained down to M_w of approximately 1.0 kDa. In the case of other polymers, for which dn/dc equals 0.05, the size of the signal is only about 7% of the polystyrene-in-THF signal at the same concentration and molecular weight, making reliable evaluation at low MW impossible.[106] dn/dc of *l*-PCL, M_w = 10 kDa (THF, 30 °C) was found to be 0.056 ± 0.006.

Membrane osmosis suffers from underestimation of the average molecular weight for the same reason as vapor pressure osmometry. Since both methods are based on the absolute number of particles in solution, hyperbranched polymers having inherently broad polydispersities and low molecular weight oligomer fractions are underestimated.

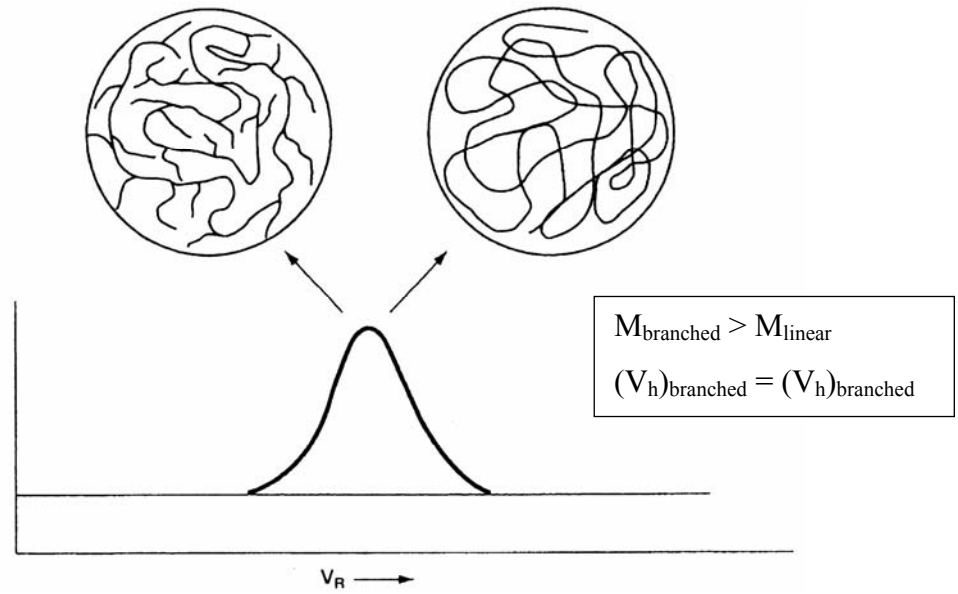

Figure 3-5: GPC elution profile of linear and branched samples of similar hydrodynamic volumes, but different molecular weights.[1]

Another method that overcomes these difficulties, is the so-called *universal calibration* technique, which was introduced by Grubisic et al.[107] It is based on the consideration that GPC does not separate macromolecules by molecular weight, but by the size of the solute molecule in solution. This concept is demonstrated in Figure 3-5 which shows a highly branched chain eluting at the same retention volume as a linear, lower-MW polymer of similar hydrodynamic volume.

Likewise, solutes of similar MW but different molecular conformation will elute at different retention volumes.

In order to relate MW to molecular size, the concept of intrinsic viscosity is often used. The intrinsic viscosity [η] of a polymer solution can be easily determined and is related to MW, size and shape of the macromolecule in solution. To date, viscosity detectors that allow online viscosity measurements, which produce reliable data and reduce experimental effort dramatically. In Table 3-1 viscosity values obtained by i) solution viscosity measurements using an Ubbelohde viscometer and ii) GPC-online viscosity detection are summarized for a series of *hb*-PCLs.

In an universal calibration the classical log MW plot against the elution volume V_{el} is replaced by log [η]·M vs. V_{el}. While the MW to V_{el} relationship depends on the type of polymer in the classical plot, these curves merge into a single plot in the universal calibration plot (Figure 3-6). The validity of this concept to produce highly reliable molecular weight estimations was examined in a number of publications investigating a variety of polymers, different in shape and in chemical nature.[107-113] For low molecular weights, the sensitivity of the viscosity detector exceeds that of light scattering even at high dn/dc.[106]

Table 3-1: Viscosity data obtained by i) GPC-online viscosity detection (TCM, 30°C) and ii) solution viscometry (TCM, 30 °C) for a series of *hb*-PCLs. *) $[\eta]_{GPC}/[\eta]_{Visc}$ is a measure of deviation; similar values express linear deviation.

Copolymer	[η] [cm^3/g] i)	[η] [cm^3/g] ii)	$[\eta]_{GPC}/[\eta]_{Visc}$ *
hb-PCL-99	28.9	33.2	1.15
hb-PCL-97	21.3	24.1	1.13
hb-PCL-95	16.8	21.2	1.13
hb-PCL-93	8.7	1.2	-

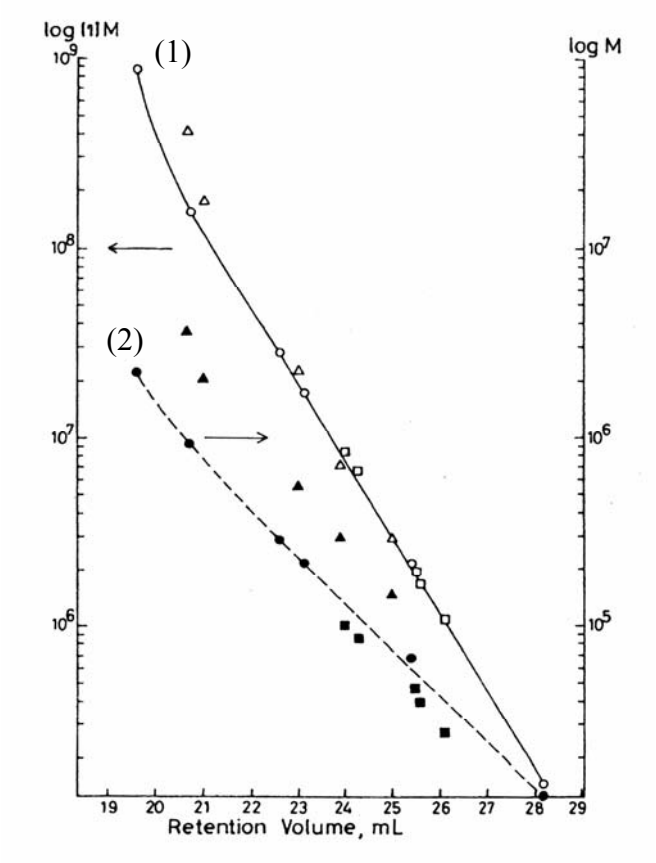

Figure 3-6: Universal calibration curve (1) and peak position calibration curve (2). Universal calibration curve: ● PS, ■ PVC, ▲ PS (comb); peak position calibration curve: ○ PS, □ PVC, Δ PS (comb). The solvent used is THF.[3]

3.2.3 MALDI-TOF Mass Spectroscopy

Structural information on the molecular scale, e.g., the comonomer incorporation pattern or the presence of macromolecular cycles, is difficult to obtain in polymer science. So far, the only method is MALDI-TOF MS, but spectra are highly questionable with respect to representative, reliable data. In Table 3-2 monoisotopic masses of the relevant fragments are summarized.

Table 3-2: MALDI-TOF MS: Monoisotopic masses of relevant fragments

Fragment	Origin	Formula	Monoisotopic mass of fragment
L_L	CL	$[C_6H_{10}O_2]$	114.068
D	BHB	$[C_6H_9O_2]$	113.060
L	BHB	$[C_6H_{10}O_3]$	130.063
-	-	H_2O	18.011

As consequence, a clear distinction between D and L_L units is difficult because both fragments have very similar masses. Considering a molecule of 1.5 kDa, being composed of 12 to 13 fragments, it may consist exclusively of L_L units, but also of (L_L-1) and one D unit. At 1.5 kDa MW, 1 a.m.u. difference is caused either by i) structural difference (see above), ii) H/D exchange or iii) difference in the geometry of the path of flight depending on the position of the spot on the sample plate.

However, incorporation of linear-dendritic fragments L is clearly indicated by the difference in mass and cyclization is recognized by signals that are 18.01 a.m.u. beneath the signal of the linear species.

Finally, one should keep in mind that MALDI-TOF MS is not a reliable tool for molecular mass determination of polydisperse samples because of mass discrimination effects, which lead to underestimation of very low- and very high-MW species [114].

3.2.4 Physical Properties

In the case of the samples prepared in kg-charges, the hot crude *hb*-PCLs had a clear yellowish color. Dramatically slowed down crystallization of the final product was observed in the case of *hb*-PCL-42 caused by the highly branched structure of the sample: While all of the low-DB samples crystallized readily upon cooling to ambient temperature, *hb*-PCL-42 remained a clear, viscous liquid for at least one day after sample preparation. Permanent solidification was achieved after cooling the sample to -20 °C for 5 hours.

All of the high DB samples (DB > 20 %) remained rather waxy whereas low DB samples were rather hard and brittle like commercial linear PCL (*l*-PCL) is. *l*-PCL prepared by enzyme-catalyzed bulk polymerization as reference material looks alike.

hb-PCL is not soluble in water or lower aliphatic alcohols but in a number of organic solvent, e.g. tetrahydrofurane (THF), chloroform (TCM), 1,4-dioxane, 1,2-dichloro ethane, toluene and pyridine.

DSC measurements confirmed that all *hb*-PCLs are flexible polymers, manifested by glass transitions between - 48 °C and - 56 °C. Melting points were found to be between 27 °C and 57 °C, strongly depending on the DB. The melting endotherm is usually shaped as double endotherm. *hb*-PCL samples of DB > 35 % are completely amorphous, as determined by means of DSC analysis.

3.3 Hyperbranched Poly(ε-caprolactone) by Polymerization in Solution

Initial experiments on the enzyme-catalyzed polymerization of CL were carried out according to the protocol developed by Skaria.[67] The results are summarized and compared to selected data of Skaria in Table 3-3 and Table 3-4.

Although prepared strictly according to the quoted protocol, neither the author nor Ursu were able to reproduce the molecular weights obtained by Skaria. However, incorporation of BHB was found to be closer to stoichiometric insertion and higher yields were obtained than in the initial work. Results produced by the author are in good agreement to those obtained by Ursu.

Table 3-3: Characterization data of *hb*-PCL samples prepared by solution polymerization.

Copolymer	DB_f mol-%	DB_p mol-%	Yield %	M_n (GPC) g·mol^{-1}	PDI
hb-PCL-96s	3.9	3.9	98.1	6,800	2.0
hb-PCL-90s	9.5	10.2	99.7	3,800	1.8
hb-PCL-83s	18.2	17.5	99.7	1,750	2.5
hb-PCL-74s	26.1	25.6	91.1	1,500	2.0
hb-PCL-98s[1)]	1.9	1.6	90.0	9,000	2.1
hb-PCL-97s[1)]	3.9	2.9	95.0	7,200	2.0
hb-PCL-92s[1)]	11.3	8.4	97.0	3,500	1.8
hb-PCL-87s[1)]	14.2	12.8	85.0	2,500	1.6
hb-PCL-77s[1)]	40.0	33.1	73.0	1,100	1.1

[1)] Experiments carried out by Ursu[80]

Table 3-4: Characterization data of *hb*-PCL samples prepared by Skaria.[67]

Copolymer	DB_f mol-%	DB_p mol-%	Yield %	M_n (GPC) g·mol^{-1}	PDI
hb-PCL-100s	0	0	80	34,600	1.8
hb-PCL-98s	3.9	3	75	53,100	1.4
hb-PCL-96s	7.7	4	78	24,800	1.6
hb-PCL-92s	14.8	10	84	23,900	1.3
hb-PCL-90s	16.7	13	74	12,900	1.5
hb-PCL-75s	40.0	23	58	8,000	1.2
hb-PCL-50s	66.7	33	61	6,600	1.2

3.4 Hyperbranched Poly(ε-caprolactone) by Bulk Polymerization

Polymerizations in organic media usually lack scalability because larger quantities in the synthesis require large volumes of solvent. Besides difficulties in solvent handling, removal of water, which is formed by the condensation process, becomes a critical issue. Most water removal methods commonly used in laboratory synthesis are not scalable conveniently either.

For that reason, one aim of the present work was to establish a protocol offering polymerization of CL and BHB using bulk techniques and enzymatic catalysis. In addition, cyclization is expected to be suppressed in bulk;[115] water, which is formed *in situ*, should be removed by vacuum.

In the final protocol, bulk polymerizations were carried out *in vacuo* at 85°C for 24 hrs, using immobilized Lipase B from *Candida Antarctica* (CALB, Novozyme 435), leading to the desired hyperbranched structure. It is noteworthy that BHB dissolves in CL above 76 °C, forming a colorless, clear solution. During polymerization a remarkable increase in viscosity was observed, which caused the rotation of the magnetic stirrer to stop after 3-5 hrs of operation depending on the fraction of BHB.

3.4.1 Reaction Kinetics

Reaction times often reflect arbitrary periods chosen by the researcher's convenience.[116] In order to optimize reaction parameters, kinetic experiments were carried out. As depicted in Figure 3-7 final molecular weight was achieved after 2-5 hours. Careful interpretation of the data led to the conclusion that there is a small decrease in molecular weight after 20 hours. The weight-loss of the polymer chains may be caused by transesterification that is also catalyzed by Novozyme 435. The decrease amounts to ca. 6 % for both $<M_n>$ and $<M_w>$.

Polydispersity (PDI) and yield reveal information about the ongoing polymerization. If PDI is high after short reaction periods, but decreases with longer intervals, random polymerization may be assumed. In this case, PDI is 1.7 – 1.8 for all samples, indicating either that the molecules' growth occurs evenly or that final conversion is reached very soon. According to Figure 3-7, yield, and thus conversion, assume a maximum after 5 – 10 hrs. After 20 hrs, no significant change in conversion is observed any more.

In conclusion, molecular weights and yields reach a maximum after 10 hrs. Between 10 and 20 hours, a weight loss of 5 - 6 % is observed, which was ascribed to trans-

esterification also mediated by the enzyme. Final molecular weights and constant yields were obtained after 20 hours of reaction. This equilibrium state was chosen as end point of the reaction.

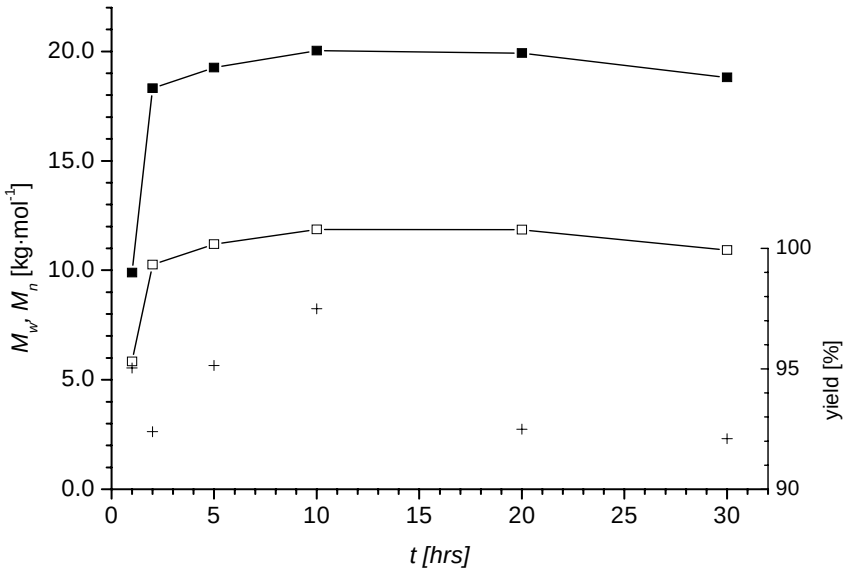

Figure 3-7: *hb*-PCL Polymerization: Kinetics - Molecular weight as a function of reaction time; ■ <M_w>, □ <M_n>,, + yield.

3.4.2 Degree of Branching

DB and, consequently, the number of hydroxyl end groups, is a central parameter in determination of the properties of *hb* polymers. It defines not only the statistical extent of branching within one macromolecule, but also the number of terminal, functional groups and indirectly the average length of linear segments (<DP_s>). In classical AB_2 polycondensations, DB approximates a certain maximum, but individual control is not feasible.

Hedrick et al. [4] as well as Choi et al. [2] exactly defined <DP_s> by the length of the linear PCL arms that were polymerized onto the branching points prior to the hyperbranching polycondensation.

In this study, DB is controlled by the monomer ratio in the feed. As discussed in section 3.2.1, the amount of AB_2 units in the copolymers was determined by integration of ^{1}H-NMR signals. The fraction of BHB incorporated into the *hb* copolymers was generally lower than in the monomer feed. CALBs preference to mid-sized and large cyclic substrates[65,117-120] is known to limit copolymerizations.

On the other hand homopolymerization of BHB was unsuccessful since large amounts of polar solvents were required to solubilize the monomer, which impaired the activity of CALB[67]. This is visualized in Figure 3-8 correlating DB values calculated from ^{1}H-NMR spectra with theoretical values set by the initial monomer ratio.

DB of the copolymers was in the range of 1 to 33 %, according to the Frey definition for AB/AB_2.copolymerizations[55] Comparing this data with samples prepared by solution polymerization similar values and trends are observed up to a DB of 20 %. At higher DB solution polymerization results in near to stoichiometric ratio of comonomer insertion (Table 3-3). In the case of bulk polymerization, the deviation from the ideal insertion is more pronounced (Table 3-4). However, even in this concentration range, control of DB is given for both systems, since the deviation from ideal behavior can be anticipated and the desired DB reproduced.

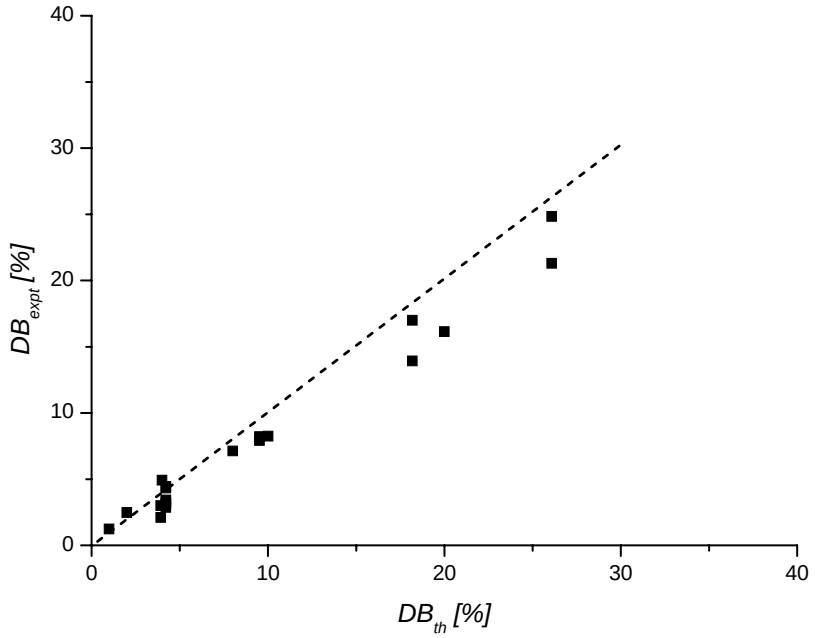

Figure 3-8: Degree of branching as determined from ^{1}H-NMR analysis correlated to theoretical degree of branching by feed. The straight line marks stoichiometric copolymerization.

As discussed elsewhere[67] yields and molar masses of *hb*-PCLs exhibit a decreasing tendency with increasing fraction of the branching component BHB. However, GPC characterization of hyperbranched multi-functional polymers whose number of functional groups per molecule is subjected to change, is problematic and can lead to questionable results, if common linear standards are employed[63] (*cf.* section 3.2.2). By means of GPC,

a change of the functional density per molecule results in different species that one cannot compare directly.[55,63,121] Thus other techniques to determine the molecular weight were taken into account. A universal calibration curve was established, which is a base for absolute molecular weights.[107] In addition, measurements of vapor pressure osmometry (VPO), which is independent of the chemical nature of the sample and therefore more reliable for hyperbranched polyfunctional polymers, were carried out. The data is summarized in Table 3-5, the relationship between $<M_n>$ and DB is shown in Figure 3-9.

In standard calibration mode, molecular weights decreased rapidly from $<M_n>$ = 10.0 to 0.4 kDa upon increasing the DB from 0.5 % to 33.3 %. PDI is in the range of 1.6 – 2.4 showing a decreasing tendency with higher DB.

Universal calibration mode was used to determine absolute molecular weights.[7,107] Since the viscosity detector is more sensitive than refractive index detectors in the case of PCL, a broadening in the molecular weight signals is a common phenomenon for the samples of *hb*-PCL. As consequence, PDI values were somewhat higher than they appeared in standard mode. Unfortunately, this detection mode is limited by weak signal intensity. Hence only samples with DB ≤ 10 % resulted in reliable data.

The absolute $<M_n>$ measured by VPO analysis was in the range of 1,000 – 1,300 Da, but in contrast to GPC only little dependence on DB was observed. All samples showed excellent linear correlation. Thus, aggregation due to polar groups can be excluded (Figure 3-3).

Table 3-5: Molecular weights and viscosity of *hb*-PCLs obtained by various methods; the samples were produced by variation of the copolymer ratio in feed.

Copolymer	DB_f mol %	DB_p mol %	$<M_n>^1$ g·mol^{-1}	PDI[1]	$<M_n>^2$ g·mol^{-1}	PDI[2]	$<M_n>^3$ g·mol^{-1}	$\eta_{intr.}{}^4$ cm^3/g	MH-K[4]	MH-α[4]	$\eta_{intr.}{}^5$ cm^3/g
l-PCL[6]	-	-	5,800	3.6	2,000	5.4	-	25.6	0.15	0.56	25.5
hb-PCL-99	1.0	1.2	10,000	2.4	4,300	2.6	1,300	28.9	0.18	0.55	33.2
hb-PCL-97	2.0	2.5	6,700	2.4	3,600	2.4	1,200	21.3	0.18	0.52	24.1
hb-PCL-95	4.0	4.9	5,700	2.0	2,300	3.0	1,200	16.8	1.72	0.26	21.2
hb-PCL-93	8.0	7.1	2,200	2.4	2,000	2.5	1,100	8.7	1.06	0.26	1.2
hb-PCL-92	10.0	8.2	2,300	2.1	2,200	2.3	1,100	7.8	0.49	0.34	1.7
hb-PCL-84	20.0	16.1	900	2.2	-	-	900	-	-	-	1.2
hb-PCL-66	50.0	33.7	400	1.6	-	-	1,000	-	-	-	-

[1] Det. by GPC (TCM, 30°C, PS-Calibration)
[2] Det. by GPC (TCM, 30°C, Univ. Calibration)
[3] Det. by VPO (TCM, 30°C)
[4] Det. by GPC-online viscometer (TCM, 30°C)
[5] Det. by solution viscometry (TCM, 30°C)
[6] produced according to the *hb*-PCL protocol

Comparing the molecular weight values obtained from these two methods it was observed that the results obtained by VPO were distinctly lower than the ones obtained by GPC (Figure 3-9). Since VPO is a colligative method, molecular weights are more likely to be underestimated because traces of solvent or oligomers will have a strong effect on molecular weights measured.

In this case, VPO data expresses rather the lower $<M_n>$ of those oligomers that were not removed by post reaction work up than the true $<M_n>$ of the sample complimentary to GPC. As discussed in section 3.2.2 data based on standard calibration may serve for comparison with other publications but universal calibration yields appropriate molecular weights that can be confirmed by absolute methods, e.g. MALDI-TOF MS, if monodisperse samples are used.

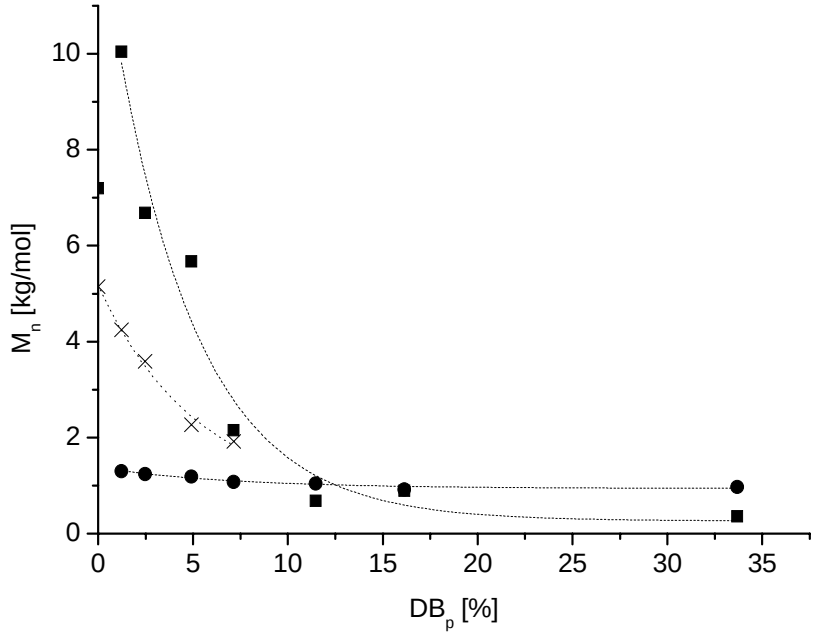

Figure 3-9: Comparative graph of $<M_n>$ against DB_p determined by: ■ GPC (polystyrene calibration, TCM), x GPC (universal calibration, TCM) and ● VPO (T = 30 °C, TCM).

As important as elucidation of structure and actual molecular weight is the determination of the materials´ properties in solution by viscosity measurements. On the one hand information on the shape of the polymer chains in the respective solvent is obtained, but on the other hand knowledge for material processing is achieved as well.

The dependence of the intrinsic viscosity [η] on molecular weights as well as the DB has been investigated for all copolymers. These measurements were performed on an

automatically recording Ubbelohde viscometer and compared with the data obtained by an online viscosity detector attached to the GPC (*cf*. Table 3-5).

Figure 3-4 depicts the results of viscosity measurements in TCM at 30 °C. The linear relationship between η_{sp}/c and concentration demonstrates that no aggregation occurs in the investigated concentration range, which corresponds to observations discussed in the GPC section. The slope of the lines flattens out with increasing DB of the sample which means that highly branched samples have a very compact structure in solution. Both techniques online viscosity detection and Ubbelohde viscometry are in good agreement. This is noteworthy, since online viscosity detection is a rather simple and efficient routine compared to common solution viscosity measurements.

As before, the values of intrinsic viscosity of the *hb*-PCLs with different DB were lower than those of *l*-PCL. This is related to the different structure and architecture of the linear and hyperbranched samples. Intrinsic viscosity depends on the ratio of the hydrodynamic volume to molecular weight. The structures of hyperbranched polymers are denser, resulting in smaller hydrodynamic volumes compared to those of linear polymers with comparable molecular weights, thus leading to smaller viscosities (*cf.* Figure 3-5). Only 5 % of branching cause a drop in viscosity to 50 % of the original value (Table 3-1).

This explanation is supported by the Mark-Houwink parameter α which is calculated from online viscosity measurements in TCM. While α equals 0.6 for *l*-PCL prepared by enzymatic catalysis, it decreases the more BHB is inserted. 5 % of branching induce a decrease of α to 0.3.

The *K* parameter, which is also obtained by the Mark-Houwink-Sakurada equation (*cf.* section 1.2) is a measure for the strength of polymer/solvent interactions. Higher values reflect stronger interactions. In the case of *hb*-PCLs no trend was observed but relatively large K values were obtained indicating strong polymer/solvent interactions.

Bulk polymerization technology is expected to yield products with lower content of cyclic species than solution techniques.[115,122] Since distinction of dendritic BHB (113 amu) and linear CL (114 amu) units is a rather difficult and not absolutely consistent issue (*cf*. Table 3-2), we were mostly interested in details on cyclization. MALDI-TOF characterization was carried out with three different samples: *hb*-PCL-98, a long-chain branched PCL, *hb*-PCL-84, a moderately branched sample and *hb*-PCL-66 representing a hyperbranched material. The respective spectra are shown in Figure 3-10-Figure 3-12. In all spectra a repetitive signal pattern was observed, which was most complex for the long-chain branched *hb*-PCL-98. The series of signals were assigned to the hyperbranched

copolymer structure. Generally, the signals were observed at regular intervals of 114 amu, corresponding to the molecular weight of the CL repeating unit or of branched BHB, respectively.

In the long-chain branched sample (*hb*-PCL-98, Figure 3-10) exclusively linear species, cyclic and non-cyclic, were dominant and a small peak referring to a branched cyclic species was also detected. The signal "L_8-nc" refers to linear HCL_8K^+. One of the CL groups might have been replaced by a dendritic BHB group, thus, a neutral species $L_7BHB^-K^+$ might have been desorbed alike. "H-nc1" stands for linear $HCL_8BHB_1K^+$. Both of them "L_8-c" and "H-c1" originate of condensed "L_8-nc" and "H-nc1" respectively, which yield cyclic species by the loss of H_2O (-18 amu). "H-nc2" represents $H\text{-}CL_7BHB_2K^+$.

This relation is inverted at DB = 16 % (Figure 3-11), in which mainly non-cyclic branched and little linear species were found. In the highly branched sample (Figure 3-12) only the two non-cyclic, branched species "H-nc1" and "H-nc2" were detected. These results confirm theoretical considerations that cyclization is suppressed the higher the DB.

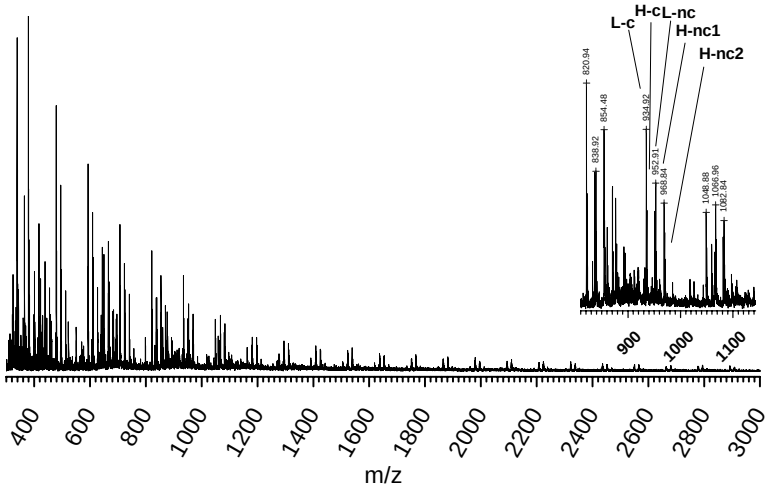

Figure 3-10: MALDI-TOF spectra of *hb*-PCL-98.

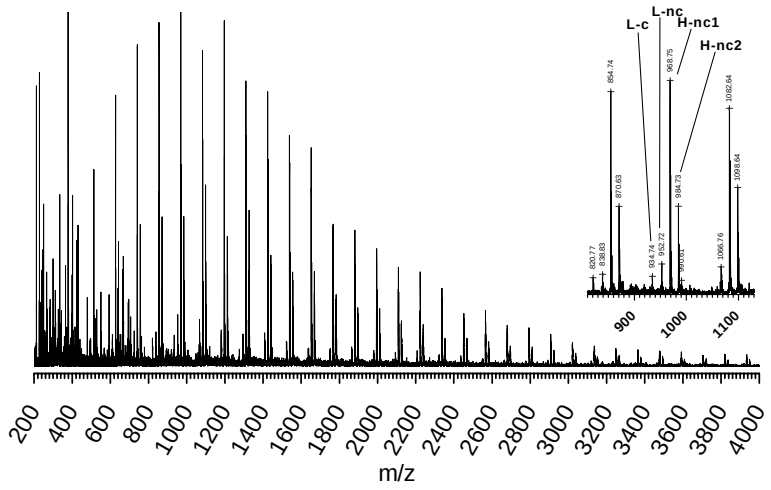

Figure 3-11: MALDI-TOF Spectra of *hb*-PCL-84.

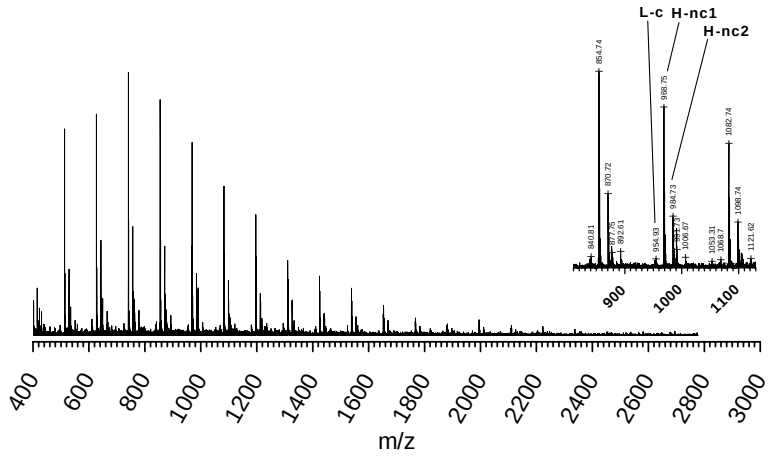

Figure 3-12: MALDI-TOF Spectra of *hb*-PCL-66. L refers to linear, H to hyperbranched, c – cyclic and nc – not cyclic. H-nc1 and H-nc2 are both branched, but differ in one linear-dendritic building unit.

Not only cyclization but also thermal properties depend strongly on the DB. Typical DSC diagrams for a series of samples obtained upon heating are shown in Figure 3-13. All DSC diagrams exhibit a characteristic double endotherm. The more intensive upper part represents the melting process, which was confirmed by optical microscopy. *Hb*-PCLs of DB > 35 % are completely amorphous by means of DSC analysis. The melting temperatures (T_m) in Table 3-6 are reported as the peaks of the higher temperature peak of the double endotherm.

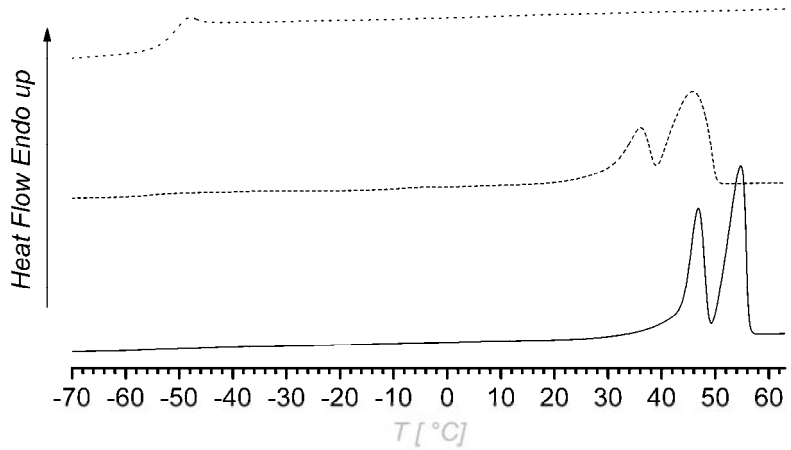

Figure 3-13: DSC diagram of *hb*-PCLs upon heating; straight line - *hb*-PCL-93, dashed line - *hb*-PCL-84, dotted line - *hb*-PCL-76.

In contrast to this study, Choi and Kwak did not observe double melting endotherms in their recent work,[2] in which a macromonomer concept for the synthesis of hyperbranched PCL was used. Since the combined area under the peaks of both endotherms in our study is equal to the area of the exotherm caused by solidification in the cooling step, this phenomenon is attributed to the presence of a wider linear segment distribution. Using polarizing microscopy Ursu observed the isothermal formation of well-grown spherulites of 200 μm in size at T_c = 35.8 °C for *l*-PCL that was prepared by polymerization in solution.[68] The spherulites were very tightly spaced and regular in shape. *Hb* materials, however, formed fewer and less developed spherulites. They were about 30 μm in size and irregular in shape. Extended amorphous regions were observed between the crystallites. These observations may tentatively explain the appearance, and moreover, the broadening of the melting endotherm.

Molecular parameters like molecular weight distribution and DB strongly influence crystallization and melting behavior. An increase of the DB_p from 1.2 to 33.7 % caused a

Table 3-6: Theoretical and experimental degree of branching (DB), the average segment length (<DP_s>) and thermal properties of selected *hb*-PCLs.

Copolymer	DB_f mol%	DB_p mol%	BHB_p mol	r	DP_s	T_g °C	T_m °C	ΔH_f $J \cdot g^{-1}$	X_c %
l-PCL*	-	-	-	-	-	-64.6	58.0	65.4	48.4
hb-PCL-99	1	1.2	0.6	165.7	83.3	-52.3	56.7	80.5	59.6
hb-PCL-97	2	2.5	1.3	75.9	38.5	-57.2	54.9	79.6	59.0
hb-PCL-95	4	4.9	2.5	39.0	20.0	-55.7	58.6	80.4	59.6
hb-PCL-93	8	7.1	3.7	26.0	13.5	-54.5	54.9	81.9	60.7
hb-PCL-92	10	8.2	4.3	22.3	11.7	-50.7	53.7	77.1	57.1
hb-PCL-84	20	16.1	8.8	10.4	5.7	-49.5	46.0	67.7	50.2
hb-PCL-66	50	33.7	20.3	0.3	2.1	-50.6	27.2	40.1	29.7

*) CAPA 6100™

decrease of T_m from 56.7 °Cto 27.2 °C. Correlating T_m with DB_p, and thus indirectly with <DP_s> of the *hb*-PCLs, it becomes clear that T_m is determined by the average length of the linear CL segments between two branching points, lowering its values with decreasing <DP_s> (Figure 3-14).

Another parameter that also reflects the crystalline fraction is the heat of fusion ΔH_f. It is represented by the area under the melting endotherm and a virtual baseline connecting both ends of the peak. As expected, a decreasing trend with increasing incorporation of AB_2-comonomer is found. Since ΔH_f of completely crystalline *l*-PCL is known, the degree of crystallinity, X_c, was calculated according to:

$$X_c = 100 \cdot \left(\frac{\Delta H_f}{\Delta H_f^0} \right) \qquad \textbf{(3-3)}$$

in which: ΔH_f – measured heat of fusion; ΔH_f^o – heat of fusion of 100 % crystalline *l*-PCL; ΔH_f^o (*l*-PCL) = 3.69 kcal/mol or 135 J/g.[123]

Intuitively, one may assume that hyperbranched polymers suffer from a lower tendency to crystallize compared to the linear analogue. Surprisingly, *hb*-PCL samples of DB below 10 % were found to exhibit a similar or even higher degree of crystallization than *l*-PCL. The highest value for X_c and for the melting enthalpy was found for *hb*-PCL-93 that slightly differs from *hb*-PCLs of lower DB (Table 3-6). One possible explanation for this unexpected finding is that the chain ends of the hyperbranched structure lead to an enhanced mobility that permits an alignment of linear segments, increasing the degree of crystallization in this way.

Since the glass transition T_g of a hyperbranched polymer is due to translational motions, Kim and Webster suggest the lower the polarity of hyperbranched polymers, the lower their T_g.[27] In the present study, the T_g values observed for the *hb*-PCL samples exhibit a tendency to increase as DB increases, which corresponds to the enhanced polarity of the polymers. A complimentary explanation is the mobility of the linear segments to be more and more constrained by the higher the number of branching points.

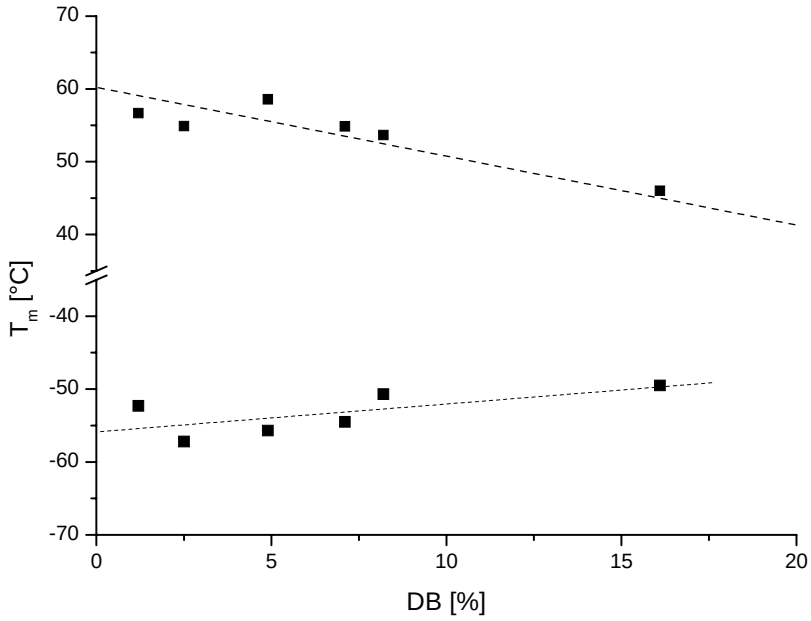

Figure 3-14: Plot of T_m vs. BHB_p of *hb*-PCLs.

3.4.3 Increasing Molecular Weights by Advanced Water Removal

High molecular weights in polycondensation reactions are only achieved at high conversion. In the present study quantitative incorporation of BHB is only realized, if the condensation competes with the ring-opening polymerization of CL. Most often, the only way to shift the equilibrium to the product side relies on efficient removal of the byproduct, e.g. water that is formed by the condensation process. Besides, the activity of Novozyme 435 is lowered the more polar groups are present in its environment and enzymatic degradation may occur.[124] Since Novozyme 435 consists of CALB that is adsorbed on Lewatit™ beads,[124] it may be washed off the beads if the medium is too hydrophilic. In this case, regeneration of the enzyme beads becomes obsolete.

For these reasons some efforts were made to improve the general protocol in terms of water removal. *hb*-PCL-96 served as reference experiment, in which no vacuum was applied.

hb-PCL-96Ar was treated as before, but an argon flux was applied for the last 5 hours. Sample *hb*-PCL-96MS was prepared like the reference sample, but 0.1 g activated molecular sieves[125] were added to adsorb water. In experiment *hb*-PCL-96Vac vacuum was applied over the whole reaction period. The results are summarized in Table 3-7.

As expected, all these measures resulted in higher incorporation of BHB, i.e. higher DB, than in the reference experiment, but only slightly increased molecular weights were observed in experiment *hb*-PCL-96MS. According to these results addition of molecular sieves or applying vacuum are best suited for driving molecular weights and DB to higher values.

Table 3-7: Experimental data of *hb*-PCLs prepared under water removal conditions.

Copolymer	DB_f mol%	DB_p mol%	$<M_n>^1$ g·mol^{-1}	PDI^1	$<M_n>^2$ g·mol^{-1}	PDI^2	$\eta_{intr.}{}^4$ cm^3/g	MH-K^4	MH-α^4 cm^3/g
hb-PCL-96	8.0	10.7	2,300	2.5	900	4.6	10.1	1.2	0.3
hb-PCL-96Ar	8.0	11.7	2,000	2.5	1,000	3.7	8.3	0.8	0.3
hb-PCL-96Vac	8.0	14.4	2,100	2.5	1,000	3.8	8.0	0.5	0.3
hb-PCL-96MS	8.0	15.7	2,400	2.6	1,000	4.3	10.4	0.9	0.3

[1)] Det. by GPC (PS-Cal.)
[2)] Det. by GPC (Univ. Cal.)
[3)] Det. by VPO (TCM)
[4)] Det. by GPC-online viscometry

3.5 Parameter Optimization for Synthesis on the kg-scale

A straight forward protocol to synthesize *hb*-PCLs in bulk employing Novozyme 435 as biocatalyst was developed and discussed in the previous sections. Since cost of the chemicals is relatively low and control over elemental product properties is achieved, parameters that gain importance in larger scale production were studied.

3.5.1 Influence of the Concentration of Novozyme 435 on the Product

The parameter, to which economic calculations are most sensitive, is the quantity of Novozyme 435 that is added to the batch. Efforts to regenerate the Novozyme beads used during a synthetic cycle were not successful yet (*cf.* section 3.5.2), therefore the cost of the enzyme will probably remain the most critical issue.

A series of samples was prepared in which the quantity of Novozyme 435 with respect to the total feed was varied. Since most protocols found in literature have chosen 10 wt% Novozyme, this amount was set as largest quantity. This can amount to relatively high

masses, but one should keep in mind that most of the weight is caused by the Lewatit^{TM} beads to which only a thin film of the active enzyme is absorbed. The molecular weights obtained after 24 hrs of reaction are shown in Figure 3-15. Although a correlation of achieved molecular weight, yield and amount of Novozyme 435 is observed, the quantity of Novozyme 435 can be reduced to 4 %, which comes along with 10 % loss of final molecular weights.

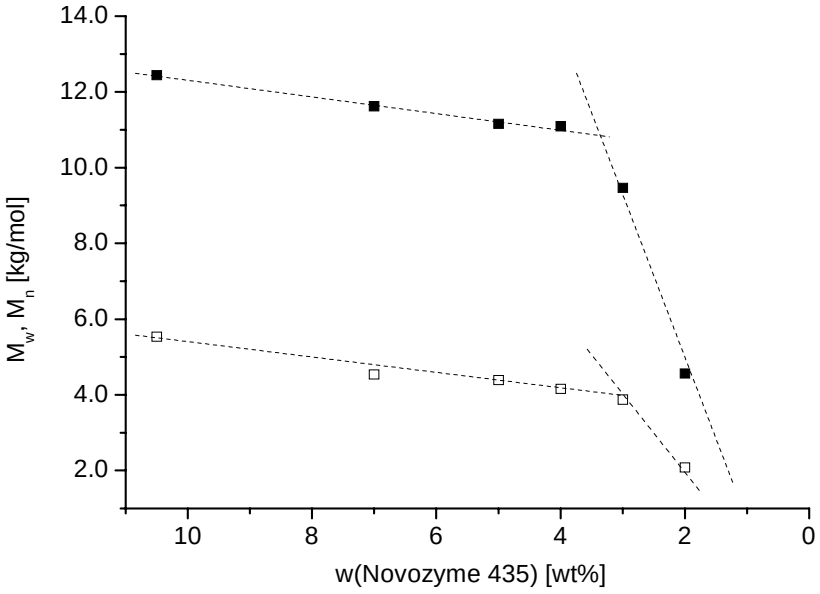

Figure 3-15:Effect of the Novozyme 435 concentration on the final molecular weight.

3.5.2 Enzyme Regeneration and Enzyme Leaching

Regeneration of the enzyme beads is also a crucial topic to achieve cost-efficient polymer production. In particular, information on eventual enzyme leaching from the beads and thus formation of a residue may gain importance if approval of the *hb* polymer as pharmaceutical compound is planned.

In each of two concurrent experiments the same lot of Novozyme 435 beads was used for the synthesis of *hb*-PCL. After each synthetic step the beads were regenerated by washing with TCM and subsequent drying. Correlating molecular weight, and yield respectively, versus production cycle, a dramatic decrease of activity between new Novozyme 435 and regenerated enzyme beads became obvious (Figure 3-16). The enzyme's activity dropped around 60 % from new to first regeneration and some more from first to second

regeneration cycle. After that only low molecular weight samples were produced but activity remained stable.

Since the loss of activity may be caused by enzyme leaching from the beads or by the regeneration process itself, new Novozyme 435 was refluxed in HPLC grade chloroform. The beads were removed from the solvent and dried according to the regeneration protocol. No significant difference between *hb*-PCL samples produced using pseudo-regenerated beads and those using new Novozyme 435 were observed.

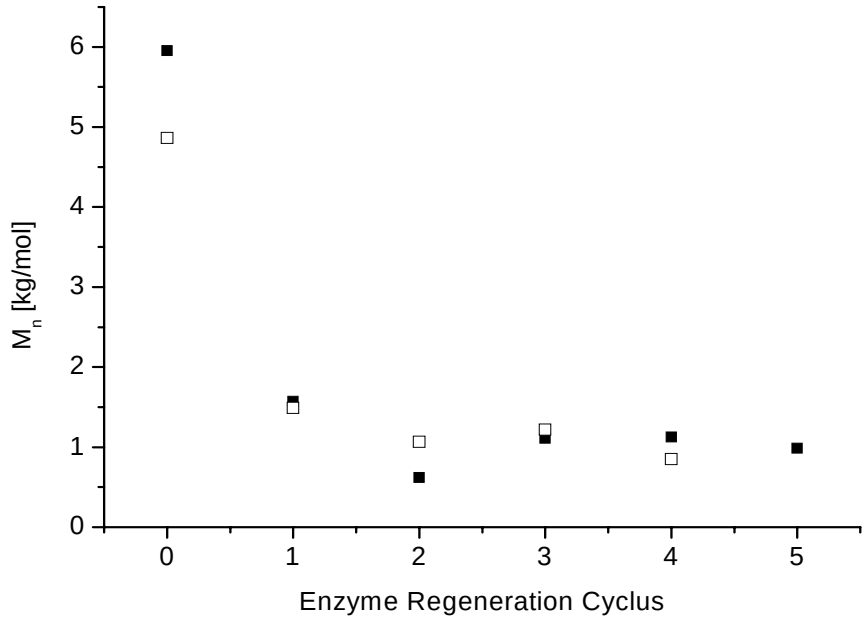

Figure 3-16: Novozyme 435 regeneration: Molecular weights by recycling cycle.

Finally, 2.7 g of new Novozyme 435 were refluxed for 24 hours with 300 ml TCM containing 1 mL methanol, which served as substitute for hydrophilic groups and water formed in the *hb*-PCL synthesis. The residue (4.7 mg) obtained after TCM evaporation was redissolved in chloroform and water prior to SDS-PAGE. While a very weak band was observed at 35 kDa in the TCM trace, the aqueous gel produced a stronger band at the same position, which corresponds to CALB. This was verified by running a solution of CALB L preparation (commercial, aqueous solution of CALB L) and size standards from 250 to 10 kD included in each gel, which were purchased from BIO-RAD (#161-0373). Additionally, a second band at 63 kDa was observed, which was not identified.[126]

In conclusion, regenerated Novozyme 435 beads are not suitable for polyester synthesis since adsorbed enzyme leaches from the Lewatit™ beads. This is caused by the hydrophilic environment generated by the increasing number of hydroxyl groups of the growing *hb*-PCL and water formed in situ.

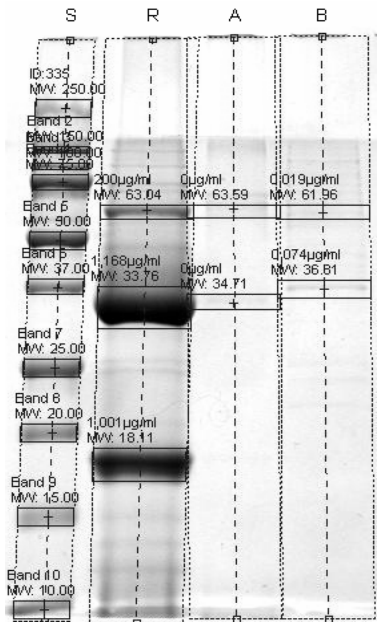

Figure 3-17: SDS-Page of the residue from refluxing Novozyme 435 in TCM containing 1 % methanol dissolved in TCM (A), in destilled water (B), a molecular weight standard (S) and CALB L preparation (R).

3.6 Preparation of hb-Poly(ε-caprolactone)s on the kg-scale

Synthesis on a larger scale is a first step to broaden experimental interest in a promising compound. Ready availability permits the use as starting material for further modifications and allows for research on blends or composites. Due to the cost of the catalyst and difficulties in catalyst regeneration, only 2% of Novozyme 435 was used (*cf.* section 3.5.1). It was chosen as compromise between achievable molecular weights and required minimal quantity of the catalyst. In Table 3-8, the results are summarized.

Table 3-8: Experimental data of *hb*-PCLs prepared in the scale-up reactor.

Copolymer	DB_f mol%	DB_p mol%	$<M_n>^1$ g·mol^{-1}	PDI^1	$<M_n>^2$ g·mol^{-1}
hb-PCL-90sc	15.0	10.0	1,600	1.8	1,300
hb-PCL-86sc	20.1	13.9	1,200	2.0	1,300
hb-PCL-78sc	30.9	21.9	800	2.3	1,300
hb-PCL-59sc	50.1	40.9	400	1.6	1,300
hb-PCL-78sc-p	21.9*	13.5	1,200	2.5	-
hb-PCL-78sc-d	21.9*	12.8	1,000	2.6	-

[1)] Det. by GPC (PS-Cal.)
[2)] Det. by VPO (TCM)
[*)] as in *hb*-PCL-78sc.

At first glance, these samples have similar molecular weights and PDI like those prepared in 5g-charges (*cf.* Table 3-3). However, work-up of the crude product implied only filtration to remove the Novozyme beads, thus no fractionation in terms of molecular weight, e.g. by washing or dialysis, occurred. Considering the 5g-charges being purified by washing, one may conclude higher synthetic efficiency in the kg-reactor, e.g. due to more effective water removal by tighter vacuum. Also distillation of CL directly prior to use could have been an asset.

According to the experiments in section 3.5.1 final DB and molecular weight were expected to be somewhat lower, compared to copolyesters that were prepared using 10 % catalyst. As shown in Figure 3-18, around 3 % less BHB is incorporated if the Novozyme 435 concentration is reduced from 10 to 2 %. Two methods of purification, precipitation and dialysis, were examined. In both cases, the $<M_n>$ increased at the expense of lower DB_p values. MALDI-TOF MS revealed a clear cut at 1 kDa for the precipitated sample (*hb*-PCL-78sc-p). Copolymers that were purified by dialysis (*hb*-PCL-78sc-d), however, had a slightly minor DB_p, but branched macromolecules of higher molecular weight were able to pass through the membrane to a certain extent. In addition, this method is only suitable for small amounts of polymer.

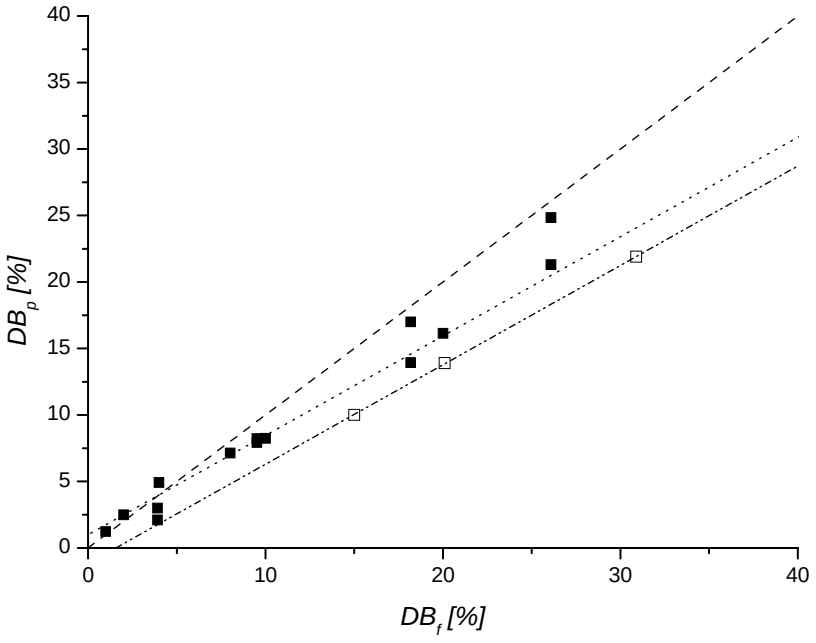

Figure 3-18: Degree of branching as determined by ^{1}H-NMR analysis correlated to the degree of branching by feed.; Dashed line - stoichiometric ratio; ■ / dotted line - 10 % catalyst; □ / dash-dotted line - 2 % catalyst.

3.7 Conclusions

In this chapter, the successful transfer of the enzyme-catalyzed hyperbranching copolymerization of CL and BHB from solution to bulk conditions was described, which allows to avoid toxic solvents and catalysts in the process. The hyperbranched samples were characterized by NMR, GPC, VPO, DSC and MALDI-TOF and compared to samples produced by solution polymerization. Insertion of BHB, and thus DB, were calculated from ^{1}H-NMR spectra.

Comparing both strategies, near stoichiometric copolymerization of BHB as branching unit was observed, though bulk conditions caused a stronger deviation at high branching ratios. Molecular weights were elucidated by VPO and by GPC applying polystyrene standard and universal calibration. In all cases, universal calibration, which is considered to provide absolute molecular weights, resulted in lower values than standard GPC calibration. VPO experiments indicated relatively low molecular weights of 1–2 kDa. Although this method is considered to provide absolute data the results are questionable in this special case. Due to the synthetic procedure and the polydisperse molecular weight distribution of these hyperbranched materials, ranging from oligomers to polymers within one single sample, VPO evaluates the lower $<M_n>$ limit rather than the overall average $<M_n>$.

Viscosity measurements were recorded by an Ubbelohde viscometer in order to confirm values obtained by GPC-online viscometry with an independent method. The data obtained by both techniques is in good agreement. Furthermore, it was observed that little branching results in a strong decrease of viscosity, which is an important asset for processing and application.

Thermal analysis provides T_g and T_m data. T_g increases from -57 °C to -49 °C where as T_m decreases from +58 °C to +27 °C the higher the feed of BHB. These effects confirm a loss in crystallinity caused by the incorporation of branching points in the linear chain.

MALDI-TOF spectroscopy was used to elucidate structural information. While long-chain branched samples have both cyclic and non cyclic species, samples with a higher degree of incorporation of BHB consist only of non cyclic, branched chains.

Reaction conditions were varied with respect to optimization for larger scale synthesis. High reaction rates were observed, thus final molecular weights are obtained after 2–5 hrs. Enhanced water removal was achieved by adding molecular sieves or applying vacuum during reaction. Novozyme 435 regeneration is not favorable in this process since the regenerated enzyme lost the major part of its original activity. Further considerations sug-

gest leaching of the active enzyme from the support in hydrophilic environments. Finally, samples produced on the kg-scale were presented. The results are compared to those obtained by synthesis in the carousel reactor (5 g per charge).

4 REKNITTING AS NOVEL ROUTE TO HYPERBRANCHED POLY(ε-CAPROLACTONE)

Recycling of polymers is a topic of current interest. To preserve primary resources, research in this field usually deals either with the combustion of plastics and composites (*thermal recycling*) or with the monomer/oligomer regeneration as secondary feedstock for a new production cycle. Recently, even recycling of synthetic, biodegradable materials has been addressed because of future limited carbon resources.

In this chapter, we introduce *reknitting* as a new concept of polymer modification. It is born by the idea of recycling and re-using polymers. In the following, reknitting is used to designate a reaction that relies on transesterification, i.e. reknitting of a linear chain structure into a hyperbranched topology (Figure 4-1). The hyperbranched polymer that acts as an additive or drug carrier is not produced from primary resources any more.

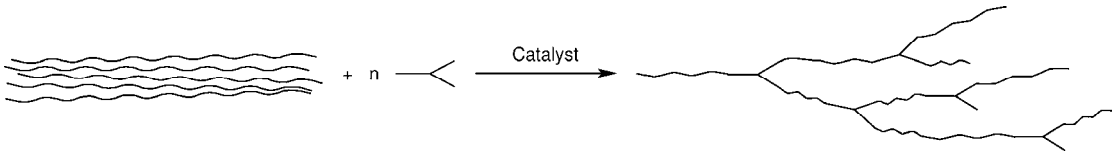

Figure 4-1: The concept of reknitting.

4.1 Preparation of *hb*-Poly(ε-caprolactone) from the Linear Analogue

In this study commercial, linear poly(ε-caprolactone) (*l*-PCL) was reknitted by modification into hyperbranched PCL (*hb*-PCL) taking advantage of the transesterification abilities of Novozyme 435. The calculated quantities of *l*-PCL and 2,2'-bis(hydroxymethyl) butyric acid (BHB) were placed into a reaction tube; Novozyme 435 and a magnetic stirring bar were added. The reaction was carried out at 80 – 90 °C under reduced pressure, to remove water formed as by-product during the reaction. After 24 hrs of reaction, the mixture was dissolved in TCM, filtered to remove the catalyst and dried. Employing this technique, isolation and purification of monomers or oligomers, which presumably affords additional energy and usually implies the use of further solvents and thus waste generation, was avoided.

4.2 Characterization

Since the materials prepared by reknitting of *l*-PCL were identical in chemical nature, they were characterized according to the description for *hb*-PCL in section 3.2.

4.3 Results and Discussion

Three sets of experiments were carried out, two of which were fed with 11.1 wt% of BHB (resulting in DB_f = 19 %) and one with 5.9 wt% BHB (resulting in DB_f = 10 %). All experiments were carried out in bulk, the reaction time ranged between 8 and 48 hrs. The experimental parameters and data obtained by analysis are summarized in Table 4-1.

Structural details were obtained from ^{1}H-NMR analysis using $CDCl_3$ as deuterated solvent (Figure 4-2). A pronounced increase of signal *a*, the methyl group of BHB, with respect to the normalized signal *d* (CL) was observed. Peak assignments and calculations of DB_p were achieved according to the expressions described for *hb*-PCL in section 3.2.1. It is an interesting observation, that none of the samples, which were fed with 11.1 % of BHB (entry 4-17), had nearly such high quantity in the final product, not even after 48 hrs. However the polymers, of which the fraction of BHB was set to 5.9 %, incorporated high amounts (up to 80 % with respect to the feed). Since the linear segments of the reknitted chain are supposed to possess sufficient length to connect to the active site of the enzyme without any difficulties, inhomogeneous mixing and diffusion of BHB in the highly viscous PCL melt, and thus reduced rates of incorporation may have caused this phenomenon.

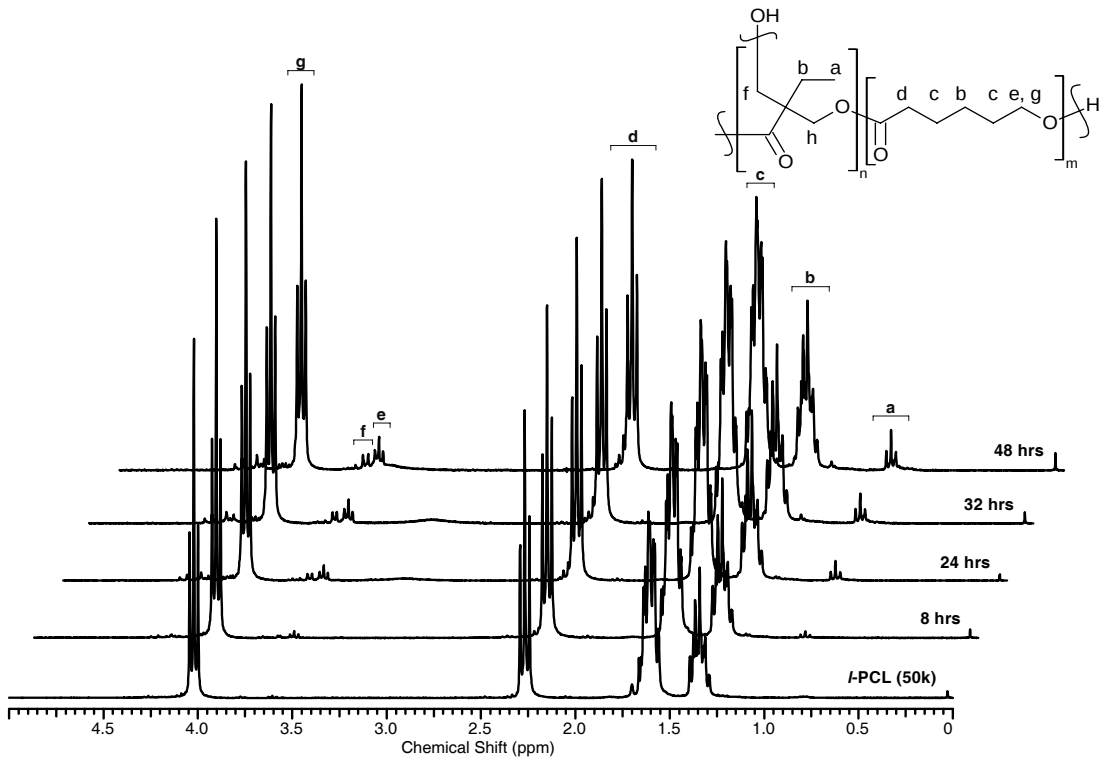

Figure 4-2: ^{1}H-NMR spectra of *l*-PCL and *hb*-PCL prepared by reknitting.

Table 4-1: Experimental data and characterization of *hb*-PCL prepared by reknitting.

Entry	Sample	Time [hrs]	DB_f [mol%]	DB_p [mol%]	T_g [°C]	T_m [°C]	M_n [1)] [g·mol^{-1}]	M_w [2)] [g·mol^{-1}]	M_n [2)] [g·mol^{-1}]	PDI[2)]	M_w [3)] [g·mol^{-1}]	M_n [3)] [g·mol^{-1}]	PDI[3)]	$[\eta]$ [3)] [cm^3·g^{-1}]	MH-K[3)]	MH-α[3)]
1	*l*-PCL (50k)	-	- Commercial -			58.0	-	100,300	62,000	1.6	40,100	19,500	2.1	132.3	2.77	0.37
3	*l*-PCL (7.2k)	24	0.0	0.0	-64.5	55.2	750.0	23,000	4,700	4.9	12,000	2,050	5.9	40.3	0.05	0.68
4	*hb*-PCL(8, 1.2)	8	19.1	1.2	n.a.	59.1	1610	63,600	9,500	6.7	32,600	3,000	10.9	71.6	0.06	0.67
5	*hb*-PCL(24, 2.9)	24	19.1	2.9	n.a.	56.5	1470	42,100	3,600	11.7	27,100	2,100	12.9	46.5	0.03	0.70
6	*hb*-PCL(30, 4.4)	30	19.1	4.4	n.a.	53.2	1370	25,800	2,200	11.7	20,500	2,100	9.8	22.6	0.08	0.58
7	*hb*-PCL(48, 5.7)	48	19.1	5.7	n.a.	52.1	1240	17,100	1,500	11.4	17,500	1,800	9.7	12.2	0.06	0.57
8	*hb*-PCL(8, 3.6)	8	19.1	3.6	-67.5	55.8	1200	102,000	10,300	9.9	63,800	1,100	58.0	85.1	0.07	0.63
9	*hb*-PCL(12, 4.5)	12	19.1	4.5	-61.5	56.5	1360	66,500	5,400	12.3	42,100	800	52.6	63.0	0.11	0.58
10	*hb*-PCL(24, 8.4)	24	19.1	8.4	-60.0	52.7	1120	15,500	2,700	5.7	12,300	1,800	6.8	16.2	0.30	0.44
11	*hb*-PCL(36, 12.0)	36	19.1	12.0	-52.6	49.4	1180	5,100	1,900	2.7	6,110	1,500	4.1	5.6	1.55	0.16
12	*hb*-PCL(48, 11.1)	48	19.1	11.1	-	49.7	1220	5,200	1,900	2.7	n.a.	n.a.	n.a.	n.a.	n.a.	n.a.
13	*hb*-PCL(8, 3.1)	8	10.6	3.1	-65.6	56.7	1250	81,600	9,000	9.1	44,400	1,100	40.4	82.0	0.07	0.65
14	*hb*-PCL(12, 4.8)	12	10.6	4.8	-63.2	55.5	1150	68,100	6,400	10.6	39,300	1,100	35.7	73.7	0.04	0.68
15	*hb*-PCL(24, 6.5)	24	10.6	6.5	-63.3	53.3	950	29,300	2,800	10.5	19,700	2,100	9.4	39.3	0.03	0.70
16	*hb*-PCL(36, 8.0)	36	10.6	8.0	-60.9	50.3	980	6,300	2,100	3.0	6,000	1,700	3.5	7.7	0.53	0.32
17	*hb*-PCL(48, 8.0)	48	10.6	8.0	-59.7	50.2	1130	6,900	2,500	2.8	n.a.	n.a.	n.a.	n.a.	n.a.	n.a.

[1)] det. by VPO (TCM, 30 °C)
[2)] det. by GPC (TCM, 30 °C, PS-calibration)
[3)] det. by GPC (TCM, 30 °C, universal calibration)
[4)] det. by solution viscometry (TCM, 30 °C)

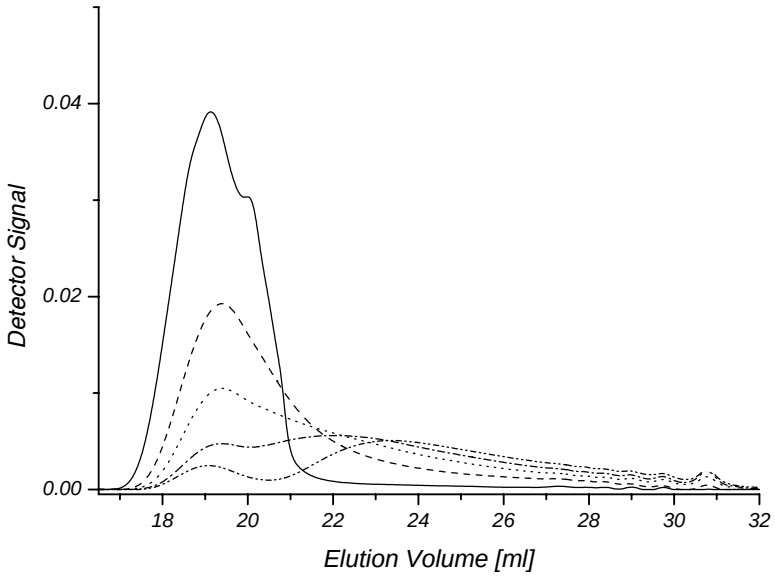

Figure 4-3: Superposition of GPC traces after 8 – 48 hrs of reaction. Straight line – *l*-PCL (CAPA 6500), dashed – 8 hrs, dotted – 24 hrs, dash-dotted – 32 hrs and dash-dot-dotted line – 48 hrs.

Molecular weights, $<M_n>$, $<M_w>$, were determined by means of GPC, employing polystyrene standard calibration and universal calibration.[107] Vapor pressure osmometry (VPO) measurements were recorded in order to investigate $<M_n>$ by a complimentary method. This effort was made because of the known difficulties in molecular weight determination for highly branched polymer samples that are in addition chemically different to the employed polystyrene standards (*cf*. section 3.2.2).[23,127]

In standard calibration mode, molecular weights steadily decreased with exposure to the active enzyme. In general, the molecular weight distribution (PDI) was broad on completion of the reaction. GPC traces showed the disappearance of the initial narrow *l*-PCL signal in favor of a broad peak that built up at higher retention time (Figure 4-3). At high elution volume even oligomers were observed, confirming the random transesterification of the enzyme in chemically indifferent environments. Similar observations were reported by Bankova et al. for the transesterification of *l*-PCL with n-Hexanol in 2002.[128]

Comparing the molecular weights ($<M_n>$) of *hb*-PCL samples that were prepared by synthesis from the comonomers (*cf*. Chapter 3) with those prepared by reknitting, compliance was observed (Figure 4-4).

Depending on the point of view, either similar molecular weights or polymers that require the same hydrodynamic volume in TCM solution were obtained. This is noteworthy since both approaches, the one “bottom-up”, the other “top-down” with respect to molecular weight yield similar material.

Universal calibration mode was used to determine absolute molecular weights.[7,107] Since viscosity detectors are different in sensitivity from refractive index detectors, a shift in molecular weights is a common phenomenon for polydisperse samples.[129] As a consequence, after short reaction times PDI was higher than it appeared in standard mode. However after 24 hours, the ratio of molecular weights determined by standard mode and universal calibration mode $M_{n,PS}$ / $M_{n,UC}$ approximated to 1.0 – 1.5 kDa and the PDI of both methods became similar.

The absolute $<M_n>$ measured by VPO was in the range of 1.7 – 1.0 kDa (Figure 4-5). Only little dependency on the DB was observed. Since VPO is a colligative method, molecular weights are rather underestimated, because traces of solvent or oligomers will have a strong effect on molecular weights measured. In this case, VPO data expresses rather the $<M_n>$ of those oligomers that were not removed by the washing process during work-up.

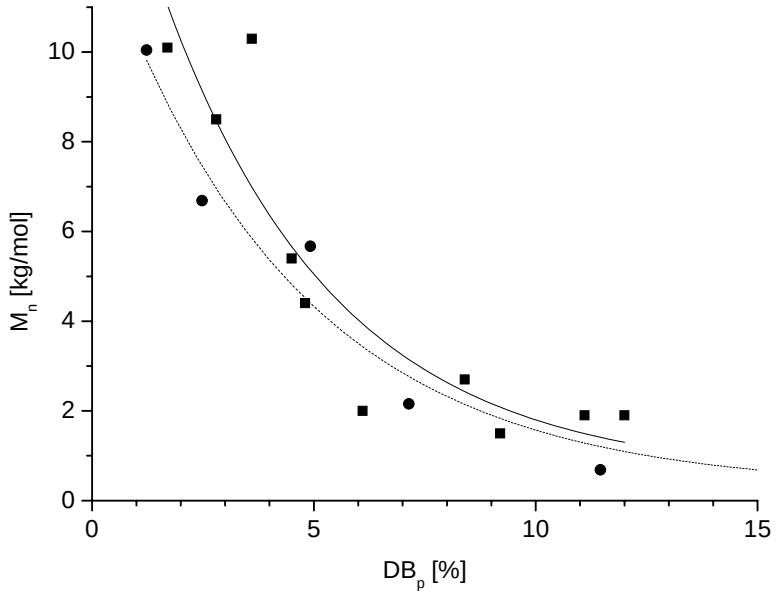

Figure 4-4: M_n (PS-GPC) of *hb*-PCL: straight line - prepared by monomer synthesis (*cf.* Chapter 3), dashed line by Reknitting of CAPA 6500.

In agreement with the considerations and results of section 3.2.2 and 3.4.2, it is recommended to accept GPC values obtained by polystyrene standard calibration as common reference to other materials, but to consider data obtained by universal calibration to reflect absolute molecular weights. Again, it should be noted that the molecular weight of samples with higher polydispersity index is generally underestimated when universal calibration is applied.[112] However, the higher the molecular weight the more

overestimated are linear aliphatic polyesters by conventional GPC.[130] Considering both effects and the experimental data obtained by measurements of high-MW *l*-PCL, overestimation of the polyesters apparently dominates underestimation because of the *hb* structure in the present study (Figure 4-5).[131]

Since fragmentation of linear polymers by enzymes, in analogy to biodegradation, is a random process, insertion of BHB is also supposed to be random. Thus, final molecular weights are likely to depend only on the time of exposure to the enzyme (Figure 4-3). To obtain more information on these hypotheses, fractionation of sample *hb*-PCL (36, 12.0) (Table 4-1, entry 11) by preparative GPC was carried out. Besides quantification of yield per fraction, the DB of all fractions was determined by ^{1}H-NMR. In addition, GPC traces were recorded by analytical GPC and MALDI-TOF MS experiments were carried out to obtain information on the composition of the respective fractions (*cf*. Appendix A.1).

Since the weight distribution of the fractions was in good agreement with the trace recorded in the preparative GPC experiment, the fractionated material was expected to be present in fraction 14 – 50 out of 60 slices taken (Figure 4-6, bottom graph). GPC analysis of all fractions within this range resulted in a linear log M versus t (equals number of fraction or V_{el}) relationship between fraction 14 and fraction 44. Samples beyond fraction 44 were considered to represent low molecular weight impurities washed out by the eluent (Figure 4-6, upper graph). This was confirmed by running a sample of pure toluene that eluted from the column at the same V_{el}.

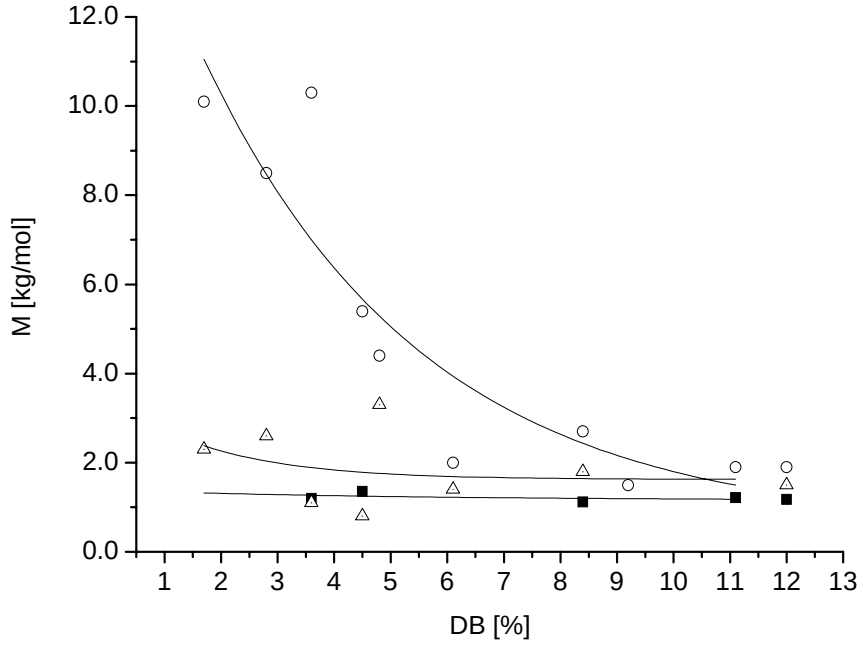

Figure 4-5: M_n determined by GPC (PS- and universal calibration, TCM) and VPO (TCM); ■ <M_n> (VPO), ○ <M_n> (GPC PS-Cal), Δ (GPC Uni-Cal).

GPC analysis of fraction 14-44 resulted in $<M_w>/<M_n>$ between 39/35 kDa and 400/300 Da (Figure 4-6, upper graph). The PDI was in the range of 1.1 – 1.3 for each fraction (Figure 4-6, middle). The maximum of the PGPC trace was collected between fraction 27 to 33, which corresponds to $<M_w>$ = 5.3 to 2.3 kDa and $<M_n>$ = 4.5 to 2.0 kDa. $<M_p>$ was around 4.0 kDa (fraction 29).

The DB calculated from ^{1}H-NMR analysis was in the range of 12 to 25 %. It increased with higher elution volume or lower average molecular weight of the fraction respectively, but it was always equal or higher than the DB of the corresponding, non-fractionated sample ($DB_{hb\text{-}PCL(36,12.0)}$ =12 %). This is an obscure result and not yet understood since the DB of both high and low molecular weight fractions is higher than the overall, average DB calculated from the sample as obtained after synthesis.

MALDI-TOF MS is an important technique to obtain information of a polymer's composition. In general, molecular weight distributions should not be determined by MALDI-TOF because of mass discrimination effects, which lead to underestimation of very low- and very high-MW species even for narrow-disperse samples on the one hand, on the other hand equal detection with respect to molecular weight or type is not assured. [132,133]

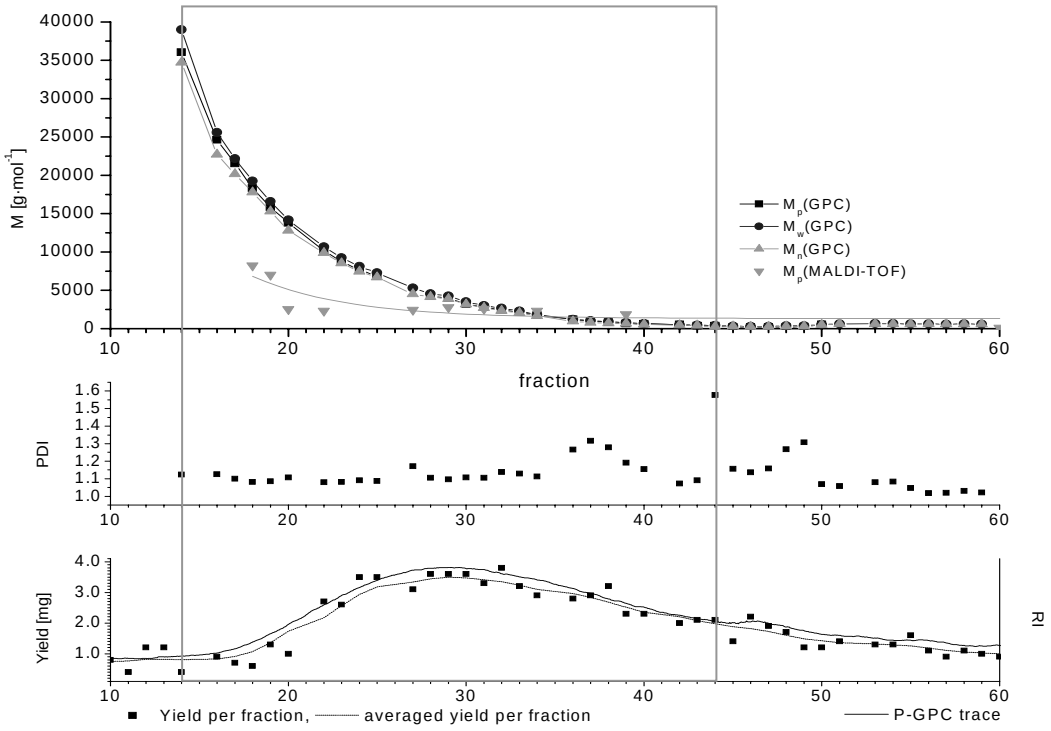

Figure 4-6: Fractionation of *hb*-PCL(36, 12.0). Upper graph: Molecular weights of the fractions obtained by GPC and MALDI-TOF; Middle: PDI of the fractions;
Bottom graph: dots / dotted line – Yield per fraction, solid line – RI signal from preparative GPC.

However, the maximum peak position (<M_p>) can be determined for samples, in which the polydispersity is sufficiently low[114].

Due to the inherent molecular weight distribution of hyperbranched samples no information on <M_p> was extracted, but the repeating unit of 114.18 Da was confirmed. In case of the fractionated sample our findings were different (Figure 4-6, upper part). Since most of the fractions were monodisperse (PDI ≤ 1.2), <M_p> was calculated for each fraction. The <M_p> values obtained by MALDI –TOF MS were considerably lower than those obtained by GPC employing PS standard calibration. Comparing data Table 3-5, in which universal GPC and standard calibration data of not fractionated samples were compared, MALDI-TOF MS and UC-GPC experiments seem to yield similar <M_p> values for a given polymer.[134] All these results were confirmed by a second run of the same sample, in which first fractionation and then analysis were repeated.

Solution properties of the non-fractionated samples were recorded by online viscosity measurements that were calculated by an iterative approach. In the case of some samples a necessary minimal signal to noise ratio was not given to produce these values. As observed earlier, hyperbranched samples possess distinctively lower viscosities than their linear analogues, which was attributed to their inherent broad molecular weight distribution.[80] At DB_p = 5 – 10 %, the intrinsic viscosity was reduced to 10 % of the value of the original, linear sample (CAPA 6500™). This result was achieved after 24 hours of reaction.

Since molecular weights were known from universal calibration mode, the Huggins coefficient *K* and the form factor α were obtained by transformation of the Mark-Houwink-Sakurada Equation.[135]

$$\eta = K \cdot M^{\alpha} \qquad \textbf{(4-1)}$$

The Huggins coefficient *K* describes the extent of binary polymer solvent interactions. It usually depends on the polymer structure and molecular weight. The lower the values of *K*, the stronger are the polymer-solvent interactions.[136] In the presented experiments no distinct correlation between DB, molecular weight and *K* was observed, but *K* was significantly lower for all the branched samples compared to *l*-PCL (50kDa).

The form factor α varied between 0.55 - 0.75 for moderately branched samples (DB ≤ 10 %). This was remarkably higher than the value for *l*-PCL (50kDa) (α=0.37). Highly branched samples had α values of 0.1 – 0.3. In conclusion, TCM is a better solvent

for *hb*-PCLs with DB ≤ 10 % than for *l*-PCL (50kDa). Highly branched samples form rather dense globular spheres.

Comparing the results obtained for [η], *K* and α in the case of *l*-PCL (50kDa) and *hb*-PCL, not only the shape of the molecule should be taken into account. The commercial *l*-PCL (50kDa) sample we used had narrow polydispersity, but considerably higher molecular weight compared to the *hb* samples.

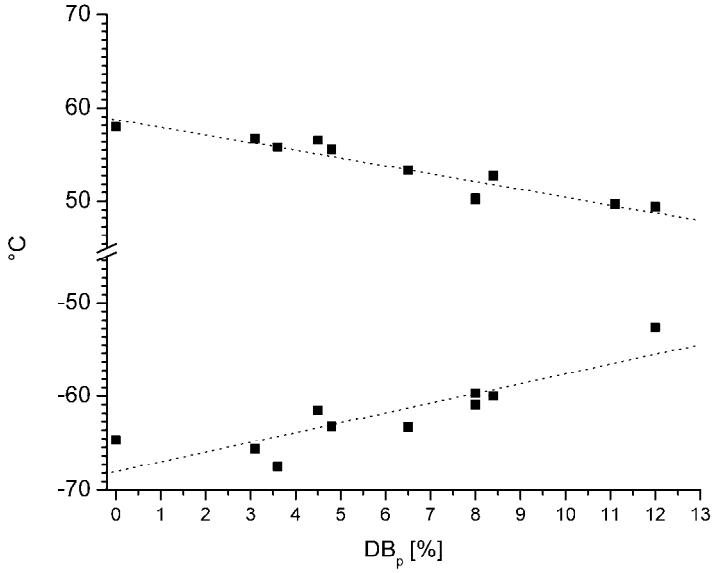

Figure 4-7: T_g, T_m plotted against the DB_p.

Therefore, another sample of *l*-PCL (7.2kDa) of lower molecular weight but broad PDI similar to the hyperbranched samples was synthesized by enzymatic catalysis to estimate the influence of molecular weight and polydispersity. As expected, [η] was considerably lower than for *l*-PCL (50k) and the Huggins-Parameter *K* was similar to that of the hyper-branched samples. The form factor α was also similar to samples of the reknitting experiments after short reaction times. This indicates that the Huggins coefficient *K* depends strongly on the size and functionality of the polymer, while α mainly depends on the size, or the length of the linear segments, respectively.

Thermal properties are of great importance to evaluate potential application and limitations. DSC diagrams of the *hb*-PCL samples showed a characteristic double endotherm, of which the more intensive upper part was recognized to be the melting peak (*cf*. Figure 3-13).[80] As discussed there (section 3.4.2), this phenomenon is caused by irregular crystallites, the formation of which is promoted with increasing DB of the sample. Since the DB directly correlates to the statistical length of the linear, crystalline

segments, the DB has strong influence on thermal properties.[80] As shown in Figure 4-7 a linear correlation of T_m with respect to DB_p is observed.

In addition, T_g was observed for all samples. In contrast to T_m, T_g increased with increasing DB, which indicates i) the mobility of the linear segments being hindered and ii) the increasing polarity of the macromolecule with increasing density of the branching points.[27]

4.4 Conclusions

Reknitting, i.e., transesterification of linear polymers as a novel route to hyperbranched materials has been introduced. As proof of evidence, modification of *l*-PCL into *hb*-PCL was investigated using BHB as AB_2 branching monomer and Novozyme 435 as catalyst under bulk conditions. The resulting samples were characterized by ^{1}H-NMR, GPC, VPO, MALDI-TOF and DSC and compared to the original and to *hb* samples prepared from copolymerization of CL and BHB (*cf*. Chapter 3).

GPC was used to monitor the change in molecular weight and molecular weight distribution. Comparing samples prepared by reknitting, which is a *top-down* approach in terms of molecular weight development, to those prepared by copolymerization of the respective comonomers, referred to as *bottom-up* approach, both of them are characterized by a similar M_n/DB relationship. This proves that final molecular weights are not limited by the topology of the active site of Novozyme 435. Moreover, molecular weights apparently depend on DB.

Separation of one sample (*hb*-PCL(36, 12.0)) by preparative GPC results in monodisperse fractions that were characterized by ^{1}H-NMR, (analytical) GPC and MALDI-TOF. DB calculated from ^{1}H-NMR analysis was in the range of 12 to 25 %, which was always higher than the DB of the original sample and still lacks explanation. Since the fractionated samples were monodisperse, it was possible to collect information on M_p by MALDI-TOF. M_p values were considerably lower than GPC data calculated in standard mode. Although universal calibration (UC) was not available at this time, indirect comparison using UC-GPC data of comparable, non-fractionated *hb*-PCLs led to the conclusion that UC-GPC and MALDI-TOF yield similar M_p values.

DSC measurements were carried out to obtain information on the thermal properties. A linear correlation of T_m, T_g with DB was observed. The decrease of T_m with increasing DB indicates a loss of crystallinity on the incorporation of branching points into the (previ-

ously) linear chains. However, the mobility of the linear segments is hindered, thus T_g increases with higher DB.

Finally, solution properties were recorded by online viscosity measurements (of the not fractionated samples). A DB of 5-10 % induced a drop of the intrinsic viscosity to 10 % of that of the parent sample (CAPA 6500^{TM}). Hence, highly branched samples possess considerably lower intrinsic viscosities than their linear analogues. The Huggins-Parameter *K* and the form factor α have also been calculated. *K* was remarkably lower compared to *l*-PCL. The form factor α suggests a dense globular shape of the *hb* molecule in TCM solution.

5 STRUCTURED POLYMER NETWORKS

5.1 Introduction

Polymer networks are interesting structures, in which linear polymer segments are interconnected at both ends.[137] The central process in network preparation is cross-linking. The materials' properties are determined by the choice of precursor, the adjusted cross-linking density of the network formed and eventual fillers and additives.[138] Usually, not the chain ends but pendent functional groups of a polymer backbone are interconnected. These networks are often classified by their purpose, the major representatives include vulcanized rubbers, thermosetting materials, adhesives, polymeric sorbents and electronic materials. Peculiarities of polymer networks in comparison to not cross-linked polymers are dimensional, thermal, physical and chemical stability.

Reaction between functional groups of the precursor and the cross-linker initially forms small branched ensembles. Subsequently, cross-linked network structures are formed. Like conversion, molar mass and polydispersity (PDI) increase up to a critical state. The gel point is reached, when the largest molecules become "infinite" (gel) while soluble molecules (sol) are still available.[139]

One recent concept for the development of ultra low-shrinkage dental materials is based on the use of hyperbranched or dendritic monomers.[140] Their compact structure and high number of functional groups render them interesting candidates for dental applications in general. But also in other medical discipline, applications, e.g., as a high-loading, biodegradable cross-linked drug carrier or as carrier for MRI or X-ray opaque contrast agents are discussed. Adhesives are another promising field for hyperbranched aliphatic polymers: low T_g and high functionality are perfect prerequisites for high tack.

Poly-(2-hydroxyethyl methacrylate) (PHEMA) has been used in biomedical application for a while, e.g. for soft contact lenses, as bone substitutes or to immobilize proteins or cells.[141,142] The hydroxyethyl pending species of the polar polymer confers a high hydrophilicity, good biocompatibility and can be used - after chemical modification or grafting - to complex various types of molecules or ions.[143,144] Networks made of PHEMA and *hb*-PCL are expected to retain both hydrophilic and hydrophobic drugs. Diffusion, but mainly biodegradation of the *hb*-PCL structure will determine the drug release rate.

In this chapter, ways to create partially methacrylated *hb*-PCLs are described. In section 5.3, 2-hydroxyethyl methacrylate (HEMA) is mixed with these polar *hb* precursors.

The binary mixtures are cross-linked by UV irradiation to form polymer networks, which are characterized with respect to swelling behavior, mechanical and thermal properties.

5.2 Methacrylation of *hb*-PCL

A simple and fast way to prepare polymer networks is cross-linking by UV-curing of double bonds. Usually only seconds to a minute of exposure to a strong UV-source are required. The main benefit lies in the application at the site, on which the network is required. For this reason, dentistry was one of the major fields, in which this technique was widely employed since the 1980s.[145]

In our efforts to create partially methacrylated *hb*-PCLs three different routes were examined with respect to i) efficiency, ii) convenience, iii) green and acceptable chemistry from a medical point of view (Figure 5-1). *Hb*-PCL-22 was used as starting material.

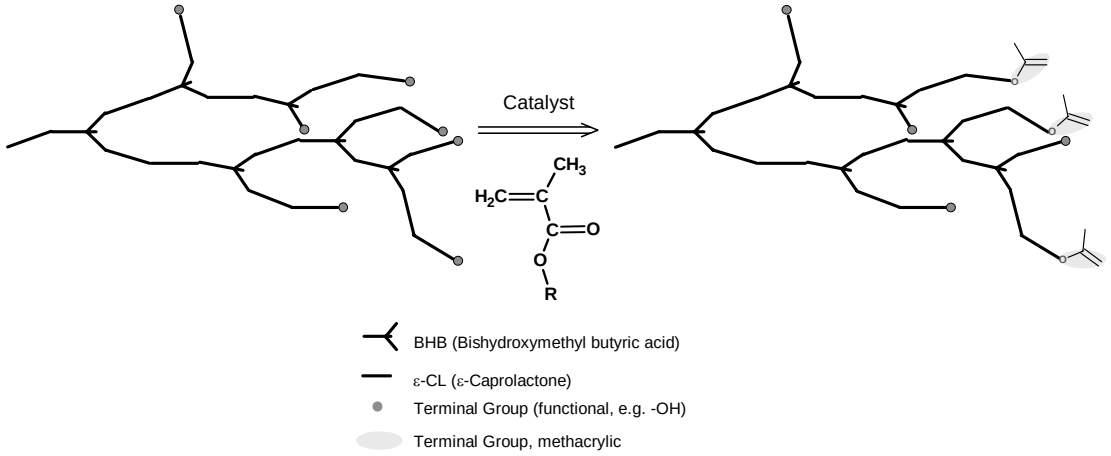

Figure 5-1: Schematic of methacrylation of *hb*-PCL.

Methacrylic chloride (MACL) / NEt_3 is often used to methacrylate alcohols since handling is rather simple. THF was used as solvent. Another approach that was expected to be useful in sample preparation was methacrylic acid in dry toluene, to which a Hafnium catalyst ($HfCl_4 \cdot 2$ THF) was added. Representative data of samples that were prepared in these ways are listed in Table 5–1.

To achieve a high degree of functionalization, a 1.25 to 5 fold excess of the acid compound was added. Regarding entry 1-4, yields were usually high. The functionalization, correlated to the initial number of available hydroxyl groups, was around 21 %, no matter what excess of the acid compound was used. Apparently, conversion is limited by structural parameters and diffusion.

In entry 5–7, results obtained for the methacrylation of *hb*-PCL-22 using methacrylic acid (MAOH) that was added to a stirred solution of *hb*-PCL-22 in dry toluene, are listed.

$HfCl_4 \cdot 2$ THF is a catalyst, which is known to promote esterification but does "not catalyze the transesterification at all".[146] Results were not consistent, and especially Dean-Stark conditions, which are supposed to increase the yield of condensation reactions by azeotropic distillation of water that is formed *in situ*, did not show any methacrylation at all. We tentatively explain this by the quantitative removal of methacrylic acid with the water.

A number of methacrylation reactions, which are catalyzed by Novozyme 435, are described in literature.[147-150] In particular, a patent,[151] in which the esterification of polyoxyalkylenes is described, gave guidance for the development of a route to methacrylated *hb*-PCL-22 using Novozyme 435. In this method butyl methacrylate (BUMA) was employed, which was transesterified by Novozyme 435. The byproduct, n-butanol, was removed by vacuum distillation. High conversion is reported for this process.

In Table 5-2 the initial experiments (2-10g/charge) are described in entry 1-4. Entries 5-7 describe samples that were prepared in 50 g per charge. Since the reaction was carried out in bulk and Novozyme 435 was again used as catalyst, no new material, such as a toxic heavy metal catalyst, that would later be found as a trace in the product were added. Finally this approach was selected for further esterification towards network precursors.

An average functionalization of 25–30 % with respect to the number of hydroxyl groups in the *hb*-PCL was achieved. In this case, yields did not relate to true conversion, since residual BUMA, which was not completely removed by work-up, also contributed. BUMA removal turned out to be a challenge which we overcame only lately in the 50g charges. Because of its high boiling point, vacuum distillation off the product did not succeed.

Table 5-1: Methacrylated *hb*-PCL-22 using MACl / NEt_3 (X=Cl or MAOH / $HfCl_4 \cdot 2$ THF (X=OH.

Entry	MA-X mol%	Yield %	reaction time / hrs	DB	x(MA)[1)] %	f[1,2)] %
1	125	70	15	21.9	7.5	94.3[5)]
2	125	31	25	16.4	1.2	21.4
3	500	83	15	-[3)]	-	-
4	500		25	17.5	1.3	21.7
5	100		15	22.8	4.0	47.3
6	170	3	15	7.9	0.2	8.2
7[4)]	300	26	15	8.5	0	0

[1)] correlated to the number of OH-groups.
[2)] functionalization.
[3)] crosslinked, no characterization done.
[4)] Dean-Stark conditions.
[5)] excess of MACl in product.

Table 5-2: Methacrylated *hb*-PCL-22 using BUMA / Novozyme 435 catalysis.

Entry	Sample	Starting material	BUMA mol%	Yield %	DB %	x(MA)[1)] %	f[1,2)] %
1		*hb*-PCL-22	110	110*	36.4	4.7	25.5
2		*hb*-PCL-22	110	91	28.4	2.9	24.2
3		*hb*-PCL-22	500	109*	36.8	6.2	33.1
4		*hb*-PCL-22	500	143*	36.4	5.6	30.2
5		*hb*-PCL-22	430		58.6	22.5	37.4
5a		*hb*-PCL-22	420	85	31.3	6.8	48.6
5b	*hb*-PCL-22MA	*hb*-PCL-22	420	69	38.5	6.6	31.9
6	*hb*-PCL-14MA	*hb*-PCL-14	420	83.9	31.4	3.6	25.6
7a		*hb*-PCL-42	420	-[3)]	39	5.8	27.6
7b	*hb*-PCL-42MA	*hb*-PCL-42	420	78.1	41	2.1	8.8

[1)] with respect to the number of hydroxyl groups of *hb*-PCL-22
[2)] functionalization
[3)] crosslinked during work-up
*) excess because of residual butyl methacrylate

1 g of the crude product (entry 5) was dialyzed in TCM for 2 days in order to remove residual BUMA. Around 20 % of weight loss (entry 5a) were recorded, which was ascribed to the loss of free BUMA, but also to the loss of a low MW fraction of *hb*- PCL-22. A functionalization of 49 % was calculated from ^{1}H-NMR spectra (Figure 5-2).

Since dialysis is not adaptable to larger amounts of product, an alternative method to purify methacrylated *hb*-PCL was sought. Precipitation from TCM solution into cold methanol did not succeed, because colloidal precipitates were formed. Finally, solubility experiments led to an efficient procedure: Both the crude product (entry 5) and BUMA dissolve in diethyl ether but only BUMA also dissolves in n-pentane. Hence, batch samples (entry 5–7) were dissolved in ether, and BUMA was washed out by repeated shaking of the solution with n-pentane for 2 hours in an extraction funnel.

The purified products (entry 5b–7b) had a light yellowish color. The functionalization was between 9 and 32 % with respect of the total number of hydroxyl groups in the starting material. Yields of 69–84 % were observed. 2,6-Di-tert-butyl-4-methylphenol (BHT) was added to the purified product immediately after washing in order to avoid spontaneous polymerization.

^{1}H-NMR spectra were recorded in order to obtain structural evidence. A typical spectrum is shown in Figure 5-2. Compared to figure 3-1, the new signals of the methacrylic ester were clearly identified. The singlets at δ = 6.07 and 5.52 ppm were ascribed to the vinyl protons (m,k), as well as δ = 1.91 ppm to the vinylic methyl group (j). At δ = 5.4–4.8 ppm,

a broad signal of terminal hydroxyl groups was observed. All other signals were related to the *hb*-PCL molecule and described in section 3.2.1. The integrals of signal m,k or j/3 and a, d were used to calculate the degree of functionalization:

$$f = \frac{\frac{1}{2}\left(I(k) + I(m)\right)}{x(BHB)} = \frac{\frac{1}{2}\left(I(k) + I(m)\right)}{\frac{I(a)/3}{I(d)/2}} \qquad \textbf{(5-1)}$$

Surprisingly, the observed DB was higher than in the starting material. Taking into account that not only terminal (T, T_L), but also linear-dendritic hydroxyl groups (L) of the branching unit were esterified, a formal increase of DB is acceptable and thus explained by the expressions used for the calculation of DB (*cf.* section 1.5) that do not distinguish between functionalized terminal units and actual branching points.

Since *hb*-PCL-MA exhibits a high tendency to cross-link at ambient conditions, BHT was added as an inhibitor. Auto-initiated polymerization of *hb*-PCL-42MA, to which no BHT was added, was observed on solvent evaporation during post reaction work-up. Therefore no GPC chromatograms were recorded given that separation of BHT from the macro-monomer in the columns bears a high risk of spontaneous polymerization.

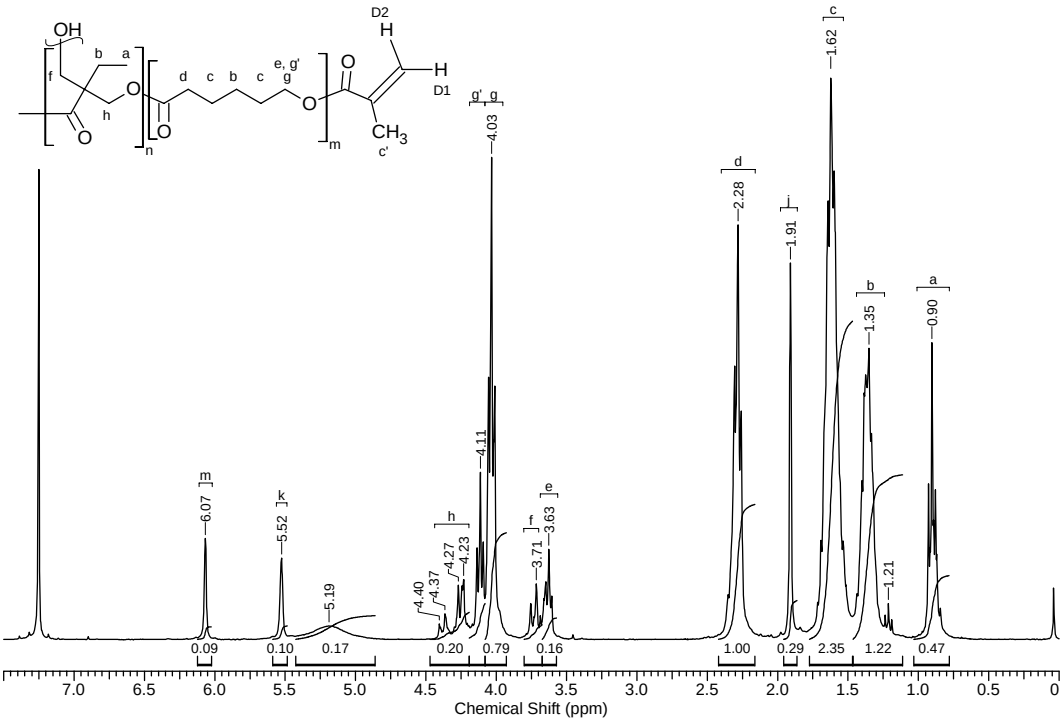

Figure 5-2: ^{1}H-NMR of *hb*-PCL-22MA (DB = 22 %, f(MA) = 32 %).

5.3 UV-Curing / Networks

Cross-linking by UV irradiation is a reaction that usually requires only some tens of seconds. Industrial curing stations are widely adapted in size and power according to the need of production. Easy integration in continuous processes, e.g. a production chain is another advantage. Only the curing of thick layers may cause difficulties because of heat dissipation, which induces irregular material flow in the polymerization process.

In the present study, mixtures of methacrylated *hb*-PCL and HEMA in various compositions were cured in mold forms to produce several types of test specimens for mechanical testing.[152] Cured bars and disks, which were 4-5 mm in height, had mostly an uneven surface due to convection caused by heat dissipation in the curing process. Therefore, 5 x 5 cm^2 plates ($d \approx 1$ mm) were cast, which had an even surface. They were heated to their glass transition temperature and specimens for the subsequently described mechanical testing were produced using stamps. In Table 5-3 the main parameters of these experiments are summarized.

All networks were analyzed with respect to their thermo-mechanical properties (DSC, torsion DMA, tensile test) and the extent of swelling in water and toluene. The data obtained from the measurements are summarized in Table 5-4, swelling experiments are collected in Table 5-5.

Table 5-3: Crosslinking experiments by UV curing - experimental parameter. Nomenclature NW-xx-yy ; xx = DB of *hb*-PCL, yy = fraction of *hb*-PCL in the network.

sample	linear precursor	hyperbranched precursor	amount *hb*-PCL wt%
PHEMA	HEMA	-	0
NW-14-20	HEMA	*hb*-PCL-14MA	21
NW-14-40	HEMA	*hb*-PCL-14MA	40
NW-14-60	HEMA	*hb*-PCL-14MA	60
NW-22-20	HEMA	*hb*-PCL-22MA	21
NW-22-40	HEMA	*hb*-PCL-22MA	40
NW-22-60	HEMA	*hb*-PCL-22MA	60
NW-41-20	HEMA	*hb*-PCL-41MA	21
NW-41-40	HEMA	*hb*-PCL-41MA	40
NW-41-60	HEMA	*hb*-PCL-41MA	60

Table 5-4: Summary of thermal analysis and mechanical testing of networks prepared by UV curing. (data of *l*-PCL were kindly provided by M. Ursu.)

Sample	T_g (DSC) °C	T_g (DMA) °C	E_a kJ/mol	<E> MPa	σ_y MPa	ε_y MPa	$<\sigma_y>$ MPa	L_B [1] %	G' (20°C) MPa	G' (@ Tg) MPa
l-PCL	-55	-49.8	-	267	9.2	-	15.9	4.9	-	-
PHEMA	86.9[2]	118	n.d.	1075	B	B	20.5	1.0	1020	1.5
NW-14-20	75.0	100	156	B	B	B	B	B	600	2
NW-14-40	n.d.	85	174	128	4.9	0.04	4.8	1.6	180	0.7
NW-14-60	n.d.	68	155	44	1.6	0.04	4.1	2.2	58	0.6
NW-22-20	67.2	78	175	B	B	B	B	B	750	.25
NW-22-40	70.3	76	230	329	9.9	0.03	11.6	1.7	280	1.8
NW-22-60	27.8	40	143	14	0.7	0.05	3.8	2.2	50	0.9
NW-41-20	n.d.	82	174	B	B	B	B	B	900	0.47
NW-41-40	n.d.	67	152	286	7.3	0.03	8.5	2.3	250	0.76
NW-41-60	≈ 35	41	105	3	0.2	0.06	2.4	4.0	20	1

[1] elongation at break: $L_B = (L-L_0) / L_0$
[2] T_m (DSC) = 127.7 °C, T_m (DMA) = 118 °C
B = brittle failure; n.d. = not determined.

5.4 Dynamic Mechanical Testing and Tensile Tests

Dynamic Mechanical Analysis (DMA) is one of the methods most often used in polymer characterization because of its sensitivity to determine T_g, which is about 100 times higher than that of DSC. In DMA measurements, the viscoelastic behavior of the sample is examined as a function of frequency and temperature. The measurements are carried out in the linear viscoelastic region, i.e. the test specimens are not destroyed. A sinusoidal mechanical strain is induced and the materials' resulting stress is recorded. Analysis of the test specimen's response provides information on molecular mobility reflected by i) the storage modulus G' – energy that is reversibly stored during deformation, ii) the loss modulus G", which offers information on the extent of energy irreversibly dissipated into heat during deformation, and iii) the loss factor tan δ, which is defined by the phase shift:

$$tan\,\delta = \frac{G''}{G'} \qquad \textbf{(5-2)}$$

A temperature scan at constant frequency over a wide temperature range allows for determination of T_g, which is verified by variation of the frequency at various temperatures. These curves, obtained at several temperatures, are fitted into one single master-curve

employing the principle of time-temperature superposition, i.e. the WLF equation (William, Landel & Ferry).[153]

T_g is an important parameter of a polymer network since its properties change dramatically. As indicated, it is determined by the freezing of the motion of longer chain segments, thus is dependent on the cross-link density. Below T_g, the storage modulus (G') is high, the polymer is hard and brittle. If the working temperature is higher than T_g, G' decreases while the loss factor (tan δ) increases. *tan* δ = G"/G' reaches a maximum at T_g. Above T_g G' levels out on a plateau, which is an indication for a physical network. In Figure 5-3 an exemplified graph is depicted.

Figure 5-4 shows the dependence of T_g as a function of the weight fraction of *hb*-PCL-MA. The more the fraction of the *hb* precursor in the polymer network increases the more the T_g is lowered. *Hb*-PCL-MA was expected to have an even lower T_g than *hb*-PCL since the number of hydrogen bonds is reduced. However, this was not detected due to experimental difficulties.[154] Finally, in copolymerizations of a low-T_g and a high-T_g monomer, T_g was expected to depend highly on the ratio of both comonomers.

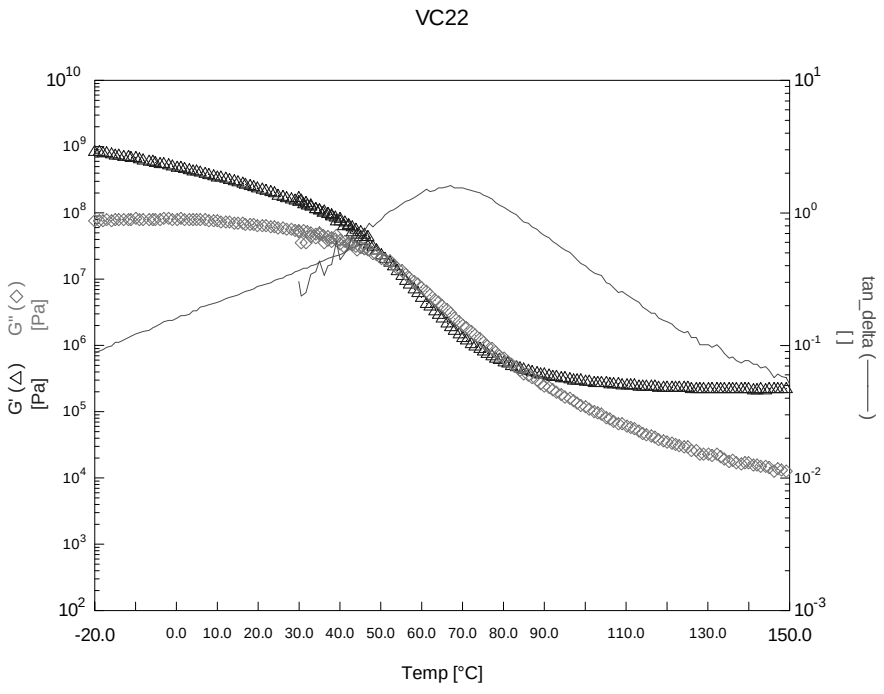

Figure 5-3: Shear storage modulus G', shear loss modulus G'' and tan δ against temperature for NW-41-40. The curves were obtained by combining data obtained in the analysis of dynamic torque of bars (left side) and disks (right side).

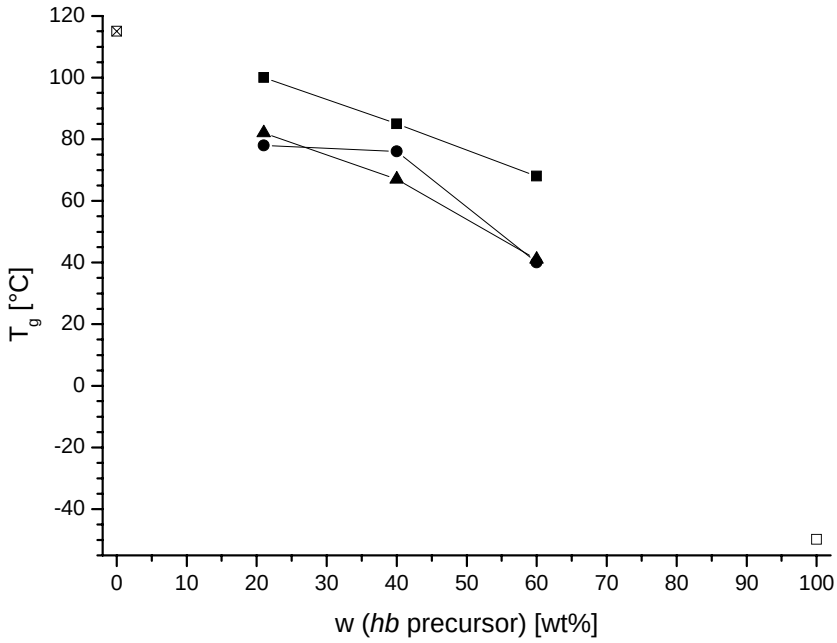

Figure 5-4: Polymer networks - T_g detected by torsion DMA plotted against the weight fraction of the cross-linking precursor. ■ NW-14-xx, ▲ NW-22-xx, ● NW-41-xx, □ *l*-PCL, ☒ PHEMA.

Comparing the T_g values obtained by DSC and DMA measurements, the latter appeared shifted about 7-10 K to higher temperatures. In both methods, T_g is a function of the experimental conditions. While T_g is affected by the thermal history in DSC, it depends on the radian frequency ω in DMA. However, T_g values obtained by DSC and DMA are supposed to be proportional and can be anticipated, once the correlating factor is determined. Some of the samples showed irregular behavior with respect to the T_g correlation between DSC and DMA values, which cannot be explained yet.

Young's modulus, <E>, is another important parameter in characterization of the mechanical properties of polymers. It was obtained by tensile tests, in which the sample stiffness is measured. Young's modulus is defined as the stress per unit area divided by the strain resulting from the applied force.

$$<E> = \frac{\sigma_y}{\varepsilon_y} \qquad \textbf{(5-3)}$$

Therefore it is a measure of the material's resistance to deformation, the higher the modulus the more rigid the material is. It is noteworthy that the definition given in eq. 5-3 for Young's modulus does not take time of applied stress into account. For materials that exhibit time-invariant deformation, e.g. metals and ceramics at room temperature, any measurement of strain will lead to a constant value of modulus. However for materials that

exhibit time-dependent deformation, such as polymers, the quoted modulus is only valid for instant, short-time deformation. Prolonged deformation results in creep.

Tensile test diagrams were recorded at 20 °C and varied according to section 10.3. The diagram of NW41-40, which is a viscoelastic sample, is shown in Figure 5-5. Four characteristic regions were observed: Near A, at little deformation, bending occurs fully elastic (A→B). Young's modulus is obtained by the calculation of the tangent at zero deformation.

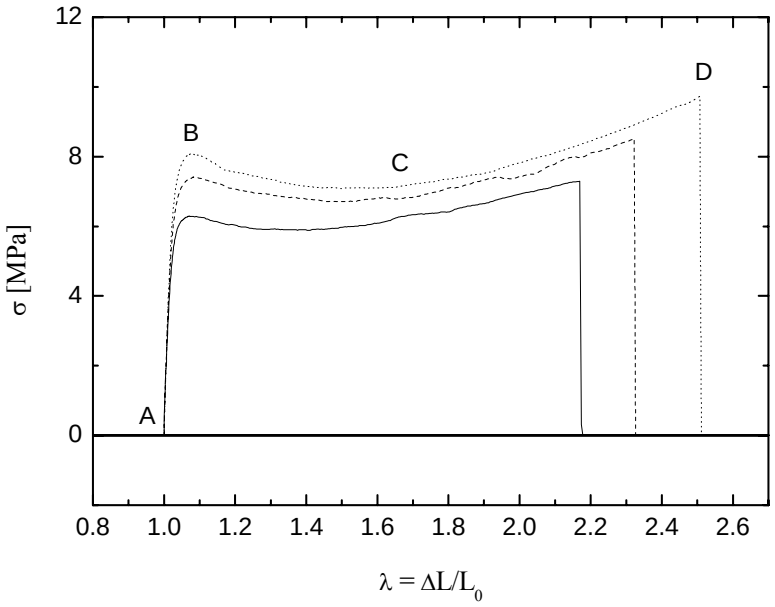

Figure 5-5: Load-extension curves of NW41-40, 3rd run recorded at 20 °C.

B is called the yield point. If the extension exceeds the yield point, irreversible elongation – yielding – occurs. This phenomenon is marked by stress softening, also referred to as cold flow (B→C) and shear hardening (C→D). Finally the sample fails in λ = D.

Of course, as shown in section 10.3, only few samples, in which the quantity of *hb* precursor was high (w = 60 wt%), exhibited this behavior. The other samples were dominated by high stiffness (w = 20 wt%) or little elasticity (w = 40wt %), since T_g was clearly above room temperature.

Since a copolymer's stiffness is a function of contributions of its components, the ratio of both comonomers, in consideration of <E> of their homopolymers, may produce a reasonable guess. A similar relationship is expected for the type of polymer network discussed in this study. In all the three samples, <E> was not obtained for w = 20 % because the test specimens showed brittle failure. However, the two experimental points of network varying only in the weight fraction, but not in the type of *hb* precursor, were extended to a linear fit to w = 0 % (Figure 5-6).

In the case of w = 60 % of any *hb* precursor, Young's modulus was in the range of 3-50 MPa, which is low and similar to the stiffness of silicon rubber. At w = 40 %, NW-14 differed distinctively from NW-22 and NW-41. The modulus of the NW-22 fell nicely on a straight line drawn between NW-14-60 and *l*-PCL, which indicates the dominance of the *hb*-PCL structure in the network.

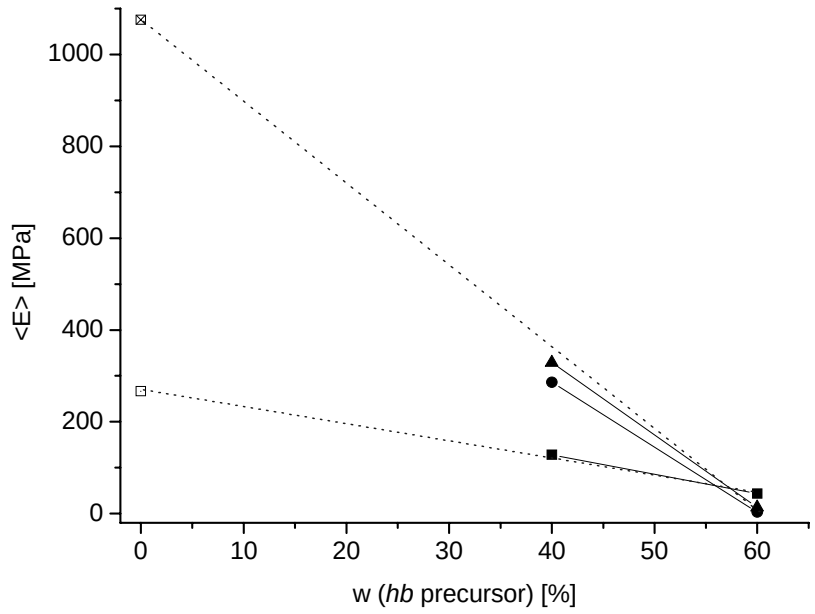

Figure 5-6: Young's modulus of PHEMA cross-linked with hb-PCL-MA plotted against weight fraction of the *hb* precursor. ■ NW-14-xx, ▲ NW-22-xx, ● NW-41-xx, □ *l*-PCL, ☒ PHEMA.

Young's modulus of NW-22 and NW-41 was around 300 MPa at w = 40 %. This represents a strong increase in toughness (like wood, perpendicular to the director of growth). Drawing a straight line between <E> at w = 60 % and <E> of pure PHEMA, the stiffness of NW-22-40 and NW-41-40 hit again the fit.

It is an interesting result that a highly methacrylated moderately branched *hb*-PCL-22MA (DB = 22 %, f = 32 %) and a low methacrylated highly branched *hb*-PCL-42MA (DB = 42 %, f = 9 %) induced similar properties to a network if used as precursor. However the "little" branched, but highly methacrylated *hb*-PCL-14MA (DB = 14 %, f = 26 %) yielded the largest effect on the softening of the resulting network. This behavior is illustrated in Figure 5-6. (*n.b.*: the explanation by means of fit lines is not meant to be applicable for the whole range of compositions, i.e. one should not expect a virtual sample NW-14-10 to obey to the fit showing <E> = 200 MPa.)

However, these results are in contradiction to the behavior of normal polymer networks. Introduction of, and in particular increasing the number of cross-links is expected to

increase Young's modulus. The appropriate model describing this phenomenon is a net: The tighter the net the more it keeps its shape and the less it is expanded if strain is applied. In the present case, the *hb* precursor obviously "dilutes" the net resulting in a looser structure that is more easily bended. It is assumed that the flexible, expandable structure of the *hb* material acts on the one hand like a polymeric, physically integrated plasticizer and as a cross-linker on the other. The biggest softening is observed, when using a cross-linker having a relatively low DB and high functionalization with methacrylate groups.

Measurements of the elongation at break yield information on the highest possible bending, tension and on the characteristics of the break – brittle failure or viscoelastic behavior. Similar to T_g data, the properties of the polymer networks were between those of *l*-PCL and PHEMA, representing two antipodes – brittle failure and viscoelastic deformation. In this experiment (Figure 5-7), samples containing *hb*-PCL-14MA and *hb*-PCL-22MA behaved similarly, but fairly moderate. NW-41 networks however exhibited a big dependence of their elongation at break with respect to the weight fraction of *hb* precursor. Although they were quite tough, they are highly expandable. Both of them, NW-41-40 and NW-41-60 showed classical viscoelastic behavior, the first of a polymer near T_g, the latter that of a polymer at T_g.

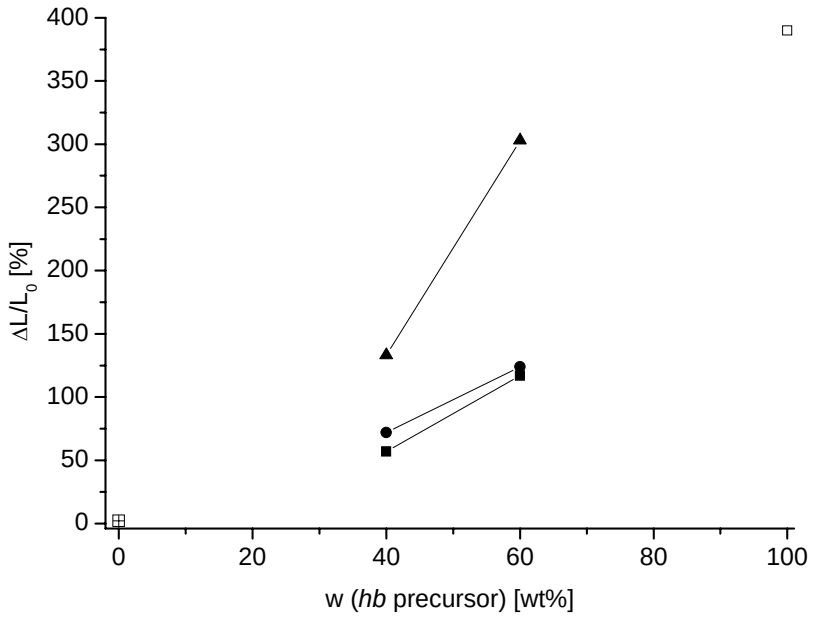

Figure 5-7: Elongation at break plotted against weight fraction of hb-PCL-MA. ■ NW-14-xx, ▲ NW-22-xx, ● NW-41-xx, □ *l*-PCL, ⊠ PHEMA.

While tensile tests were carried out at ambient temperature, viscoelastic DMA data are a function of temperature and frequency. The complex shear modulus G^* is calculated according to:

$$G^*(\omega) = G'(\omega) + i \cdot G''(\omega) \quad \textbf{(5-4)}$$

in which G' - the shear storage modulus, G'' - the shear loss modulus.
The value is calculated by:

$$|G| = \sqrt{G'^2 + G''^2} \quad \textbf{(5-5)}$$

In a first approximation, G' >> G" is assumed:

$$G \approx G' \quad \textbf{(5-6)}$$

This approximation is valid for the investigated samples, because $G'_{T=20°C}$ is far below T_g and hence, the loss modulus *G"* is one order of magnitude lower than G'. In Figure 5-8, the shear storage moduli (G') are plotted against the weight fraction of *hb*-PCL-MA. Since a similar approximation as in Eq. 5-5 is valid for E and E', <E> and G'(T=20°C) are comparable and are expected to be proportional:

$$E \approx E' = k \cdot G' \approx k \cdot G \quad \textbf{(5-7)}$$

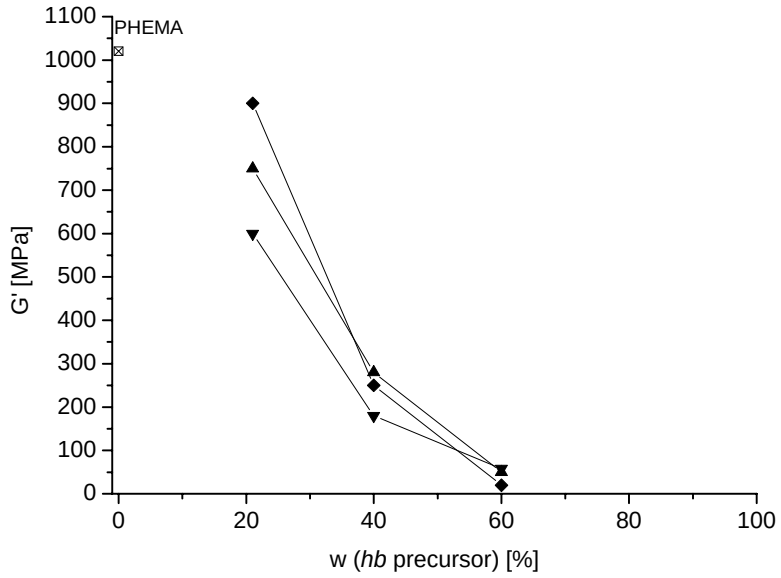

Figure 5-8: Shear stroage modulus (G') against weight fraction of hb precursor. ■ NW-14, ▲ NW-22, ● NW-41, □ l-PCL, ☒ PHEMA.

Assuming the *hb* precursor "to dilute" a pure PHEMA polymer, which has a characteristic G'/<E> ratio may give a lucid explanation of the results visualized in Figure 5-9. the *hb* precursor. Similar to the results obtained by T_g or elongation at break experiments, the values of the networks were found to be between those of the pure components. At w = 20 wt%, G' is highly proportional to the DB of the *hb* precursor.

However, at higher weight fraction, G' mainly depends on the weight fraction, but only little on the nature of the *hb* precursor. Once again, *l*-PCL was used as representative of a pure *hb*-PCL-MA network, assumed to produce a value of G' in the same magnitude like a virtual pure *hb*-PCL-MA network.

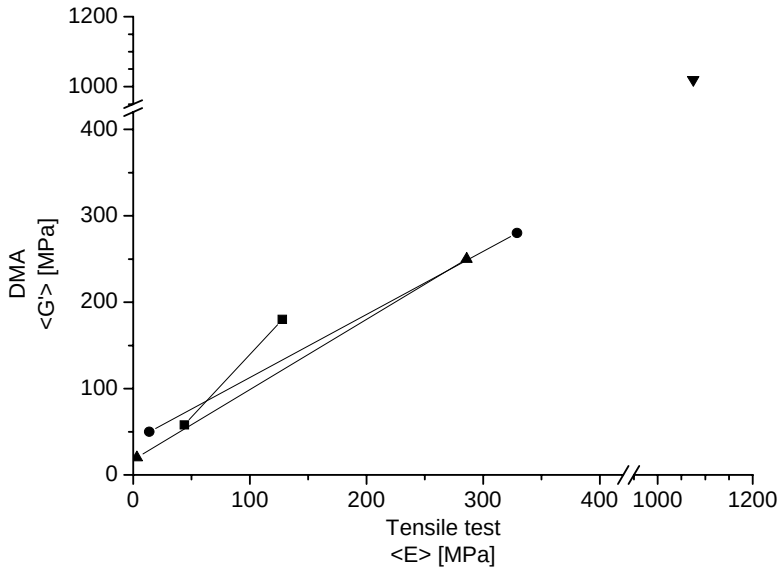

Figure 5-9: Shear modulus (G') at 20 °C against Young's modulus (<E>) . ■ NW-14-xx, ▲ NW-22-xx, ● NW-41-xx, ☒ PHEMA.

5.5 Swelling Experiments

Copolymerization of linear HEMA with the methacrylated *hb*-PCLs on the one hand increases the cross-link density and introduces free hydroxyl groups into the network on the other. As it is obvious from Table 5-5, the weight swelling degree in a solvent strongly depends on the amount and type of the hyperbranched *hb*-PCL-MA. Increasing the amount of the *hb*-PCL-MA induced an increase of the solvent take-up in the case of toluene and a decrease in the case of water.

While the weight swelling degree in toluene showed a strong increase in NW-14 and NW-22, almost no change was observed for NW-41. This was in line with expectation, since there are three parameters to be considered: a) osmotic pressure of the solvent to

dilute the network, b) compatibility between network chains and solvent and c) restoring forces of the network. NW-41 is the most lipophobic network, thus the weight take-up in toluene is the lowest of the three networks.

Swelling in water strongly depends on the number of free hydroxyl groups, i.e. NW-14-60 may be assumed to exhibit the highest weight take-up. However, of the three NW-41 samples, NW-41-20 (w = 20 %) showed the biggest water take-up and NW-41-60 (w = 60 %) the lowest. Network hydrophilicity was constrained by network stiffness and hydrophobic interactions caused by the plasticizer's backbone. Similar results were obtained in the case of NW-14 and NW-22.

Finally, one may estimate the cross-linking density of a polymer network. This is best performed, when other strong interactions, e.g. dipole-, hydrogen-interactions, can be excluded. In the case of strongly hydrophilic polymers, this was realized in hydrocarbons. PHEMA was considered as blind test.

Table 5-5: Swelling experiments of *hb*-NWs (t = 48 hrs.) - experimental data

Sample	Comonomer	Amount wt%	Q(H_2O) $\Delta m/m_0$	Q(Toluene) $\Delta m/m_0$
PHEMA	-	0	45.1	0.0
NW-14-20	*hb*-PCL-14MA	21	20.7	5.6
NW-14-40	*hb*-PCL-14MA	40	12.8	16.7
NW-14-60	*hb*-PCL-14MA	60	7.8	36.3
NW-22-20	*hb*-PCL-22MA	21	27.3	0.2
NW-22-40	*hb*-PCL-22MA	40	13.5	5.6
NW-22-60	*hb*-PCL-22MA	60	9.4	12.7
NW-41-20	*hb*-PCL-41MA	21	27.1	-0.2
NW-41-40	*hb*-PCL-41MA	40	18.9	-0.3
NW-41-60	*hb*-PCL-41MA	60	11.0	4.7

Table 5-5 clearly shows significantly increasing cross-link densities for those networks consisting of precursors having higher DB while the weight fraction of the precursor was kept constant, i.e. the toluene weight take-up went down the more the *hb* precursor was branched, respectively, the cross-link density increased. However, an increase of the weight fraction of the same *hb* precursor in a network resulted in highly increased toluene take-up of the test specimens. The higher the weight fraction of the *hb* precursor the more the cross-link density decreased. High fractions of this *hb* precursor apparently suppressed cross-linking efficiency.

5.6 Conclusions

hb precursors for cross-linking were prepared by methacrylation of *hb*-PCL. Amongst other routes, transesterification of BUMA to methacrylated *hb*-PCL catalyzed by Novozyme 435 was chosen, since i) moderately functionalized precursors were obtained and ii) simple removal of the immobilized catalyst was considered as an advantage.

Cross-linking of binary mixtures of HEMA and the methacrylated precursor was achieved by exposure to a UV source giving the desired networks. These networks were examined by thermal and mechanical testing as well as experiments on their swellability, and thus, cross-link density. The trends are visualized in Table 5-6.

Reading this table in a horizontal manner, i.e. considering only one type of precursor at a time, the network polymers act as follows: one may imagine a net in which the knots represent the *hb* precursor having long elastic arms. The more knots or cross-linking points respectively, the lower is the average distance between two of them. The long elastic arms at the cross-linker cause a lowered T_g, reduced stiffness <E> and shear modulus <G'>, but higher maximal elongation of the material. Swelling in toluene is simply characterized by the portion of hydrophobic plasticizer in the network and the ability of the network backbone structure to bend. In the case of interaction with H_2O, the hydrophobic net collapses and hydrophilic interactions between solvent and hydroxyl groups of the polymer are overcompensated. The linear analogue, PHEMA takes-up 45 % H_2O of its original weight within 48 hours. Swelling properties may be recognized as the sum of the individual contributions of the number of respective repeating units, in which the *hb*-PCL unit induces stronger effects than the PHEMA.

Observing trends "in columns", e.g. NW-14-21, -40 and -60 (expressed as 'trend' in Table 5-6) a complex relationship was observed, which lacks explanation so far. In a first approximation, *hb*-PCL-MA is again best described as a star-shaped plasticizer having long linear arms, which causes effects ascribed to cross-linking (swelling properties, elongation at break) and to blending (<E>, $T_{g;}$, G'). All samples with relatively low content of *hb*-PCL-MA (NW-xx-20) were brittle, whereas higher portions of *hb*-PCL-MA (NW-xx-40, NW-xx-60) yielded rather elastic materials. Further experiments to gain a better understanding of these effects have to be carried out.

The cross-link density was evaluated by analysis of the swelling in toluene, since solvent interactions with hydroxyl groups of the backbone are excluded. The more the precursor was branched, the higher was the cross-link density (w = const.). However, the higher the weight fraction of any precursor, the more was the cross-link density decreased (same

precursor). High weight fractions of precursor reduced cross-link efficiency in the curing process.

Table 5-6: Trends summarized according to the type of analysis and the nature of cross-linker. Arrows indicate trends with respect to the weight fraction of the cross-linker unless otherwise stated.

Precursor	T_g/w	<E>/w	L/w_3	G'/w	G'/<E>	G'(@T)/w	Swelling H_2O	Swelling Toluene
hb-PCL-14MA	↘	↘	↗	↘	↗	↗	↘	↗
hb-PCL-22MA	↘	↘	↗	↘	↗	↗	↘	↗
hb-PCL-41MA	↘	↘	↗	↘	↗	↗	↘	↗
trend[1)]	↘	↗	↗	↘	↘	↘	↘	↗
PHEMA							+	0
l-PCL							0	*
hb-PCL							0	*

[1)] observed in direction of NW-14, NW-22, NW-41, while w = const.
[2)] dissolves in toluene.
[3)] elongation at break

6 HYPERBRANCHING POLYMERIZATION OF ANALOGOUS LACTONES AND CARBONATES

6.1 Introduction

The hyperbranching concurrent copolymerization of an AB- and an AB_2- monomer is a powerful concept to create novel materials in a straight one-pot reaction. Chemical and physical properties are closely related to the degree of branching (DB) and functionality which are adjusted by the AB/AB_2 comonomer ratio in feed.[29,155-157]

The proof of concept is laid out in chapter 3, in which the copolymerization of ε-caprolactone (CL) and 2,2'-bis(hydroxymethyl) butyric acid (BHB) was discussed. The influence of the DB was examined with respect to characteristic parameters, such as molecular weight, viscosity and thermal properties.

In this study, cyclic compounds of similar structural identity that may serve as AB-monomer are sought, to which this concept is transferable. Since Novozyme 435 is a biocatalyst, chemical similarity of structure is not the only criterion for successful copolymerization, moreover steric issues, such as the length of the linear segment or the repeating unit may play a crucial role.

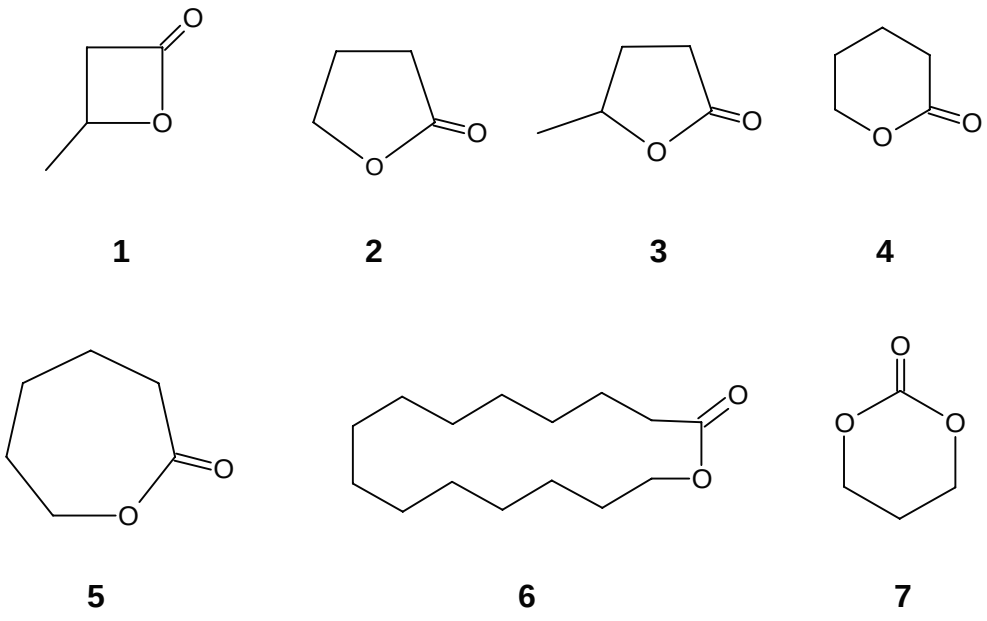

Figure 6-1: Cyclic compounds tested in the screening experiment: (1) β-butyrolactone, (2) γ-butyrolactone, (3) γ-valerolactone, (4) δ-valerolactone, (5) ε-caprolactone, (6) ω-pentadecalactone and (7) trimethylene carbonate.

An initial screening experiment of the selected compounds is described. Although Novozyme 435 is known to catalyze most of these monomers, reaction kinetics of both the cyclic lactone and BHB must be similar to make insertion of the branching points possible. In section 6.3 (hyperbranched poly(δ-valerolactone)s and 6.4 (hyperbranched poly(trimethylene carbonate)s), the two most promising systems are investigated in detail. In both cases, *l*-PVL and *l*-PTMC are bioresorbable and biodegradable.[79,83,97]

6.2 Screening of Cyclic Esters for Hyperbranching Polymerization

The comonomers were chosen by similarity in structure compared to CL, availability and cost (Figure 6-1). To the best of our knowledge, 8- to 15-membered cyclic esters and carbonates are not available on the market. Besides γ-valerolactone (3) all of them are known to be polymerized by Novozyme 435.[60-62,82,118,158] TMC was synthesized in our laboratory according to Takeshi's procedure.[159]

The experiments were carried out in toluene solution in analogy to Skaria's protocol.[67] A degree of branching in the feed (DB_f) of 18.0 was chosen. The results are summarized in Table 6-1. Yield and appearance after work-up, i.e. the physical state, was chosen as indicators of success or failure of the polymerization. In brief, the samples made from BHB and i) δ-valerolactone (VL, entry 4), ii) ω-pentadecalactone (PDL, entry 6), and iii) trimethylene carbonate (TMC, entry 7) were polymerized under these conditions.

The copolymerizations of BHB and i) β-butyrolactone (entry 1), ii) γ-butyrolactone (entry 2) and iii) γ-valerolactone (entry 3), however, were not promising at all employing these reaction conditions and were not pursued any further. The formation of *hb*-PCL (entry 5) comfirmed that suitable (co-)polymerization conditions were met according to Skaria.[67]

Table 6-1: Screening experiment - characterization of the copolymerization of cyclic esters / trimethylene carbonate and BHB.

Entry	Monomer	DB_p	Yield [%]	Appearance
1	β-butyrolactone	n.d.	4.9	liquid, 1 drop
2	γ-butyrolactone	n.d.	19.7	liquid, <1 drop
3	γ-valerolactone	n.d.	33.2	Liquid
4	δ-valerolactone	20.2	56.2	highly viscous
5	ε-caprolactone	11.7	53.3	Solid
6	ω-pentadecalactone	0	97.7	Solid
7	trimethylene carbonate	7.4	65.9	Solid

[1)] n.d. = not determined.

^{1}H-NMR analysis of sample 4 – 7 was used to evaluate BHB incorporation. While branched polymers were obtained in the case of VL, CL and TMC copolymerization with BHB, PPDL was observed to yield a linear homopolymer, i.e. no copolymerization took place. This is in good agreement with data reported by Gross et al., who tried to copolymerize CL and PDL using Novozyme 435.[120] They observed that the homopolymerization of PDL proceeds about 13 times faster than CL, i.e. about >10 times faster than BHB copolymerization.

6.3 Hyperbranched Poly(δ-Valerolactone)s

Hb-PVL was synthesized in bulk in analogy *hb*-PCL. BHB dissolves in VL at elevated temperature, thus a homogenous binary mixture of the two comonomers was formed. Yields between 74 % and 40 % were obtained strongly depending on the DB. Work-up of high-DB samples was impaired by loss of product, since phase separation during purification of the organic phase was incomplete, also after a day of delay. There difficulties were ascribed to the polymer's amphiphilic properties. The samples were waxy and had a light yellowish color. They were characterized using NMR, GPC, VPO and viscosity measurements. Thermal properties were obtained by DSC analysis.

In Figure 6-2, a typical ^{1}H-NMR spectrum of *hb*-PVL is depicted. Signal c, d, e, f and f' represent the linear VL segments. They match the chemical shifts reported for *l*-PVL by Báez et al.[160] As in the case of *hb*-PCL, DB was calculated by the ratio of signal a (-C$\underline{H}_3$, BHB) and c (-O-CO-C$\underline{H}_2$-R) according to the Frey equation (*cf*. section 1.4). The results are summarized inTable 6-2.

DB of *hb*-PVL was in the range of 0.8 to 24 %. While a deviation from stoichiometric insertion was negligible up to DB_f = 12 %, it became significant at higher values (Figure 6-4). The structure of *hb*-PVL is inherently more compact, since the number of methylene groups, acting as spacer between two connecting points, is smaller than in *hb*-PCL. At higher DB, the statistically distributed branching points cause a more condensed structure which presumably prevents the growing polymer from binding to the active site in CALB and thus reduces the incorporation rate of BHB. For *hb*-PVLs, this effect is observed at lower DB_p than for *hb*-PCL.

^{13}C-NMR spectra yielded further information on the *hb* structure (Figure 6-3). As DB increases, a new signal appears in the carboxyl region at 173.7 ppm, which was ascribed

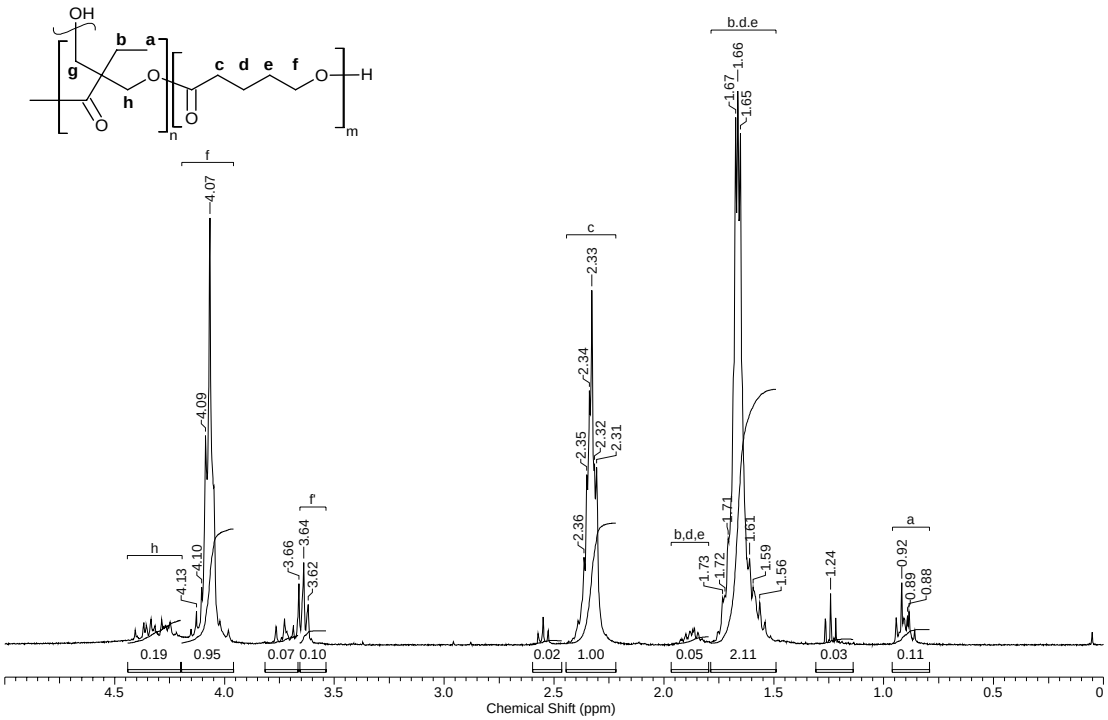

Figure 6-2: ^{1}H-NMR spectrum of *hb*-PVL-80, DB = 20.2.

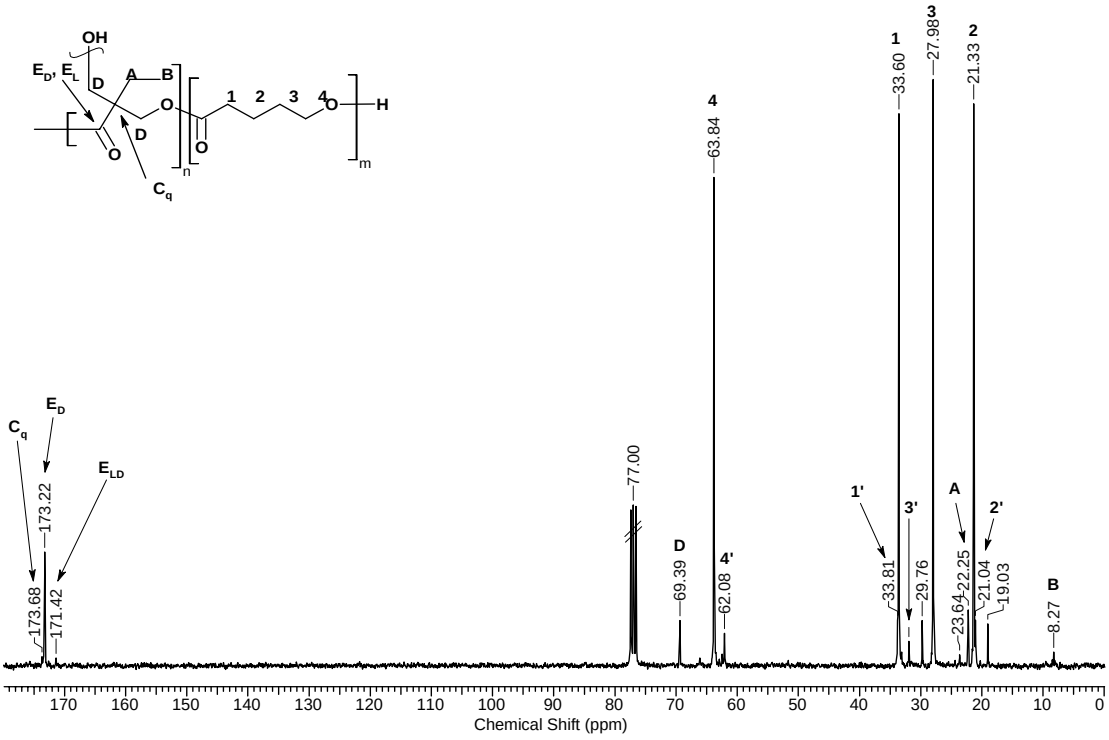

Figure 6-3: ^{13}C-NMR of *hb*-PVL-89 containing 5.7 mol-% BHB.

Table 6-2: Characteristic data of *hb*-PVL samples.

Copolymer	DB_f mol%	DB_p mol%	Yield %	M_n (GPC)[1] g·mol^{-1}	PDI[1]	M_n(UC)[2] g·mol^{-1}	PDI[2]	M_n (VPO) g·mol^{-1}	$\eta_{intr.}$ cm^3/g
l-PVL	0	0	92.1	3,400	1.7	-[4)]	-[4)]	1,200	13.6
hb-PVL-99	1.5	0.8	57.6	4,500	1.8	2,900	1.7	1,300	17.5
hb-PVL-98	2.8	1.5	69.5	5,100	1.9	3,200	1.9	-	18.5
hb-PVL-95	5.5	5.0	59.9	3,800	2.1	-[3)]	-[3)]	1,200	17.2
hb-PVL-89	10.7	10.8	45.1	2,700	1.9	-[3)]	-[3)]	-	13.1
hb-PVL-88	13.3	11.6	74.1	2,100	2.1	-[3)]	-[3)]	1,200	11.7
hb-PVL-80	37.2	20.2	48.3	-	-	-[3)]	-[3)]	730	9.4
hb-PVL-76	57.8	24.4	38.8	300	2.7	-[3)]	-[3)]	-	
hb-PVL-71	25.5	29.3	45.9	700	1.9	-[3)]	-[3)]	-	-

[1)] PS-Calibration [2)] universal calibration [3)] no signal obtained [4)] no η-detector available

to the quaternary carbon C_q in α-position to the carboxylic function of BHB indicating the higher number of branching points, and, to the same extend, new terminal, linear groups. However, signal E_L at 171.42 ppm disappears, which refers to BHB groups that are incorporated in a linear manner. This led to the conclusion that linear VL units first react with free BHB end groups prior to addition of another BHB branching unit. This observation supports the explanation for the DB-deviation. All other signals related to groups of terminal CL units became more pronounced with higher DB.

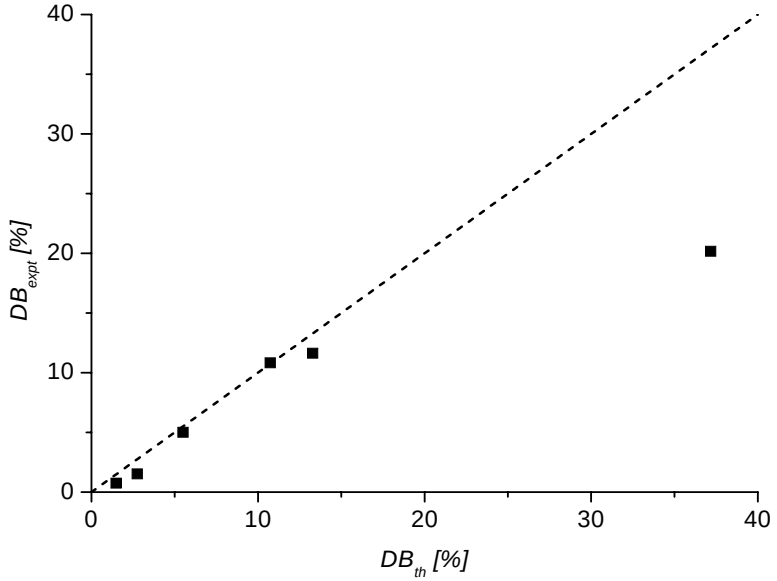

Figure 6-4: Degree of branching of *hb*-PVLs calculated from ^{1}H-NMR integrals correlated to the theoretical degree of branching in the feed. The straight line marks stochiometric insertion.

Experiments varying the time of reaction were carried out to identify the state of maximal conversion. After 20 hours, molecular weights did not increase any more and remained stable. In contrast to *hb*-PCL, no loss of molecular weights due to transesterification was observed at longer *reaction* times. Yields of the final product increased to 55 % in the 10 hour-experiment. At longer reaction times, yields dropped to 40-45 % of the theoretical value. It is assumed that a portion of the highly hydrophilic samples having a high DB was carried through to the aqueous phase during the washing step in post reaction work-up.

In the 24 hour-experiments, molecular weights were found to depend strongly on DB, and thus the degree of functionalization. 10 % of branching induced a drop in $<M_n>$ to 50 % of the original value. Since the viscosity signal was too weak, universal calibration was not applicable. However, $<M_n>$ was obtained for *hb*-PVL-99 and *hb*-PVL-98 in universal calibration mode. The $<M_{n(UC)}>$ was 64 % of $<M_{n(PS)}>$.

$<M_n>$ calculated from VPO measurements, ranging between 1300 and 800 Da, showed little dependency on DB (Figure 6-5). Since *hb* polymers usually have a composition comprising oligomers that consist of only a couple of repeating units, and longer polymer chains, VPO values reflect the lower end of the corresponding $<M_n>$ distribution (*cf*. section 3.4.2).

Viscosity data were recorded by an automatic Ubbelohde viscometer. All samples showed linear behavior of η_{sp}/c vs. c, which demonstrates that no aggregation occurred.

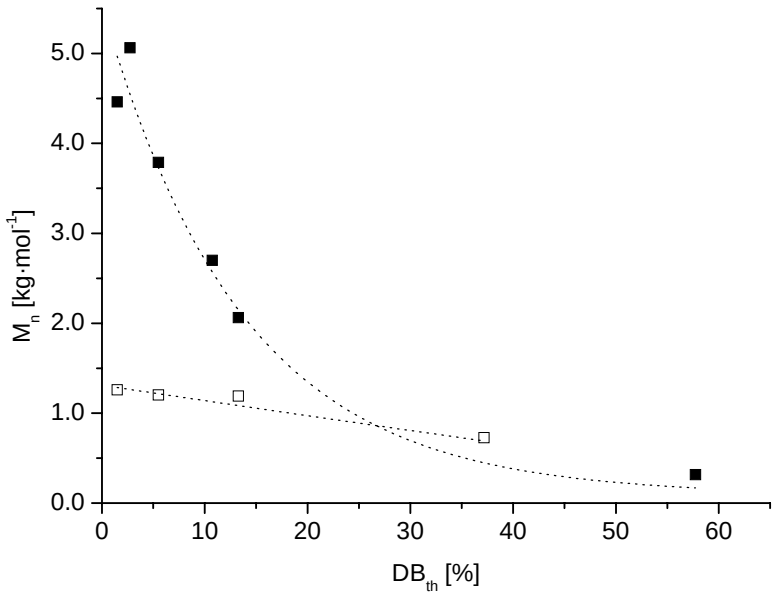

Figure 6-5: $<M_n>$ of *hb*-PVL determined by ■ GPC (TCM) and by □ VPO (TCM).

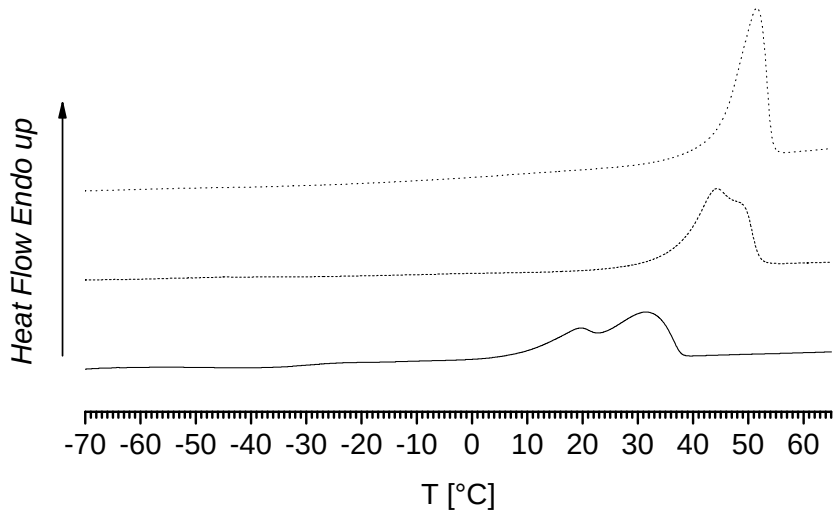

Figure 6-6: DSC diagrams of *hb*-PVLs: dotted line - *hb*-PVL-99, dashed line - *hb*-PVL-89, and straight line - hb-PVL-80

Little branched samples had higher viscosities than the highly branched. Compared to *hb*-PCL this trend was less pronounced, given that lower molecular weights were realized for *l*-PVL. Samples that have similar molecular weights (<M_n>) produced similar viscosity numbers.

DSC measurements confirmed that all *hb*-PVLs are flexible polymers, manifested by glass transitions (T_g) in the range of -54°C to -73°C (Table 6-3). It is noteworthy that the little branched samples showed a single melting endotherm. However, at higher DB (*hb*-PVL-89, *hb*-PVL-88), a shoulder emerges from the melting peak and for sample *hb*-PVL-80 and *hb*-PVL-76, double melting endotherms are observed. As in the case of *hb*-PCL (*cf*. section 3.4.2), this observation was ascribed to different qualities of crystallites. High DB impairs the formation of uniform crystallites, thus fewer and undeveloped spherulites, much smaller in dimension and less regular shape than those of *l*-PVL were formed.

The degree of crystallinity is another parameter, which allows statements on the rate of degradation, since degradability decreases with increasing degree of crystallization. Absolute values were calculated according to expression 3-3 (*cf*. section 3.4.2), if the heat of fusion ΔH_f^0 of the linear, completely crystalline homopolymer is given. In the case of fully crystalline *l*-PVL it is available from a web based source.[161]

Intuitively, one may assume that *hb* polymers suffer from a lower tendency to crystallize than their linear analogues. But similar to *hb*-PCL, the highest value of X_c was detected at

DB = 12 %. A better alignment of linear segments due to enhanced mobility may be a valid explanation.

Table 6-3: Theoretical and experimental degree of branching (DB), the average segment length (<DPs>) and thermal properties of selected *hb*-PVLs. Thermal data of *l*-PVL are reported elsewhere.[162]

Copolymer	DB_f mol%	DB_p mol%	BHB_p Mol	T_g °C	T_m °C	ΔH_f $J \cdot g^{-1}$	X_c %
l-PVL	-	-	-	-67.0	59.0		
hb-PVL-99	1.5	0.8	0.4	-57.7	51.5	79.5	42.3
hb-PVL-98	2.8	1.5	0.8	-59.7	50.4	77.9	41.4
hb-PVL-95	5.5	5	2.6	-55.2	47.1	78.5	41.8
hb-PVL-89	10.7	10.8	5.7	-54.0	n.d.	76.0	40.4
hb-PVL-88	13.3	11.6	6.2	n.d.	45.1	82.7	44.0
hb-PVL-80	37.2	20.2	11.2	-72.6	31.3	48.1	25.6
hb-PVL-76	57.8	24.4	13.9	-62.5	41.8	56.8	30.2
hb-PVL-71	25.5	29.3	17.2	-67.3	28.7	41.8	22.2

6.4 Hyperbranched Poly(trimethylene carbonate)s

Poly(trimethylene carbonate)s (PTMCs) are interesting biodegradable materials since they are completely amorphous.[95] Surprisingly, their biodegradability is much higher *in vivo* than *in vitro*. This is ascribed to the degrading enzyme's active site specificity.[95] A biotechnological approach to *l*-PTMC preparation was reported by Kobayashi in 1997 using CALB as well as other enzymes.[158] In 2002, Zhuo et al. reported the enzymatic synthesis of high MW samples up to 48 kDa.[163]

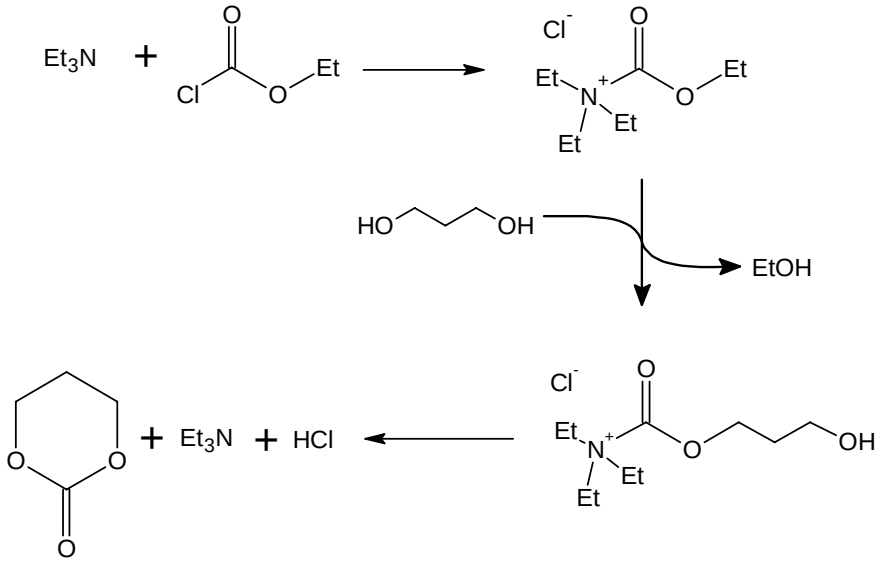

Figure 6-7: Synthesis of trimethylene cyrbonate.

However, low glass transition temperatures (T_g) and the absence of crystallinity come along with poor mechanical properties. For that reason, PTMC is mostly used in copolymers to tailor the flexibility and biodegradability of polymeric biomedical devices.[94,164]

TMC is not available on the market, thus it was prepared in a one pot reaction according to Takeshi's procedure reported in 1993 (Figure 6-7).[159] The precipitated product was obtained in 48 - 55 % yield.

In the initial screening experiment enzymatic preparation of TMC-BHB copolyesters was successful. The biodegradability, already observed for *l*-PTMC, will turn *hb*-PTMC into an interesting functional polymer for controlled drug release applications. Therefore a systematic evaluation of the synthetic conditions and properties of these novel materials was carried out. Characterization was done in a similar way as described in section 4.2.

The polymer structures were analyzed by using ^{1}H and ^{13}C-NMR spectroscopy. In Figure 6-8 a typical ^{1}H-NMR spectrum of *hb*-PTMC is shown. ^{1}H NMR spectra displayed mainly two peaks: a triplet peak (*c, e*) and a quintet peak *d*, which were ascribed to α-and β-methylene protons of the carbonate moiety of the polymer. In addition, three smaller, characteristic peaks *c'*, *d'* and *e'* were observed, which were ascribed to terminal TMC units of the polymer. Structural features of the BHB branching unit were found in signal *a* and *b*.

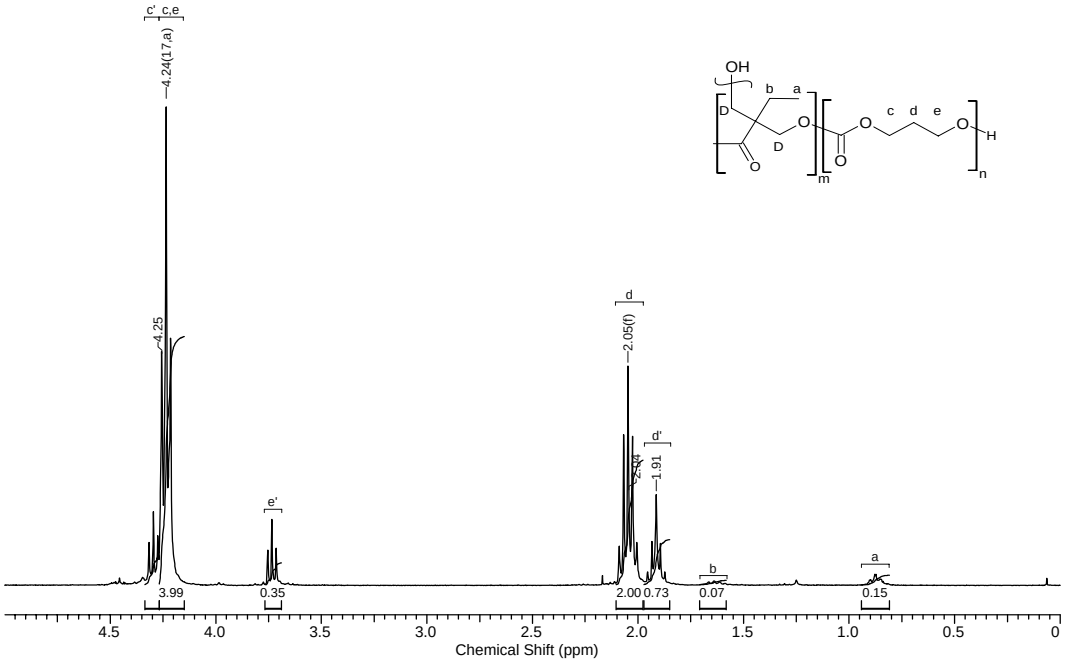

Figure 6-8: ^{1}H-NMR spectrum of *hb*-PTMC-94. DB = 6.3 %.

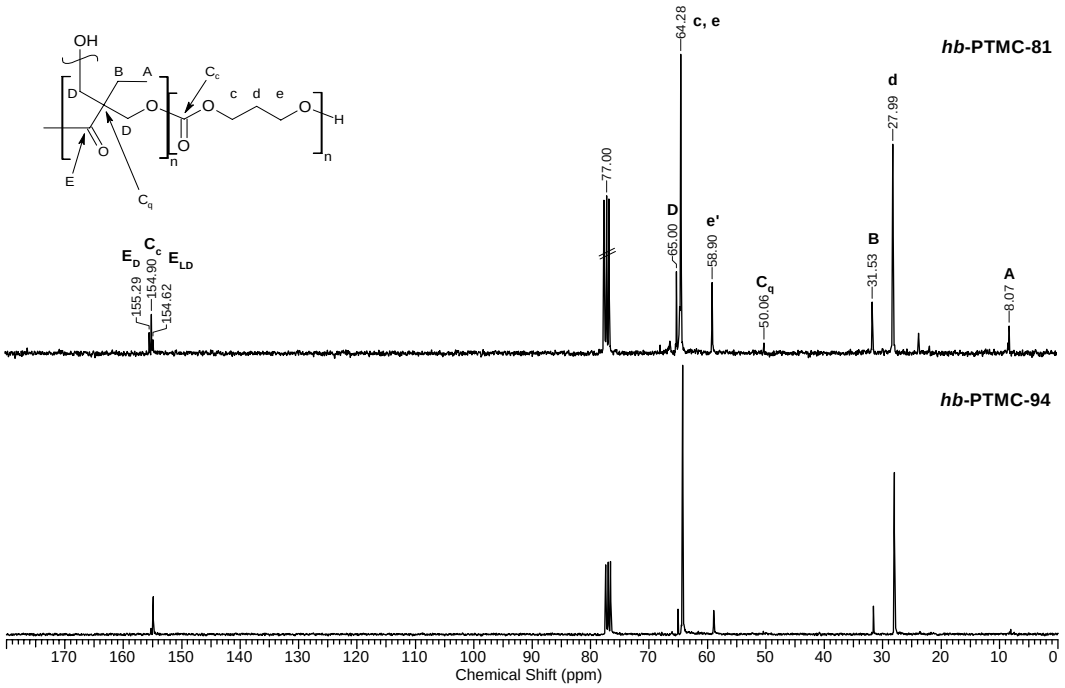

Figure 6-9: ^{13}C-NMR spectra of two *hb*-PTMCs.

The integrals of signal *a* and signal *d* were used to calculate DB according to the Frey equation (*cf.* section 1.4). No peak was observed around δ = 3.2 ppm,[159] suggesting the absence of ether units formed by decarboxylation. NMR spectra made further information available: Signal C_c, which refers to the carbonate carbon, *c, d* and *e* were assigned to the TMC building unit. The carboxylic carbons of BHB are represented by signal E_D (dendritic incorporation) and E_{LD} (linear-dendritic incorporation). They appeared only at higher DB. Signal D, C_q, B and A ($\underline{C}H_3$) were ascribed to the BHB unit. e' refers to terminal methylol groups (-C$\underline{H}_2$OH) (Figure 6-9).

The DB_p of the product was calculated and plotted against DB_f in the feed. Deviation from regular stoichiometric insertion (dashed line) was observed but highly linear up to DB_f = 38.0 % (*hb*-PTMC-68) as shown in Figure 6-10. This is in good agreement with the results obtained for *hb*-PCL and *hb*-PVL, indicating that the length of the linear segments determines the rate and hence the efficiency of BHB insertion. Accessibility of the binding pocket in CALB by the terminal hydroxyl group of the growing chain is seen as the crucial kinetic parameter.

Experiments, in which the reaction time was varied, were carried out in order to elucidate the optimal time in terms of molecular weight and distribution. Final molecular weights were achieved after 10 to 20 hours. No relevant changes were observed at longer reaction times. Therefore 24 hours were chosen as standard reaction time.

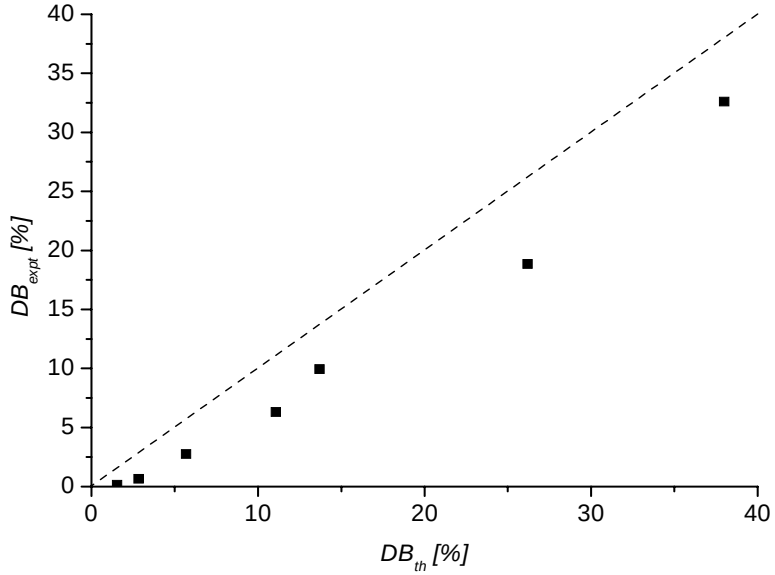

Figure 6-10: Degree of branching of *hb*-PTMCs calulated from ^{1}H-NMR integrals plotted against the degree of branching in the feed. The dashed line marks stoichiometric conditions.

In comparison to *hb*-PCL and *hb*-PVL, yields after work-up were quite low. While phase separation at the TCM-water interface during purification was very slow for *hb*-PVL, it became infinite for *hb*-PTMC. In addition, some of the highly functional as well as low-MW material of the sample was presumably easily carried through to the aqueous phase. Both effects contribute to small yield hence an alternative, improved purification procedure should be carried out in future.

Molecular weights were determined by GPC and VPO. As in the case of the other hyper-branched polymers examined in this study strong dependence of the molecular weight with respect to the degree of branching in the product (DB_p) was observed. Compared to

Table 6-4: Experimental data of *hb*-PTMCs.

Copolymer	DB_f mol%	DB_p mol%	Yield %	M_n (GPC)[1] g·mol^{-1}	PDI[1]	M_n (VPO) g·mol^{-1}	$\eta_{intr.}$ cm^3/g	T_g °C
hb-PTMC-100	1.5	0.1	40.2	4,300	2.2	1,300	14.8	-27.8
hb-PTMC-99	2.8	0.6	41.3	3,900	2.4	1,300	14.2	-30.2
hb-PTMC-97	5.7	2.7	12.8	3,200	2.5	1,300	8.4	-27.7
hb-PTMC-94	11.1	6.3	21.6	2,200	2.7	900	-	-31.5
hb-PTMC-90	13.7	9.9	10.2	900	1.6	900	9.4	-33.6
hb-PTMC-81	26.2	18.8	34.6	500	1.6	1,200	5.7	-31.1
hb-PTMC-74	38.0	32.6	18.6	300	1.3	1,200	-	-31.4
hb-PTMC-67	58.6	26.5	28.6	400	1.4	n.d.	-	-31.1

hb-PVL and *hb*-PCL, the relationship of DB_f against DB_p was rather linear, especially at higher molecular weights (*cf*. section 3.4.2 & 6.3). Similar to *hb*-PCL and *hb*-PVL results, VPO measurements did not encounter large changes in $<M_n>$. All data are summarized in Table 6-4; M_n against DB_p is plotted in Figure 6-11.

Viscosity data were recorded with an automatic Ubbelohde viscometer, since online-viscosity measurements returned reliable results only up to DB = 5 %. The-values were lower than those of comparable *hb*-PVL or *hb*-PCL, which is a result of the higher flexibility of the polymer chains due to complete amorphism. According to the calculated Mark-Houwink α parameters, *l*-PTMC is a random coil ($\alpha = 0.45$), all the branched samples have a dense globular shape ($\alpha \approx 0.2$).

DSC measurements confirmed the complete amorphism of *hb*-PTMC, thus the only observed transition was a T_g around -30 °C. For all samples the transitions were easily recognized, even at the lower heating rate of 10 K/min.

The physical appearance of *hb*-PTMC is a yellowish, sticky and highly viscous material.

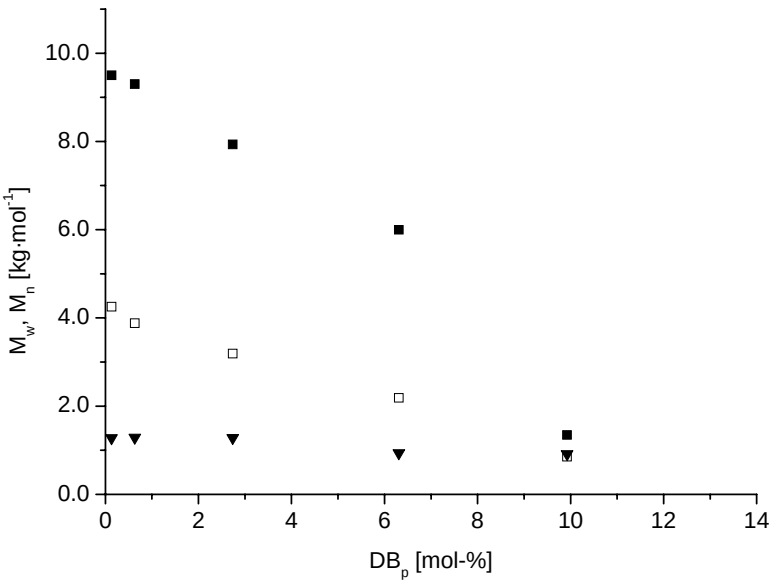

Figure 6-11: Molecular weights of *hb*-PTMCs by GPC (■ $<M_w>$, □ $<M_n>$) and VPO (▼ $<M_n>$) plotted against DB_f.

7 SUMMARY & PERSPECTIVES

The aim of the present study was a detailed investigation of the enzymatic copolymerization of ε-caprolactone and 2,2'-bis(hydroxymethyl) butyric acid in bulk and the characterization of the resulting aliphatic, hyperbranched poly(ε-caprolactone)s (*hb*-PCLs). These polyfunctional materials are promising candidates for biomedical applications because of their biocompatibility and biological clearance without the formation of toxic products. The advantage of this protocol employing an immobilized enzyme lies in the complete absence of heavy-metal compounds, e.g., as catalyst, and of organic solvents.

As an alternative to the synthesis from the monomers, the novel concept of transesterification of *linear* polymers into *hyperbranched* materials, which we termed "reknitting", was introduced as a method of preserving limited primary resources and energy that is consumed by monomer/oligomer regeneration (Figure 7-1).

Furthermore, the modification of *hb*-PCL to multi-functional cross-linkers by methacrylation, the subsequent creation of poly(2-hydroxyethyl methacrylate) (PHEMA) networks, and the investigation of their mechanical and physical properties were laid out.

Finally, *hb*-poly(δ-valerolactone)s and *hb*-poly(trimethylene carbonate)s that are structurally related to *hb*-PCL have been prepared. Their physical and chemical properties have been compared. These polymers are expected to possess an even more flexible and easier degradable structure than *hb*-PCL.

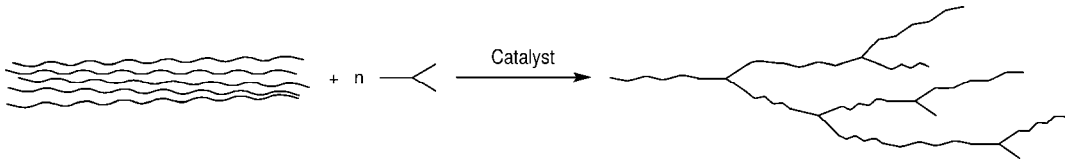

Figure 7-1: The concept of reknitting.

7.1 Hyperbranched Poly(ε-caprolactone)s

The synthesis of *hb*-PCL from CL and BHB in toluene solution was reported by Skaria et al. in 2002.[67] In the present study the successful transfer of this reaction to bulk conditions was first described, thus avoiding toxic solvents and catalysts in the process. Mild reaction conditions were achieved using Novozyme 435 as biocatalyst. Novozyme 435 is *Candida Antarctica* Lipase B (CALB) that is immobilized on nanoporous acrylate

beads (Lewatit^{TM}). This preparation improves the enzyme's tolerance to heat and organic media and allows for the complete removal of the catalyst.[117]

The important parameter in the characterization of *hb*-polymers is the degree of branching (DB). Comparing both strategies, near stoichiometric copolymerization of BHB and CL was observed, though bulk conditions caused a stronger deviation in favor of CL at high branching ratios.

All molecular weights were determined by VPO and by GPC measurements, the latter applying polystyrene standard calibration as well as universal calibration (Figure 7-2). The VPO experiments indicated relatively low molecular weights compared to the GPC data. However, these results are highly questionable in this case due to the inherent broad molecular weight distribution of hyperbranched materials. Since VPO is a colligative method, molecular weights are underestimated. In the present case the minimum of $<M_n>$ of the sample rather than the average $<M_n>$ was evaluated by VPO.

The GPC measurements of multi-functional polymers that are also chemically different from the employed polystyrene calibration are a difficult task and may lead to erroneous results. Since the number of functional groups increases with DB, the elution volume does not depend exclusively on the molecule's size but also on polymer/solvent and polymer/matrix interactions; thus, only relative molecular weights were obtained.

Universal calibration is expected to provide absolute molecular weights even for branched molecules of variable geometry.[107] The results obtained for *hb*-PCL indicate lower molecular weights and thus lower dependence of M on DB (Figure 7-2). However, this technique is somewhat limited by the signal to noise ratio of the viscosity signal. Therefore, molecular weights were determined only up to DB = 7 %.

The intrinsic viscosity was obtained by GPC-online viscometry and additionally confirmed by measurements recorded with an Ubbelohde viscometer. Data obtained by both techniques was in good agreement. Besides, a drastic drop in viscosity already induced by a low degree of branching was observed, which is an important asset for processing.

MALDI-TOF spectroscopy was used to elucidate structural information. While long-chain branched samples consist of both cyclic and linear macromolecules, only linear, branched species were observed in hyperbranched materials.

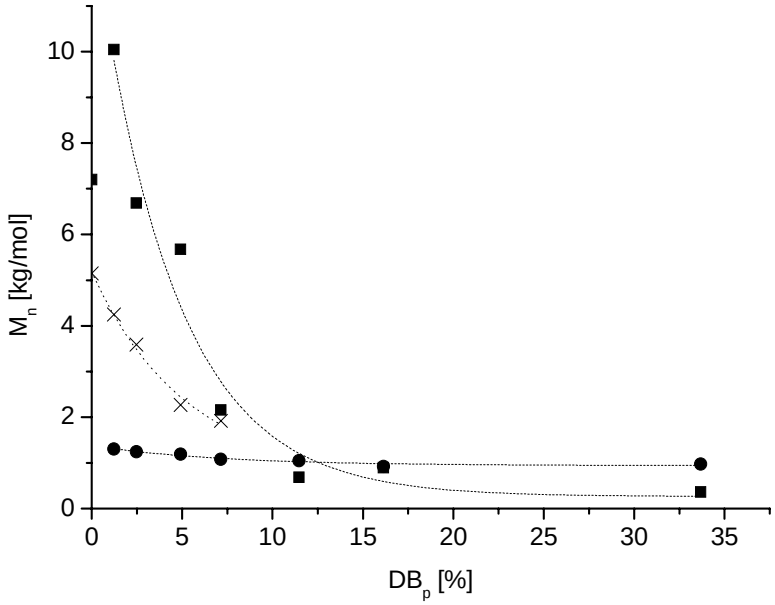

Figure 7-2: <M_n> of *hb*-PCL determined by: ■ GPC (poly styrene calibration), x GPC (universal calibration) and ● VPO (T = 30 °C, TCM).

DSC measurements were carried out to obtain information on T_g and T_m. T_m decreased from +58 °C to +27 °C with increasing fraction of BHB, which clearly confirms a reduction in crystallinity. On the other hand, T_g increased with increasing DB. According to Kim and Webster[27] this indicates that the mobility of the linear segments becomes more and more constrained, as the number of functional, polar groups increases. A complimentary explanation is that the mobility of the linear segments is more and more limited with an increasing number of branching points.

7.2 Hyperbranched Poly(ε-caprolactone)s on the kg-scale

Synthesis on a larger scale is a first step to broaden the experimental interest in a promising compound. Ready availability permits the use as starting material for further modifications and allows for research on blends or composites.

Effective preparation requires optimized reaction conditions, i.e. bulk polymerization, and catalyst recycling. High reaction rates were observed and highest molecular weights were obtained after 2-5 hours. Between 10 and 20 hours, a weight loss of 5 - 6 % due to transesterification was observed; yet, PDI became minimal. The addition of molecular sieves or the application of vacuum during the reaction led to more efficient water removal, which slightly increased molecular weights.

The amount of Novozyme 435 that is used per charge is a crucial economic factor. Although slightly higher yields were obtained employing 10 wt% Novozyme 435, which is commonly used in some reports, investigations revealed little loss in the final molecular weights down to 4 wt% in the 5g charges. Further reduction of the catalyst quantity caused a strong decrease in molecular weights for the 5g charges (Figure 3-15).

On the kg-scale, the samples possessed similar properties to those prepared in the carousel reactor (5g-charges), although the catalyst feed was further reduced to 2 wt%.

It is assumed that more efficient mixing of the melt and tighter vacuum contribute to the enhanced efficiency of the system.

Novozyme 435 regeneration was found to be disadvantageous since the regenerated enzyme lost the major part of its original activity. Further investigations pointed to leaching of the adsorbed enzyme from the macroporous support in hydrophilic environments.

7.3 "Reknitting" of Linear into Hyperbranched Poly(ε-caprolactone)

"Reknitting," i.e. transesterification of a linear polymer into a hyperbranched material as a novel recycling concept has been introduced. As proof of concept transesterification of *l*-PCL (CAPA 6500^{TM}, M_n = 62 kDa, PDI = 1.6) into *hb*-PCL was investigated using BHB as AB_2 branching monomer and Novozyme 435 as catalyst under bulk conditions. The resulting samples were characterized like *hb*-PCL prepared from the comonomers and compared to these.

GPC was used to monitor the change in molecular weight and molecular weight distribution. As shown in Figure 7-3, the signal of CAPA 6500^{TM} steadily decreased with exposure to the active enzyme in favor of a broad peak that built up at a longer retention time. The broad molecular weight distribution is a typical feature of hyperbranched polymers, which leads to lowered average molecular weights, $<M_w>$, $<M_n>$, compared to the linear analogue. At a high elution volume, even the formation of oligomers was observed, which indicates the random transesterification by the enzyme.

The molecular weight to DB relations ($<M_n>/DB_p$) of *hb*-PCL prepared by reknitting and that prepared from the comonomers were similar (Figure 7-4). This is noteworthy, since i) both preparation from comonomers as well as transesterification of a linear high-MW PCL result in similar materials, ii) the observed $<M_n>$-DB_p relationship does not indicate a limitation of the enzymatic polymerization. Moreover, it seems to describe either a peculiarity of the system or of the GPC analysis of these special materials.

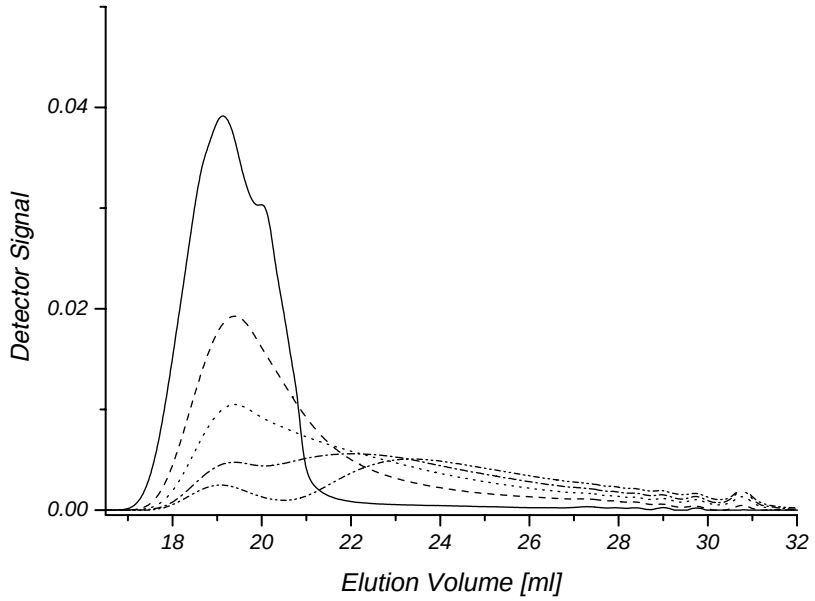

Figure 7-3: Superposition of GPC traces after 8 – 48 hrs of reaction. straight line – l-PCL (CAPA 6500), dashed – 8 hrs, dotted – 24 hrs, dash-dotted – 32 hrs and dash-dot-dotted line – 48 hrs.

Fractionation of *hb*-PCL (t=36 hrs, DB=12 %) obtained by reknitting provided a deeper insight into the composition of the sample. Thirty monodisperse fractions were obtained out of 60 slices, which were characterized by ^{1}H-NMR, GPC and MALDI-TOF MS. DB_p, which was calculated from the ^{1}H-NMR analysis was in the range of 12 to 25 %, which was always higher than the DB_p of the original, not fractionated sample. This result still lacks explanation and should be addressed in the future.

GPC experiments confirmed that the fractions were monodisperse (PDI ≤ 1.3). For that reason, it was supposed to obtain reliable data by MALDI-TOF MS. However, structure elucidation was limited, because some characteristic structural features of the studied material possessed similar monoisotopic masses (L, L_L: $\Delta m = 1$ amu).

Molecular weights obtained by MALDI-TOF MS are usually not reliable. However, MALDI-TOF and UC-GPC experiments seem to yield similar values of the maximum peak position M_p for a given narrow-disperse polymer.[114] In this case, M_p values were somewhat lower than those obtained by GPC (PS calibration). The relationship of this pair of M_p values ($M_{p,\,PS\text{-}GPC}$ / $M_{p,\,MALDI\text{-}TOF\ MS}$), however, was similar to that obtained for the ratio of $M_{p,\,UC\text{-}GPC}$ to $M_{p,\,PS\text{-}GPC}$ in the case of *hb*-PCL prepared from the comonomers. It is assumed that $M_{p,\,MALDI\text{-}TOF\ MS}$ values of each fraction will be similar to M_p values that can be obtained by GPC in universal calibration mode[134].

Thermal analysis (of the non-fractionated samples) revealed a linear relationship between the decrease of T_m and the increase of DB, which is caused by a loss in crystallinity on the

incorporation of branching points into the linear polymer chains. However, T_g increases, which is tentatively explained by the increase of the polarity of the macromolecules and reduced mobility of the linear segments with higher DB.

Finally, viscosity measurements have been carried out. A drop in viscosity to 10 % of its original value (*l*-PCL) was induced by a DB of 5 – 10 %. Hence, also long-chain branched samples possess low viscosity in solution, which is an important property for processing.

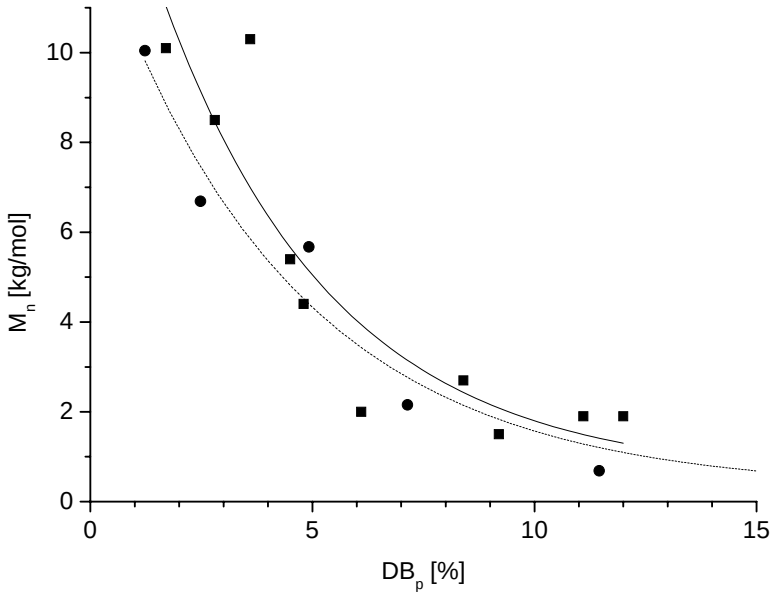

Figure 7-4: M_n (PS-GPC) of *hb*-PCL: straight line - prepared by monomer synthesis (*cf.* Chapter 3), dashed line by Reknitting of CAPA 6500™.

7.4 Structured Polymer Networks

Polymer networks are interesting structures, in which linear polymer segments are cross-linked, i.e. interconnected. The materials' properties are determined by the choice of precursor, the cross-linking density of the network formed, and fillers and additives, which are possibly present.[138] In this part of the thesis, the aim was to establish a synthetic protocol towards a *hb*-PCL precursor. Furthermore, the creation of HEMA networks and the investigation of the influence of the amount of *hb* precursor on the mechanical properties was assessed.

Hb precursors for cross-linking were prepared by methacrylation of *hb*-PCL (Figure 7-5). In continuation of the previously described synthesis, an enzymatic route, i.e. the transesterification of butyl methacrylate (BUMA) employing Novozyme 435 under bulk conditions was chosen. A functionalization of 20-30 % with respect to available

hydroxyl groups was achieved. Since *hb*-PCL-MA exhibits a high tendency to cross-link at ambient conditions, BHT was added as an inhibitor. Consequently, no GPC chromatograms were recorded, considering that separation of BHT from the macromonomer bore a high risk of spontaneous polymerization.

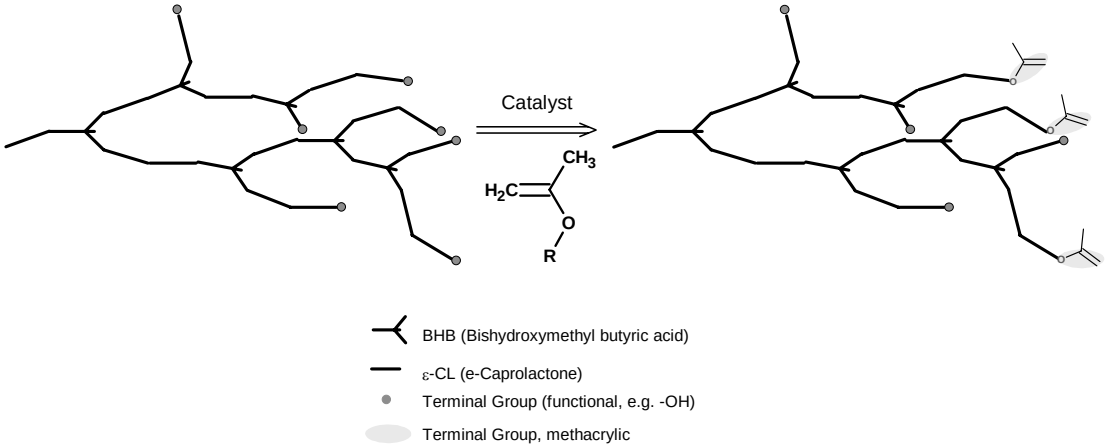

Figure 7-5: Scheme of *hb*-PCL methacrylation.

Cross-linking of binary mixtures of 2-hydroxyethyl methacrylate (HEMA) and the *hb* methacrylated precursor was achieved by exposure to a UV source. These networks were examined by thermal and mechanical testing as well as swelling experiments, and thus, cross-link density. The trends are visualized in Table 7-1.

Considering trends that depend exclusively on the weight fraction of an *hb* precursor in the network, the model of a net that is interconnected by flexible and bendable knots is applicable. The higher the network density (the number of knots per unit volume), the shorter is the average distance between two knots, i.e. the lower are T_g, <E> and <G'> but the higher is the maximal elongation at break (L).

Swelling is strongly determined by the compatibility of the swelling media to the linear or the branching part of the network respectively. Since the cross-linker is less hydrophilic than HEMA, swellability in water decreases with an increasing weight fraction of *hb*-PCL-MA in the network. The opposite is observed when toluene is used.

Trends at a given weight fraction but different cross-linkers, e.g. NW-14/22/41-40, are rather complex and cannot be explained by an ostensive model.

Table 7-1: Trends summarized according to the type of analysis and the nature of cross-linker. Arrows indicate trends with respect to the weight fraction of the cross-linker unless otherwise stated.

Precursor	T_g/w	<E>/w	L/w^3	G'/w	G'/<E>	G'(@T)/w	Swelling H_2O	Swelling Toluene
hb-PCL-14MA	↘	↘	↗	↘	↗	↗	↘	↗
hb-PCL-22MA	↘	↘	↗	↘	↗	↗	↘	↗
hb-PCL-41MA	↘	↘	↗	↘	↗	↗	↘	↗
trend[1)]	↘	↗	↗	↘	↘	↘	↘	↗
pHEMA							+	0
l-PCL							0	+[2)]
hb-PCL							0	+[2)]

[1)] observed in direction of NW-14, NW-22, NW-41, while w = const.
[2)] dissolves in toluene.
[3)] elongation at break

7.5 Hyperbranching Copolymerization of Analogous Lactones and Carbonates

The hyperbranching concurrent ring-opening polymerization / polycondensation reaction of an AB- and an AB_2-monomer is a powerful concept to create novel materials in a single one-pot reaction, in which a controlled variation of DB is assured.

In order to extend this concept, screening experiments of several cyclic lactones and trimethylene carbonate as AB-monomers, which are similar in structure to CL, and BHB as AB_2-monomer were carried out under identical reaction conditions.

The two most promising systems, δ-valerolactone/BHB and trimethylene carbonate/BHB, were investigated in further detail. Besides the ease undergoing copolymerization under the given conditions, both classes of polymers are particularly interesting for biomedical application.

In both systems, similar behavior as for *hb*-PCL was observed when DB was varied. At moderate portions of BHB in the feed (DB ≤ 10 wt%), $<M_n>$ between 5.0 and 2.0 kDa for *hb*-PVL, 4.0 and 1.0 kDa for *hb*-PTMC were obtained showing a decreasing tendency with higher DB in the product. For both systems PDI was in the range between 1.6 and 2.2. Low molecular weight samples were obtained, when the BHB fraction was large.

In contrast to *hb*-PCL and *hb*-PVL, for which an increasing deviation from stoichiometric copolymerization was observed for high DB values, *hb*-PTMC deviation of the stoichiometric copolymerization remained linear. In addition, a decrease in molecular weight with increasing DB was also less pronounced and rather linear compared to the other systems. *Hb*-PTMC is a completely amorphous material regardless of DB.

7.6 Perspectives

Hyperbranched polymers have been known for more than a decade. Although a tremendously increased interest in this fascinating field of polymers has been observed since the mid 1990s, it is an intriguing issue, whether or not control of DB can be achieved, e.g. by a concurrent ring-opening polymerization / polycondensation approach.[52,55,165]

In 2002, Skaria et al.[67] first reported the successful synthesis of *hb*-PCL, in which the DB was controlled by the comonomer ratio in the feed. Furthermore, this paper quoted the first synthesis of a hyperbranched material, in which a biocatalyst was used.

In this study, the systematic variation of DB, transfer of the synthetic concept to bulk conditions, optimization of reaction parameters and the effects of DB on the physico-chemical properties were addressed. Finally, a set-up and a synthetic protocol to prepare *hb*-PCL on the kg-scale were implemented.

Further steps should be taken based on the one-pot synthesis making the desired ***hb*-PCL** available. On the one hand, the well-known polyol chemistry might open interesting possibilities. However, the main difference is the expected degradability of these *hb* polyesters by enzymes and bacteria.[79,81,83,98,99] This assumption, in particular the biological clearance of *hb*-PCL, should be verified. Positive results will encourage research on controlled drug release, drug targeting, and pharmacokinetics, eventually leading to novel formulations based on these materials. On the other hand, tailored physical properties, such as the drastically lowered viscosity will facilitate novel applications: sustainable rheological modifiers, softeners, film formers, and glues.

Reknitting was introduced as a novel concept to transform plastics at the end of a life cycle into a new, hyperbranched material, creating another life cycle. The proof of principle was given by the transesterification of high-MW *l*-PCL into highly functional *hb*-PCL. As mentioned above, M_p of each fraction of the fractionated sample should be determined by GPC-online viscometry in order to compare this data with results from MALDI-TOF MS.

We believe it is attractive to transfer the concept of reknitting to standard polymers that are nowadays disposed or incinerated at the end of their product life-cycle. One day adhesives or multi-functional polymeric supports might be produced in this manner, saving primary carbon resources.

Polyfunctional hyperbranched precursors introduce novel aspects to polymer networks. In this study, first investigations on the extent physical properties that are affected by the *hb* structure were carried out. However, systematic studies on the influence of

i) DB / molecular weight, ii) functionalization and iii) polarity of the hyperbranched material shall be done for both structural materials and hydrogels. Drug loading is certainly an interesting issue, i.e. whether artificial bone replacements or hydrogels, the attachment and controlled release of antibiotics or growth-stimulating factors will be an asset. Drug release and biodegradation are interesting subjects.

***hb*-PVL / *hb*-PTMC** will complete the opportunities provided by *hb*-PCL: pharmacokinetics and drug release rates are supposed to be different, thus they are candidates to tailor the properties of *hb*-PCL. For sure, *l*-PVL, *l*-PTMC or copolymers consisting of these biomedical polymers will be blended in order to enhance their properties for the desired purpose.

It would be interesting to study *hb*-PVL and *hb*-PTMC in analogy to *hb*-PCL. Insight into the influence of the difference in length of the repeating unit and the A functionality, i.e. ester or carbonic ester respectively, will enhance understanding of the relation between micro- and macroscopic phenomena.

8 EXPERIMENTAL

8.1 Materials

Most materials were commercially available and thus purchased from common suppliers (Aldrich, Fluka, Acros, Sigma). ε-CL and δ-VL were refluxed over CaH_2 and distilled prior to use. Unless otherwise stated all other the compounds were used as received.

Novozyme 435 (specific activity 10,000 PLU/g) was received as a gift from Novozymes A/S, Denmark. It is characterized as:[124] Novozyme 435 beads consist of 10 wt% CALB physically adsorbed within 90 wt% Lewatit™ VPOC 1600 (supplied by Bayer). Lewatit™ is a macroporous resin comprised of cross-linked poly(methyl methacrylate-co-butyl methacrylate) with a surface area and average pore diameter of 110-150 $m^2 \cdot g^{-1}$ and 140-170 Å, respectively. CALB is found on the outer 100 μm of 600 μm average-diameter Lewatit™ beads.

8.2 Monomer Synthesis: Trimethylene carbonate (TMC)

Lit.: Ariga, T.; et al. Journal of Polymer Science: Part A: Polymer Chemistry 1993, 31, 581-584.

115 ml (1.21 mol) ethyl chloroformate and 43.5 ml (0.6 mol) 1,3-propanediol were added to 2 l of cold tetrahydrofurane in a 5 l beaker. The solution was constantly stirred while 128.9 ml (0.93 mol) triethylamine were added dropwise within 45 minutes. Immediate formation of precipitated NH_4Cl was observed. The solution was stirred another 30 minutes at 0 °C and 2 hours at room temperature. The product was separated from the precipitate by filtration and solvent was removed by distillation under reduced pressure at room temperature. The crude product was recrystallized from THF and diethyl ether and dried in vacuo over night. Yield: 29.2 g (0.32 mol, 53.3 % based on 1,3-propanediol) of a colorless solid, mp 45 °C.[166]

^{1}H-NMR ($CHCl_3$-d_1): δ = 2.13 (m, 2H, –C$\underline{H}_2$–), 4.44 ppm (t, 4H, C$\underline{H}_2$O).

^{13}C-NMR ($CHCl_3$-d_1): δ = 148.79 (O$\underline{C}$(O)O), 68.27 ($\underline{C}H_2O$), 22.18 ppm (–$\underline{C}H_2$–).

8.3 Polymerization Apparatus

8.3.1 Carrousel Reactor for Parallel Synthesis

Most polymerization reactions were carried out in a Carrousel Reactor for parallel synthesis, purchased from Zinsser Analytik GmbH, produced by Radleys Discovery Technologies, UK.

The Carousel Reactor was placed on a hot plate (Ikamag®) while the upper part was connected to a cooling circuit. The temperature sensor of the hot plate was placed into a whole in the lower part of the reactor.

The design of the reactor allows carrying out 12 reactions under identical physical conditions, magnetic stirring and the use of vacuum or inert gas conditions. Thus identical conditions were guaranteed for each set of experiments.

8.3.2 Scale-Up Reactor for Batch Synthesis

Samples were produced on kg scale in an apparatus as sketched in Figure 8-1.

The reaction vessel (A) is a double walled glass reactor with a bottom outlet. It is covered by a five-necked flat glass lid (B). The reactor is heated by a thermostat. Temperature control in the chamber was realized by a thermocouple that sits in the stopper of the bottom outlet (C). A stirring shaft (HWS Gleitring-Rührverschluss, manufactured in PEEK) (D) is attached to the central neck of the lid of the reaction vessel. The stirrer is agitated by an electrical stirrer (Heidolph RZR 2102 control) (E) that is able to maintain constant rotational speed and indicates speed (rpm) as well as applied force (Nm). A condenser (F) and an oil bubbler are attached to another neck of the lid.

Synthetic Protocol: CL was dried by reflux over CaH_2 as a prerequisite (G). The desired volume was distilled and purged into a graduated dropping funnel (H) to dose the exact volume of CL.

BHB was placed in the reactor and vacuum was applied. Then CL was sucked from the dropping funnel into the reactor and the thermostat was set to 110 °C to obtain 85 °C in the chamber. When BHB and CL formed a clear solution, argon was purged into the chamber, a stop cock was opened and Novozyme 435 was added. Vacuum was applied again to remove water formed during reaction and the chamber was kept at 85 °C under constant stirring. After 24 hours, the bottom outlet was opened and the raw product was filtered over a grid of steel to remove the Novozyme 435 beads. No further purification was done. The product is a yellowish waxy solid. Crude product yields were quantitative.

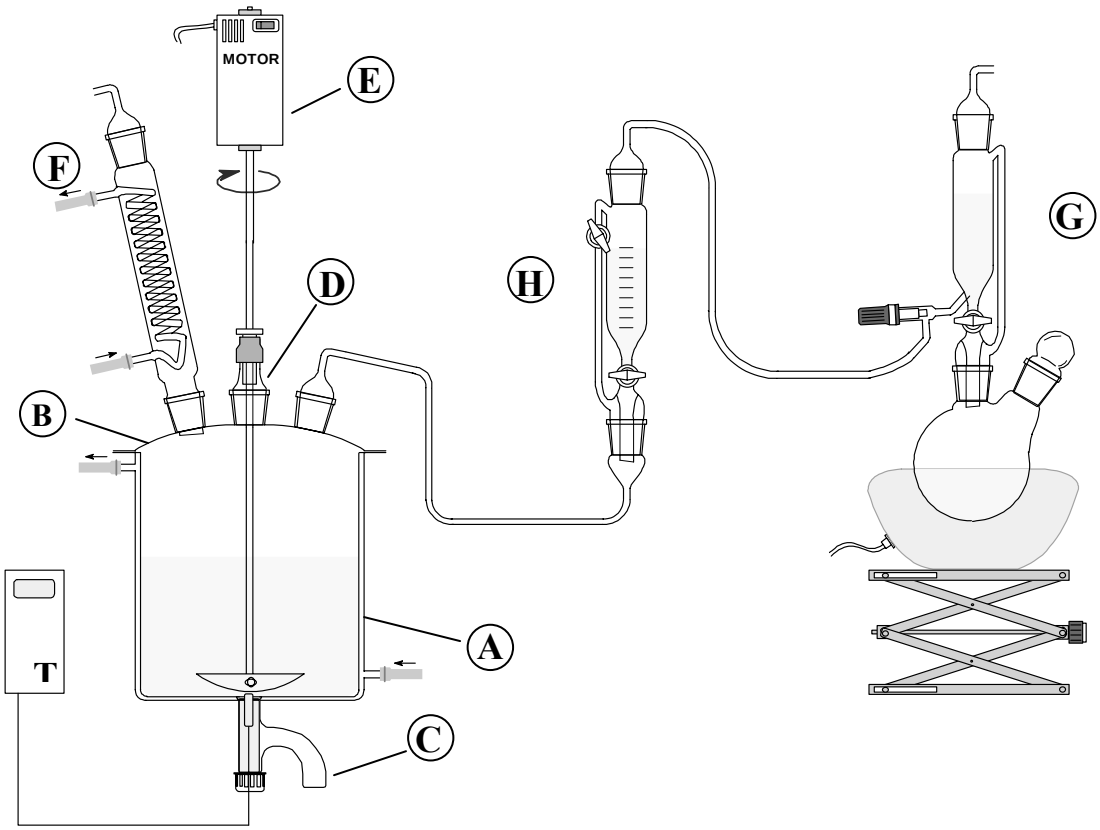

Figure 8-1: Illustration of theScale-Up.

8.4 Linear Poly(ε-caprolactone)

10 ml CL and 0.1 g Novozyme 435 were added to an oven-dried flask and vacuum was applied. The reaction was stirred at 85 °C for 24 hours. The reaction was stopped by adding cold chloroform and then filtered to remove the Novozyme beads. The beads were washed thoroughly with chloroform and the filtrate was concentrated. The oily product was redissolved in chloroform and washed twice with deionized water. The organic layer was dried over anhydrous sodium sulfate, filtered and concentrated. Remaining traces of solvent were removed by high vacuum at 40 °C over night.

The product is a colourless, brittle compound. Yield: 8.52 g (85.2 %).

^{1}H-NMR ($CHCl_3$-d_1): δ = 3.96–4.09 (t, C$\underline{H}_2$OR), 3.56–3.65 (t, RC$\underline{H}_2$OH), 2.18–2.38 (t, RC$\underline{H}_2$C(O)O), 1.48-1.67 (m, O(O)CCH$_2$C$\underline{H}_2$CH$_2$C$\underline{H}_2$CH$_2$O), 1.26-1.48 (m, O(O)CCH$_2$CH$_2$C$\underline{H}_2$CH$_2$CH$_2$O).

^{13}C-NMR ($CHCl_3$-d_1): δ = 173.49 (O–$\underline{C}$(O)CH$_2$), 64.09 (–$\underline{C}$H$_2$O), 34.06 ($\underline{C}$H$_2$C(O)–O), 28.29 ($\underline{C}$H$_2$CH$_2$O), 25.48 ($\underline{C}$H$_2$CH$_2$CH$_2$O), 24.52 ppm ($\underline{C}$H$_2$CH$_2$CH$_2$C(O)–O).

8.5 Hyperbranched Poly(ε-caprolactone)s

8.5.1 Polymerization in Solution

Lit.: Skaria, S.; Smet, M.; Frey, H. *Macromol. Rapid Comm.* **2002**, *23*, 292-296.

The synthesis protocol is exemplified for the sample *hb*-PCL-93. Novozyme (0.45 g) and BHB (0.242 g, 1.63 mmol) were added to an oven-dried flask under argon, followed by toluene (1:2 v/w with respect to total monomer weight) via a syringe. ε-CL (4.3 g, 37.5 mmol) was added and the reaction was kept at 85°C for 24 h under constant stirring. The reaction was stopped by adding cold chloroform and then filtered to remove the Novozyme beads. The beads were washed thoroughly with chloroform and the filtrate was concentrated. The oily product was redissolved in chloroform (30 mL) and washed twice with 20 mL deionized water. The organic layer was dried over anhydrous sodium sulfate, filtered and concentrated in vacuum, yielding the desired *hb*-PCL sample. Yields ranged between 73 and 97 %.

8.5.2 Polymerization in Bulk

All Copolymerizations under bulk conditions were carried out as exemplified for *hb*-PCL-93 if not quoted different: Novozyme 435 (0.45 g) and BHB (0.24 g, 1.6 mmol) were added to an oven-dried flask under argon. ε-CL (4.0 ml, 37.5 mmol) was added via a syringe. After CL and BHB had formed a homogeneous solution upon heating the reaction was kept at 85 °C for 24 hours under constant stirring while vacuum was applied to remove water formed in situ. The reaction was stopped by adding cold TCM. The crude product was filtered to remove the enzyme beads. The beads were thoroughly washed with TCM and the filtrate was concentrated. The oily product was redissolved in TCM (30 ml), washed twice with 20 ml deionized water and dried over anhydrous sodium sulfate, filtered and concentrated. Yields ranged between 70 and 97 %.

^{1}H-NMR ($CHCl_3$-*d*$_1$; Figure 3-1): δ = 3.96–4.32 (br, CH_2O–C(O)R), 3.65–3.72 (m, C_t–CH_2OH(BHB)), 3.56–3.65 (m, RCH_2OH), 2.18-2.38 (t, $RCH_2C(O)$–O), 1.48–1.75 (m, O(O)C$CH_2C\underline{H_2}CH_2C\underline{H_2}CH_2$O), 1.23–1.48 (m, O(O)C$CH_2CH_2C\underline{H_2}$, $CH_3C\underline{H_2}$–C_t(BHB)), 0.83–0.96 ppm (t, –$C\underline{H_3}$(BHB))

^{13}C-NMR ($CHCl_3$-*d*$_1$; Figure 3-2): δ = 173.52 (O–$\underline{C}(O)CH_2$), 67.02, 64.10 (–$\underline{C}H_2O$), 62.97, 62.53, 34.49, 34.18, 34.07 ($\underline{C}H_2C(O)O$), 32.23, 28.29 ($\underline{C}H_2CH_2O$), 28.07, 25.48 ($\underline{C}H_2CH_2CH_2O$), 25.24, 24.62, 24.52 ($\underline{C}H_2CH_2CH_2C(O)O$), 8.12 ppm (–$\underline{C}H_3$(BHB)). Peaks with no assignment were ascribed to terminal CL. They appeared only at higher DB.

8.6 Reknitting of Commercial Linear Poly(ε-caprolactone)

4.0 g *l*-PCL (CAPA 6500™) and 0.50 g (4.6 mmol) BHB and were placed in a carrousel reaction tube. The reaction was stirred at 90 °C for 8 to 48 hours. Vacuum (p=150 mbar) was applied to remove water formed in situ. The reaction was stopped by adding 20 ml of cold chloroform and then filtered to remove the Novozyme beads. The beads were washed thoroughly with chloroform and the filtrate was concentrated. The oily product was redissolved in chloroform and washed twice with deionized water. The organic layer was diluted with 50 ml TCM, dried over anhydrous sodium sulfate, filtered and concentrated in vacuum, yielding the desired *hb*-PCL sample.

Yield: 3.1–3.5 g (78-88 % based on m(CAPA 6500™)) of a colorless solid.

^{1}H-NMR ($CHCl_3$-d_1): *cf*. 8.5.2.
^{13}C-NMR ($CHCl_3$-d_1): *cf*. 8.5.2.

8.7 Optimization of Bulk hb-PCL Synthesis

Experiments on water removal that is formed in situ were carried out in a similar manner. Four experiments were carried out experiment no. 1 serving as reference. In experiment no. 2 an argon flux was applied within the last five hours of operation to carry out water formed in situ. Molecular sieves (4 Å, 8-12 mesh) were added to experiment no. 3. Due to the suppliers information the maximum water uptake is around 50 % by weight. Experiment no. 4 was run in vacuo over the whole period.

Experiments on Novozyme concentration were executed according to the general procedure but the weight fraction of Novozyme 435 was gradually reduced from 10 to 2 percent with respect to the comonomers' initial weight.

Regeneration of Novozyme 435: Experiments on Novozyme regeneration were carried out employing 10 weight percent of Novozyme 435 with respect to the initial weight or the comonomers. The comonomer ratio was calculated to meet DB = 4.2 %. The procedure was repeated five times as described in section 8.5.2, each one referred to as cycle, for two sets of Novozyme 435. Between two cycles, the Novozyme beads were placed in a Soxhlet apparatus and HPLC grade chloroform was refluxed for 2 hours. The beads were dried in vacuum at 40 °C for 1 hour.

8.8 Methacrylation of Hyperbranched Poly(ε-caprolactone)s

1.5 g Novozyme 435, 38.0 ml (0.24mol) butyl methacrylate and 50 g *hb*-PCL22 (n_{OH} = 56.8 mmol) were placed in a round bottom flask. 150 mg BHT (5%, based on n_{OH}) were added to prevent spontaneous polymerization. The mixture was heated to 70 °C and vacuum of 120 mbar was applied. After 20 hours, the raw product was dissolved in Et_2O and filtered to remove the Novozyme beads. The raw product solution was concentrated to 100 ml volume, overlaid by 400 ml pentane and shaken for 60 minutes. The pentane layer was decanted. This process was repeated twice prior to solvent removal in vacuum. The product, *hb*-PCL22MA, is a highly viscous yellowish substance. Yield (related to the amount of initial free hydroxyl groups): 52-58 %. Yield (related to the mass of *hb*-PCL22): 87 – 97 %.

^{1}H-NMR ($CHCl_3$-d_1): 6.06 (s, cis vinyl-H), 5.52 (s, trans vinyl-H),
4.20–4.30 (br, C$\underline{H_2}$OC(O)R), 4.08–4.16 (t, RC$\underline{H_2}$O–C(O)R (MA),
3.93–4.08 (t, C$\underline{H_2}$–OC(O)R), 3.69–3.79 (br, C_t-C$\underline{H_2}$-OH(BHB)),
3.57–3.69 (m, RC$\underline{H_2}$OH), 2.19–2.40 (t, RC$\underline{H_2}$C(O)–O), 1.91 (s, 3H, R-C$\underline{H_3}$ (MA)),
1.48-1.73 (m, O(O)CCH$_2$C$\underline{H_2}$CH$_2$C$\underline{H_2}$CH$_2$O), 1.26-1.46 (m, O(O)CCH$_2$CH$_2$C$\underline{H_2}$,
CH$_3$C$\underline{H_2}$–C_t(BHB)), 0.81-0.96 ppm (R-C$\underline{H_3}$ (BHB)).

^{13}C-NMR ($CHCl_3$-d_1)(Figure 5-2): δ = 173.76 (R$\underline{C}O_2$–, E_D), (173.53 ((R$\underline{C}O_2$–, E_{LD})),
136.40, 125.23, 66.21, 64.42, 64.09 (–$\underline{C}H_2O$), 62.50, 51.90, 49.80,
34.04 ($\underline{C}H_2$-CO(O)), 30.60, 28.25 ($\underline{C}H_2CH_2O$), 25.45 ($\underline{C}H_2CH_2CH_2O$),
24.49 ($\underline{C}H_2CH_2CH_2C(O)$–O), 23.63, 19.04, 18.24, 13.63,8.25 (–$\underline{C}H_3$(BHB)), 8.09. Signals with no assignment were ascribed to terminal CL. They appeared only at higher DB.

8.9 UV-Cross-linking of methacrylated *hb* Poly(ε-caprolactone)s

This procedure is exemplified for a 20/80 network of *hb*-PCL22MA / HEMA: 0.58 g *hb*-PCL22MA was mixed with 2.95 g (23.0 mmol) HEMA and 4.0 mg ($2.0 \cdot 10^{-5}$ mol) BPO. The homogenous solution was poured into a curing form of desired geometry and exposed to UV irradiation at a distance of 20 cm for 10 minutes. As UV source served a PowerCure 3 (manufactured by Fusion UV Systems, Inc.).

8.10 Screening Experiments

The screening experiments were carried out in toluene solution (V= 10 ml) in a Carousel Reactor Station to ensure identical polymerization conditions. β-Butyrolactone, γ-butyrolactone, δ-valerolactone, γ-valerolactone, ω-pentadecalactone (PDL) and trimethylene carbonate (TMC) were chosen as AB-monomers (*cf.* Figure 6-1. A sample of CL and BHB was used as control experiment. Novozyme 435 (10 w% of the total mass of the comonomers) and BHB (0.20 g, 1.4 mmol) were added to an oven-dried flask under argon. The AB-monomer (12.1 mmol) was added via a syringe, PDL and TMC were added using spatula. The reaction was kept at 85 °C for 24 hours under constant stirring while vacuum was applied to remove water formed in situ. The reaction was stopped by adding cold TCM. The crude product was filtered to remove the enzyme beads. The beads were thoroughly washed with TCM and the filtrate was concentrated. The oily product was redissolved in TCM (30 ml), washed twice with 20 ml deionized water and dried over anhydrous sodium sulfate, filtered and concentrated. Yields are summarized inTable 6-1.

8.11 Hyperbranched Poly(δ-valerolactone)s

All copolymerizations were carried out under bulk conditions as exemplified for *hb*-PVL-95: Novozyme 435 (0.39 g) and BHB (0.118 g, 1.1 mmol) were added to an oven-dried flask under argon. δ-VL (3.4 ml, 37.5 mmol) was added via a syringe. The reaction was kept at 85 °C for 24 hours under constant stirring while vacuum was applied to remove water formed in situ. The reaction was stopped by adding cold TCM. The crude product was filtered to remove the enzyme beads. The beads were thoroughly washed with $CHCl_3$ and the filtrate was concentrated. The oily product was redissolved in TCM (30 ml), washed twice with 20 ml deionized water and dried over anhydrous sodium sulfate, filtered and concentrated. Yields ranged between 40 and 74 %.

^{1}H-NMR ($CHCl_3$-d_1) (Figure 6-2): 4.20-4.40 (br, C$\underline{H_2}$O-C(O)R (BHB), *h*), 3.98-4.16 (br, C$\underline{H_2}$O-C(O)R (VL, *f*)), 3.60-3.74 (C$\underline{H_2}$OC(O)R), 2.21-2.44 (C$\underline{H_2}$C(O)O), 1.51-1.79 ($CH_2C\underline{H_2}C\underline{H_2}CH_2$, $CH_3C\underline{H_2}$-C_t(BHB)), 0.86-0.96 ppm (–CH_3(BHB)).

^{13}C-NMR ($CHCl_3$-d_1) (Figure 6-3): 173.68 ($\underline{C_t}CO_2R$, E_D), 173.22 (O–$\underline{C}$(O)CH_2, E_D), 171.42 (O–$\underline{C}$(O)CH_2, E_{LD}), 69.39 ($C_t\underline{C}H_2O$), 63.84 (R$\underline{C}H_2O$), 62.08, 33.81, 33.60 ($\underline{C}H_2C(O)O$), 31.93, 27.98 ($\underline{C}H_2CH_2O$), 22.25 (-$\underline{C}H_2CH_3$ (BHB)), 21.33 ($\underline{C}H_2CH_2CO_2R$), 21.04, 8.27 ppm (–$CH_3$(BHB)). Peaks with no assignment were ascribed to terminal CL. They appeared only at higher DB.

8.12 Hyperbranched Poly(trimethylene carbonate)s

All copolymerizations were carried out under bulk conditions as exemplified for *hb*-PTMC-90: Novozyme 435 (0.40 g) and BHB (0.311 g, 2.9 mmol) were added to an oven-dried flask under argon. TMC (3.4 ml, 36.2 mmol) was added via a syringe. The reaction was kept at 85 °C for 24 hours under constant stirring while vacuum was applied to remove water formed in situ. The reaction was stopped by adding cold TCM. The crude product was filtered to remove the enzyme beads. The beads were thoroughly washed with TCM and the filtrate was concentrated. The oily product was redissolved in TCM (30 ml), washed twice with 20 ml deionized water and dried over anhydrous sodium sulfate, filtered and concentrated. Yields ranged between 10 and 40 %.

^{1}H-NMR ($CHCl_3$-d_1) (Figure 6-8): 4.09–4.38(m, $OC\underline{H}_2CH_2C\underline{H}_2O$), 3.65-3.75 (t, $RC\underline{H}_2OH$), 1.95-2.07 (m, $CH_2C\underline{H}_2CH_2$), 1.80-1.94, 1.55-1.69 (br, CH_3-$C\underline{H}_2$-C_t(BHB)), 0.77-0.90 (br, R-$C\underline{H}_3$ (BHB)).

^{13}C-NMR ($CHCl_3$-d_1) (Figure 6-9): 155.28 (quart. C, *E*,C_c), 65.00 ($C_tC\underline{H}_2O$), 64.28 ($CH_2\underline{C}H_2O$), 58.90 ($R\underline{C}H_2OH$), 50.60 ($\underline{C}_q$ (BHB)), 31.53($\underline{C}_tCH_2CH_3$), 27.99 ($CH_2\underline{C}H_2CH_2$), 23.57, 21.72, 8.07 ppm (–$\underline{C}H_3$ (BHB)). Signal with no assignment were only observed in highly branched samples.

8.13 General Characterization

8.13.1 DSC

DSC measurements were carried out on a Perkin Elmer 7 Series Thermal Analysis System with autosampler in the temperature range of -95 °C to 120 °C at heating rates of 40 and 10 K/minute. Melting points are determined as peak maximum of the melting endotherm (T_m) for polymers, as onset temperature (T_o) for other compounds. The melting point of indium (T_o = 156.6 °C) and Millipore water (T_o = 0 °C) were used for calibration.

8.13.2 MALDI-TOF Mass Spectrometry

Measurements were performed with a Bruker Reflex II MALDI-TOF mass spectrometer, equipped with a nitrogen laser delivering 3 ns laser pulses at 337 nm. α-cyano hydroxyl cinnamic acid and dithranol were used as matrices. Samples were prepared by dissolving the polymer in methanol, or chloroform in the case of dithranol, at a concentration of 5 g/L. A 10 µl aliquot of this solution was added to 10 µl of a 20 g/L matrix solution and 1 µl of

a cationization agent (LiCl, KCl). A 1 µl aliquot of the resulting mixture was applied to a multistage target to evaporate the solvent and create a thin matrix/analyte film. The ions were accelerated to 21.50 kV and measured in reflectron mode. PEG-2000 was used for calibration.

8.13.3 NMR

^{1}H-NMR and ^{13}C-NMR spectra were obtained from solutions in $CHCl_3$-*d*$_1$ at concentrations of 100g/L (^{1}H) and 300-400 g/L (^{13}C) on a Bruker ARX 300 spectrometer operating at 300 and 75.4 MHz respectively.

8.13.4 VPO

Vapor pressure osmometry was carried out using a Knauer K7000 vapor pressure osmometer and chloroform solutions at 30 °C in a concentration range of 5-40 g/L. Benzil was used for calibration in a concentration range of 10-40 g/L.

8.13.5 GPC

Gel permeation chromatography was performed in chloroform on a set-up constructed by PSS. The eluent was degassed by an ERC-3315-online degasser and pumped by a TSP P100 HPLC pump at a flow rate of 1 ml/min. 150 µl of the sample solution consisting of 10 mg polymer in 4 ml solvent were injected into the column by a Waters 717_{plus} autosampler. A set of PSS-SDV 5 µ columns with 100, 1.000 and 10.000 Å porosity each was used for size separation. Molecular Weights were analyzed using a TSP UV2000 UV/VIS detector, a Showdex differential refractometer RI-71 and a WGE Dr. Bures η-1001 differential viscometer. In June 2004, the differential RI detector was replaced by an Optilab DSP Differential Refractive Index Detector of Wyatt Technology Corp. The instrument was calibrated using 12 linear polystyrene (PS) standards of Mp between $2.5 \cdot 10^6$ and 376 Da. To each sample 5 µl toluene were added as internal standard. By knowledge of the Mark-Houwink coefficient of PS[167], a universal calibration curve to determine true molecular weights[107] was established. PSS-WinGPC 7.12 was used for data evaluation.

8.13.6 Viscosity in Solution

Experiments were performed on a Lauda PVS1 Ubbelohde dilution viscometer at 30 °C using a capillary 0c with a diameter of 0.53 mm. Huggins and Kraemer plots were used to obtain the intrinsic viscosity.

8.13.7 SDS-Page Electrophoresis

Samples were dissolved in Loading buffer (Roti-Load, 4* Konz., ROTH, Art.K 929.1) and boiled for 5 min. Nine micro liters from each sample were electrophoresed in 12% SDS-PAGE. Size standards from 250 to 10 kDa, purchased from BIORAD (161-0373) were included in each gel. Protein concentration of samples was assessed by Odyssey Infrared Imaging System (LI-COR, Biosciences).

8.13.8 Dynamic Mechanical Analysis (DMA)

DMA measurements were performed on an *Advanced Rheometric Expansion System* (A.R.E.S.) manufactured by Rheometric Scientific, Piscataway, NJ, USA. Test specimens were either disks (d = 6.0 mm, $h \approx$ 1 mm) or bars (l = 30-40 mm, w = 6.0 mm, $h \approx$ 1 mm). A radian frequency ω = 10 rad/s and a heating rate HR = 2 K/min were applied. Measuring points were recorded at intervals of Δt = 30s.

8.13.9 Tensile Tests

Static properties were analyzed using a mechanical testing machine Instron 6022 (Instron Corp., High Wycombe, England). Samples of rectangular shape were cut (l = 15 mm, w = 2 mm, h ≈ 1 mm). Measurements were performed at room temperature (20°C) at a constant rate of 1mm/min. The stress σ vs. draw ratio λ was recorded where λ is the ratio of the final length L to the initial length L_0 prior to the application of stress. Young modulus was determined from the slope of the stress/draw ratio curves at zero strain. The measurements were repeated three times.

9 BIBLIOGRAPHY

[1] Figure extracted from: Mori, S.; Barth, H.G.: "Size Exclusion Chromatography", Springer Verlag Berlin, 1999, p. 18

[2] Choi, J.; Kwak, S.-Y. *Macromolecules* **2003**, *36*, 8630-8637.

[3] Figure extracted from: Mori, S.; Barth, H.G.: "Size Exclusion Chromatography", Springer Verlag Berlin, 1999, p. 109

[4] Trollsas, M.; Hedrick, J. L. *Macromolecules* **1998**, *31*, 4390-4395.

[5] Voit, B. I.; Turner, S. R. P. *Angew Makromol Chem* **1994**, *223*, 13-27.

[6] Kim, Y. H.; Webster, O. W. *Polymer Preprints (American Chemical Society, Division of Polymer Chemistry)* **1988**, *29*, 310-311.

[7] Burchard, W. *Adv Polym Sci* **1999**, *143*, 113-194.

[8] Wooley, K. L.; Frechet, J. M. J.; Hawker, C. J. *Polymer* **1994**, *35*, 4489-4495.

[9] Staudinger, H.; Husemann, E. *Liebigs Ann. Chem.* **1937**, *527*, 195-237.

[10] Meyer, K. H.; Bernfield, P. *Helv. Chim. Acta* **1940**, *23*, 875-886.

[11] Cannizzaro, S. *Ann. Chem. Pharm.* **1854**, *90*, 252.

[12] Friedel, C.; Crafts, J. M. *Bull. Soc. Chim. Fr.* **1885**, *43*, 53.

[13] Flory, P. J. *J. Am. Chem. Soc.* **1952**, *74*, 2718.

[14] Lach, C.; Müller, P.; Frey, H.; Mülhaupt, R. *Macromol Rapid Comm* **1997**, *18*, 253-260.

[15] Muzafarov, A. M.; Rebrov, E. A.; Gorbacevich, O. B.; Golly, M.; Gankema, H.; Möller, M. *Macromol. Symp.* **1996**, *102*, 35.

[16] Johansson, M.; Malmstrom, E.; Hult, A. *J Polym Sci Pol Chem* **1993**, *31*, 619-624.

[17] Yang, G.; Jikei, M.; Kakimoto, M. *Macromolecules* **1998**, *31*, 5964-5966.

[18] Uhrich, K. E.; Hawker, C. J.; Frechet, J. M. J.; Turner, S. R. *Macromolecules* **1992**, *25*, 4583-4587.

[19] Hawker, C. J.; Chu, F. K. *Macromolecules* **1996**, *29*, 4370-4380.

[20] Chu, F. K.; Hawker, C. J. *Polym Bull* **1993**, *30*, 265-272.

[21] Kim, Y. H.; Webster, O. W. *J Am Chem Soc* **1990**, *112*, 4592-4593.

[22] Odian, G. In *Principles of Polymerization*; John Wiley & Sons, Inc.: Hoboken, NJ, 2004; p 175.

[23] Sunder, A.; Bauer, T.; Mülhaupt, R.; Frey, H. *Macromolecules* **2000**, *33*, 1330-1337.

[24] Sunder, A.; Quincy, M. F.; Mülhaupt, R.; Frey, H. *Angew Chem Int Edit* **1999**, *38*, 2928-2930.

[25] Shi, W.; Raanby, B. *J. Photopolym. Sci. Technol.* **1996**, *9*, 173.

[26] Nicholson, J.; Anstice, M. *Trends Polym. Sci.* **1994**, *2*, 272.

[27] Kim, Y. H.; Webster, O. W. *Macromolecules* **1992**, *25*, 5561-5572.

[28] Massa, D. J.; Shriner, K. A.; Turner, S. R.; Voit, B. I. *Macromolecules* **1995**, *28*, 3214-3220.

[29] Sendijarevic, I.; McHugh, A. J. *Macromolecules* **2000**, *33*, 590-596.

[30] Gopala, A.; Wu, H.; Xu, J.; Heiden, P. *J Appl Polym Sci* **1999**, *71*, 1809-1817.

[31] Heinemann, J.; Walter, P.; Mäder, D.; Schnell, R.; Suhm, J.; Mülhaupt, R. In *Metalorganic Catalysis for Synthesis and Polymerization*; Kaminsky, W., Ed.: Berlin, 1999; Vol. 1.

[32] Schmaljohann, D.; Potschke, P.; Hassler, R.; Voit, B. I.; Froehling, P. E.; Mostert, B.; Loontjens, J. A. *Macromolecules* **1999**, *32*, 6333-6339.

[33] Wu, H.; Xu, J.; Liu, Y.; Heiden, P. *J Appl Polym Sci* **1999**, *72*, 151-163.

[34] Xu, J.; Wu, H.; Mills, O. P.; Heiden, P. A. *J Appl Polym Sci* **1999**, *72*, 1065-1076.

[35] Zhang, Y. D.; Wang, L. M.; Wada, T.; Sasabe, H. *Macromol Chem Physic* **1996**, *197*, 667-676.
[36] Zhang, Y. D.; Wang, L. M.; Wada, T.; Sasabe, H. *J Polym Sci Pol Chem* **1996**, *34*, 1359-1363.
[37] Percec, V. *Pure Appl. Chem.* **1995**, *67*, 2031.
[38] Percec, V.; Chu, P. W.; Ungar, G.; Zhou, J. P. *J Am Chem Soc* **1995**, *117*, 11441-11454.
[39] Kirsten, J.; Gehringer, L.; Donnio, B.; Guillon, D.; Frey, H. *Macromolecules* **2005**, *submitted*.
[40] Kirsten, J.; Neuner, I.; Frey, H. *Macromol. Chem. Phys.* **2005**, *submitted*.
[41] Knischka, R.; Lutz, P. J.; Sunder, A.; Mülhaupt, R.; Frey, H. *Macromolecules* **2000**, *33*, 315-320.
[42] Piotti, M. E.; Rivera, F.; Bond, R.; Hawker, C. J.; Fréchet, J. M. J. *J. Am. Chem. Soc.* **1999**, *121*, 9471.
[43] Weinmann, H.-J.; Ebert, W.; Misselwitz, B.; Radüchel, B.; Schmitt-Willich, H.; Platzek, J. *Eur. Radiol.* **1997**, *7*, 196.
[44] Uhrich, K. *Trends Polym Sci* **1997**, *5*, 388-393.
[45] Uhrich, K. E.; Rutger the State University: US Patent, 2000.
[46] Liu, H.; Joshi, N.; Uhrich, K. E. *Polymer Preprints (American Chemical Society, Division of Polymer Chemistry)* **1996**, *37*, 147.
[47] Liu, H.; Uhrich, K. E. *Polymer Preprints (American Chemical Society, Division of Polymer Chemistry)* **1997**, *38*, 582.
[48] Uhrich, K. E.; Cannizzaro, S. M.; Langer, R. S.; Shakesheff, K. M. *Chem. Rev.* **1999**, *99*, 3181.
[49] Knapen, J. W. J.; van der Made, A. W.; de Wilde, J. C.; Leeuwen, P. W. N. M.; Wijkens, P.; Grove, D. M.; van Koten, G. *Nature* **1994**, *372*, 659.
[50] Schlenk, C.; Kleij, A. W.; Frey, H.; van Koten, G. *Angew Chem Int Edit* **2000**, *39*, 3445-3447.
[51] Hollfelder, F.; Kirby, A. J.; Tawfik, D. S. *J. Am. Chem. Soc.* **1997**, *119*, 9578.
[52] Hölter, D.; Burgath, A.; Frey, H. *Acta Polym* **1997**, *48*, 30-35.
[53] Hawker, C. J.; Lee, R.; Frechet, J. M. J. *J Am Chem Soc* **1991**, *113*, 4583-4588.
[54] Hobson, L. J.; Feast, W. J. *Polymer* **1999**, *40*, 1279-1297.
[55] Frey, H.; Hölter, D. *Acta Polym* **1999**, *50*, 67-76.
[56] David, B. A.; Kinning, D. J.; Thomas, E. L.; Fetter, L. J. *Macromolecules* **1986**, *19*, 25.
[57] Kwak, S.-Y.; Choi, J.; Song, H. J. *Chem. Mater.* **2005**, *17*, 1148-1156.
[58] Choi, J.; Kwak, S.-Y. *Polymer* **2004**, *45*, 7173-7183.
[59] Jacob, S.; Majors, I.; Kennedy, J. P. *Macromolecules* **1996**, *29*, 8631.
[60] Würsch, A.; Möller, M.; Glauser, T.; Lim, L. S.; Voytek, S. B.; Hedrick, J. L.; Frank, C. W.; Hilborn, J. G. *Macromolecules* **2001**, *34*, 6601-6615.
[61] Gitsov, I.; Ivanova, P. T.; Frechet, J. M. J. *Macromol. Rapid. Commun.* **1994**, *15*, 387-393.
[62] Nobes, G. A. R.; Kazlauskas, R. J.; Marchessault, R. H. *Macromolecules* **1996**, *29*, 4829-4833.
[63] Burgath, A.; Sunder, A.; Neuner, I.; Mülhaupt, R.; Frey, H. *Macromol Chem Physic* **2000**, *201*, 792-797.
[64] Löfgen, A.; Albertson, A. C.; Dubois, P.; Jerome, R. *J. Macromol. Sci. Rev. Macromol. Chem. Phys.* **1995**, *C35*, 379.
[65] Gross, R. A.; Kumar, A.; Kalra, B. *Chem. Rev.* **2001**, *101*, 2097-2124.
[66] Kobayashi, S.; Uyama, H.; Kimura, S. *Chemical Reviews* **2001**, *101*, 3793-3818.
[67] Skaria, S.; Smet, M.; Frey, H. *Macromol Rapid Comm* **2002**, *23*, 292-296.

[68] Ursu, M.; Frey, H.; Neuner, I.; Thomann, R.; Rusu, M. *Romanian Reports in Physics* **2004**, *56*, 495-502.
[69] Ursu, M.; Neuner, I. T.; Thomann, R.; Rusu, M.; Frey, H. *"Blends of ε-Caprolactone and Bis(2,2'-hydroxymethyl) butyric acid", submitted.* **2005**.
[70] Sunder, A.; Turk, H.; Haag, R.; Frey, H. *Macromolecules* **2000**, *33*, 7682-7692.
[71] Möck, A.; Burgath, A.; Hanselmann, R.; Frey, H. *Macromolecules* **2001**, *34*, 7692-7698.
[72] Orlicki, J. A.; Thompson, J. L.; Markoski, L. J.; Sill, K. N.; Moore, J. S. *J Polym Sci Pol Chem* **2002**, *40*, 936-946.
[73] Yamanaka, K.; Jikei, M.; Kakimoto, M.-a. *Macromolecules* **2001**, *34*, 3910-3915.
[74] Uyama, H.; Kobayashi, S. *Chem. Lett.* **1993**, 1149-1150.
[75] Mezoul, G.; Lalot, T.; Brigodiot, M.; Marechal, E. *Macromol Rapid Comm* **1995**, *16*, 613-620.
[76] Knani, D.; Gutman, A. L.; Kohn, D. H. *J Polym Sci Pol Chem* **1993**, *31*, 1221-1232.
[77] Berkane, C.; Mezoul, G.; Lalot, T.; Brigodiot, M.; Marechal, E. *Macromolecules* **1997**, *30*, 7729-7734.
[78] Pitt, C. G.; Chasalow, F. I.; Hibionada, Y. M.; Klimas, D. M.; Schindler, A. *J. Appl. Polym. Sci.* **1981**, *26*, 3779-3787.
[79] Ali, S. A. M.; Zhong, S.-P.; Doherty, P. J.; Williams, D. F. *Biomaterials* **1993**, *14*, 648-656.
[80] Ursu, M.; Neuner, I. T.; Thomann, R.; Rusu, M.; Frey, H. *"Synthesis and Properties of Hyperbranched Poly(ε-caprolactone) Copolyesters", to be submitted* **2005**.
[81] Matsumura, S.; Ebata, H.; Toshima, K. *Macromol Rapid Comm* **2000**, *21*, 860-863.
[82] Matsumura, S.; Harai, S.; Toshima, K. *Macromol Rapid Comm* **2001**, *22*, 215-218.
[83] Matsumura, S. *Macromol Biosci* **2002**, *2*, 105-126.
[84] Sunder, A.; Krämer, M.; Hanselmann, R.; Mülhaupt, R.; Frey, H. *Angew Chem Int Edit* **1999**, *38*, 3552-3555.
[85] Broeren, M. A. C.; van Dongen, J. L. J.; Pittelkow, M.; Christensen, J. B.; van Genderen, M. H. P.; Meijer, E. W. *Angew Chem Int Edit* **2004**, *43*, 3557-3562.
[86] van Heerbeek, R.; Kamer, P. C. J.; van Leeuwen, P. W. N. M.; Reek, J. N. H. *Chem. Rev.* **2002**, *102*, 3717-3756.
[87] Kleij, A. W.; Ford, A.; J.t.B.H., J.; van Koten, G. In *Dendrimers and Other Dendritic Polymers*; Frechet, J. M. J.; Tomalia, D. A., Eds.; John Wiley & Sons Ltd., 2001; pp 485-514.
[88] Slagt, M. Q.; Stiriba, S.-E.; Klein Gebbink, R. J. M.; Kautz, H.; Frey, H.; van Koten, G. *Macromolecules* **2002**, *35*, 5734-5737.
[89] Vamvakaki, M.; Hadjiyannakou, S. C.; Loizidou, E.; Patrickios, C. S.; Armes, S. P.; Billingham, N. C. *Chemistry of Materials* **2001**, *13*, 4738-4744.
[90] Vamvakaki, M.; Patrickios, C. S. *Chemistry of Materials* **2002**, *14*, 1630-1638.
[91] Hild, G. *Progress in Polymer Science* **1998**, *23*, 1019-1149.
[92] Johansson, M.; Rospo, G.; Hult, A. *Polymeric Materials Science and Engineering* **1997**, *77*, 124-125.
[93] Stiriba, S. E.; Kautz, H.; Frey, H. *J Am Chem Soc* **2002**, *124*, 9698-9699.
[94] Wang, H.; Dong, J. H.; Qiu, K. Y.; Gu, Z. W. *J Polym Sci Pol Chem* **1998**, *36*, 1301-1307.
[95] Zhu, K. J.; Hendren, R. W.; Jensen, K.; Pitt, C. G. *Macromolecules* **1991**, *24*, 1736-1740.
[96] Schwope, A. D.; Wise, D. L.; Sell, K. W.; Skornik, W. A.; Dressler, D. P. *Transactions - American Society for Artificial Internal Organs* **1974**, *20A*, 103-107.

[97] Serrano, M. C.; Pagani, R.; Vallet-Regi, M.; Peña, J.; Rámila, A.; Izquierdo, I.; Portolés, M. T. *Biomaterials* **2004**, *25*, 5603-5611.
[98] Dawes, E. A. *Microbial Energetics*; Blackie & Son: Glasgow, 1986.
[99] Dawes, E. A.; Senior, P. J. *Adv. Microb. Physiol.* **1973**, *10*, 135.
[100] Schmitt-Willich, H.; Platzek, J.; Graske, K.-D.; Radüchel, B. S. A.: DE 19652386, 1998.
[101] Yates, C. R.; Hayes, w. *Eur. Polym. J.* **2004**, *40*, 1257-1281.
[102] Liu, M.; Vladimirov, N.; Fréchet, J. M. J. *Macromolecules* **1999**, *32*, 6881-6884.
[103] Trollsas, M.; Löwenhielm, P.; Lee, V. Y.; Möller, M.; Miller, R. D.; Hedrick, J. L. *Macromolecules* **1999**, *32*, 9062-9066.
[104] The combination of ROP with AB polycondensation has been described fort he preparation of linear polyesters in 2 works: [a] S. Kobayashi, H. Uyama, S. Namekawa, *Polym. Degrad. Stab.* **1998**, *59*, 195; [b] Z. Jedlinski, M. Kowalczuk, G. Adamus, W. Sikorska, J. Rydz, *Int. J. Biol. Macromol.* **1999**, *25*, 247.
[105] Mori, S.; Barth, H. G. In *Size Exclusion Chromatography*; Springer: Berlin, Heidelberg, 1999; p 122.
[106] Olivier, S.; Walkenhorst, R., Online (Viskoek GmbH, D-76356 Weingarten), 2002; http://www.ademe.fr/recherche/manifestations/materiaux_2002/Site/file/pdf/CM12070.PDF
[107] Grubisic, Z.; Rempp, P.; Benoît, H. *J. Polym. Sci., Polym. Lett. B5* **1967**, 753.
[108] Williamson, G. R.; Cervenka, A. *European Polymer Journal* **1972**, *8*, 1009-1017.
[109] Iwama, M.; Abe, M.; Homma, T. *Kogyo Kagaku Zasshi* **1969**, *72*, 931-934.
[110] Ambler, M. R.; McIntyre, D. *Journal of Polymer Science, Polymer Letters Edition* **1975**, *13*, 589-594.
[111] Hamielec, A. E.; Ouano, A. C. *Journal of Liquid Chromatography* **1978**, *1*, 111-120.
[112] Stogiou, M.; Kapetanaki, C.; Iatrou, H. *International Journal of Polymer Analysis and Characterization* **2002**, *7*, 273-283.
[113] Lesec, J.; Millequant, M.; Patin, M.; Teyssie, P. *Advances in Chemistry Series* **1995**, *247*, 167-179.
[114] Pasch, H.; Schrepp, W. In *MALDI-TOF Mass Spectrometry of Synthetic Polymers*; Springer-Verlag GmbH: Heidelberg, 2003; pp 107-133.
[115] Gooden, J. K.; Gross, M. L.; Müller, A.; Stefanescu, A. D.; Wooley, K. L. *J. Am. Chem. Soc.* **1998**, *120*, 10180-10186.
[116] i.e. 8 hours may be considered for a reaction that is run during one working day.
[117] Kumar, A. G., R.A. *Biomacromolecules* **2000**, *1*, 133 - 138.
[118] Bisht, K. S.; Henderson, L. A.; Gross, R. A.; Kaplan, D. L.; Swift, G. *Macromolecules* **1997**, *30*, 2705-2711.
[119] Gross, R. A.; Kalra, B.; Kumar, A. *Appl. Microbiol. Biotechnol.* **2001**, *55*, 655.
[120] Kumar, A.; Kalra, B.; Dekhterman, A.; Gross, R. A. *Macromolecules* **2000**, *33*, 6303-6309.
[121] Sunder, A.; Hanselmann, R.; Frey, H.; Mülhaupt, R. *Macromolecules* **1999**, *32*, 4240-4246.
[122] Burgath, A.; Sunder, A.; Frey, H. *Macromol Chem Physic* **2000**, *201*, 782 - 791.
[123] Crescenzi, V.; Manzini, G.; Calzolari, G.; Borri, C. *Eur. Polym. J.* **1972**, *8*, 449.
[124] Mei, Y.; Miller, L.; Gao, W.; Gross, R. A. *Biomacromolecules* **2003**, *4*, 70-74.
[125] According to the manufacturer, it can adsorb up to 50 %wt H_2O of its own weight. The added amount corresponds to a 100-fold excess of water adsorbability.
[126] Novozymes A/S referred to it as a side activity produced by the fermentation process.

[127] Burgath, A.; Hanselmann, R.; Hölter, D.; Frey, H. *PMSE Prepr. (Am. Chem. Soc., Div. Polym.Chem.)* **1997**, *77*, 166.
[128] Bankova, M.; Kumar, A.; Impallomeni, G.; Ballistreri, A.; Gross, R. A. In *Macromolecules*, 2002; Vol. 35, pp 6858-6866.
[129] Communication with Dr. A. Held of Polymer Standards Service GmbH, M., Germany. 02/2004.
[130] Chaudhary, A. K.; Beckman, E. J.; Russell, A. J. *J. Am. Chem. Soc.* **1995**, *117*, 3728-3733.
[131] l-PCL (CAPA 6500^{TM}) was measured: PS-GPC: <Mn> = 56 kDa; UC-GPC: <Mn> = 19.5 kDa.
[132] Byrd, H. C. M.; McEwen, C. N. *Anal. Chem.* **2000**, *72*, 4568-4576.
[133] Mourey, T. H.; Hoteling, A. J.; Balke, S. T.; Owens, K. G. *J. Appl. Polym. Sci.* **2005**, *97*, 627-639.
[134] Fractionation was done, when the viscosity detector was broken. UC-GPC data will be recorded as as soon as the viscosity detector will be online again.
[135] Huggins, M. L. *J. Am. Chem. Soc.* **1942**, *64*, 2716.
[136] Yurtseven, N.; Aras, L. *Polymer* **1995**, *36*, 3355.
[137] Dickie, R. A.; Labana, S. S.; Bauer, R. S., Eds. *Cross-Linked Polymers: Chemistry, Properties and Applications*; American Chemical Society: Washington, D.C., 1988; Vol. 367.
[138] Dusek, K.; Duskov-Smrckova, M. *Prog. Polym. Sci.* **2000**, *25*, 1215-1260.
[139] Flory, P. J. *Faraday Discuss.* **1974**, *57*, 7-18.
[140] Moszner, N.; Salz, U. *Prog. Polym. Sci.* **2001**, *26*.
[141] Dumitriu, S. *Polymeric Biomaterials*; Marcel Dekker: New York, 2002.
[142] Montheard, J. P.; Chatzopoulos, M.; Chappard, D. *J. Macromol. Sci. Rev. Macromol. Chem. Phys.* **1992**, *C32*, 1.
[143] Slow-release drug formulations containing polymer-protein complexes. In *Jpn. Kokai Tokkyo Koho*; (Japan Atomic Energy Research Institute, Japan). Jp, 1982; p 4 pp.
[144] Miura, Y.; Aoyagi, S.; Kusada, Y.; Miyamoto, K. *Journal of Biomedical Materials Research* **1980**, *14*, 619-630.
[145] Nowadays, blue LEDs replaced UV and Halogen curing lamps. While UV irradiation endangers eye-sight, Halogen lamps dissipate energy into excessive heat. Blue LEDs have a 100 fold higher lifetime.
[146] Ishihara, K.; Ohara, S.; Yamamoto, H. *Science* **2000**, *290*, 1140-1142.
[147] Warwel, S.; Steinke, G.; Klass, M. R. *Biotechnology Techniques* **1996**, *10*, 283-286.
[148] Park, D.-W.; Haam, S.; Ahn, I.-S.; Lee, T. G.; Kim, H.-S.; Kim, W.-S. *Journal of Biotechnology* **2004**, *107*, 151-160.
[149] Kamat, S.; Barrera, J.; Beckman, E. J.; Russell, A. J. *Biotechnology and Bioengineering* **1992**, *40*, 158-166.
[150] Derango, R.; Wang, Y. F.; Dowbenko, R.; Chiang, L. C. *Biotechnology Letters* **1994**, *16*, 241-246.
[151] Gruning, B.; Hills, G.; Josten, W.; Schäfer, D.; Silber, S.; Weitemeyer, C. In *Eur. Pat. Appl.*; (Goldschmidt A.-G., Germany). Ep, 2000; p 8 pp.
[152] Pure *hb* methacrylated material was not cured. It is anticipated not to have enhanced properties for biomedical application: i) quantitative cross-linking will result in hard, brittle material or ii) in the case of not efficient cross-linking a number of free, not favorable methacrylic groups might remain.
[153] Williams, M. L.; Landel, R. F.; Ferry, J. D. *J. Am. Chem. Soc.* **1955**, *77*, 3701.

[154] In DSC measurements, no T_g was observed. DMA measurements were not successful (Communication with Prof. Dr. T. Pakula, MPI-P, Mainz, Germany.
[155] Thompson, D. S.; Markoski, L. J.; Moore, J. S.; Sendijarevic, I.; Lee, A.; McHugh, A. J. *Macromolecules* **2000**, *33*, 6412-6415.
[156] Lee, A. T.; McHugh, A. J. *Macromolecules* **2001**, *34*, 9080-9086.
[157] Sendijarevic, I.; Liberatore, M. W.; McHugh, A. J.; Markoski, L. J.; Moore, J. S. *Journal of Rheology (New York, NY, United States)* **2001**, *45*, 1245-1258.
[158] Kobayashi, S.; Kikuchi, H.; Uyama, H. *Macromol. Rapid Commun.* **1997**, *18*, 575-579.
[159] Ariga, T.; Takata, T.; Takeshi, E. *Journal of Polymer Science: Part A: Polymer Chemistry* **1993**, *31*, 581-584.
[160] Baéz, J. E.; Martínez-Richa, A.; Marcos-Fernández, A. *Macromolecules* **2005**, *38*, 1599-1608.
[161] found at: ATHAS Data Bank, http:web.utk.edu/~athas/databank/ by Ed. M. Pyda (1994)
[162] Aubin, M.; Prud'homme, R. E. *Polymer* **1981**, *22*, 1223-1226.
[163] Feng, J.; Feng, H.; Zhuo, R. *Macromolecules* **2002**, *35*, 7175-7177.
[164] Albertsson, A. C.; Lofgren, A.; Sturesson, C.; Sjoling, M. *Acs Sym Ser* **1994**, *545*, 172-180.
[165] Hölter, D.; Frey, H. *Acta Polym* **1997**, *48*, 298-309.
[166] Saegusa, T.; Ikeda, H. *Macromolecules* **1973**, *6*, 808.
[167] Brandrup, J.; Immergut, E. H.; Grulke, E. A. *Polymer Handbook, 4th ed.*; John Wiley & Sons: New York, 1999.

10 APPENDIX – SUPPORTING INFORMATION

10.1 Chapter 4: Fractionation of hb-PCL Prepared by Rekniting

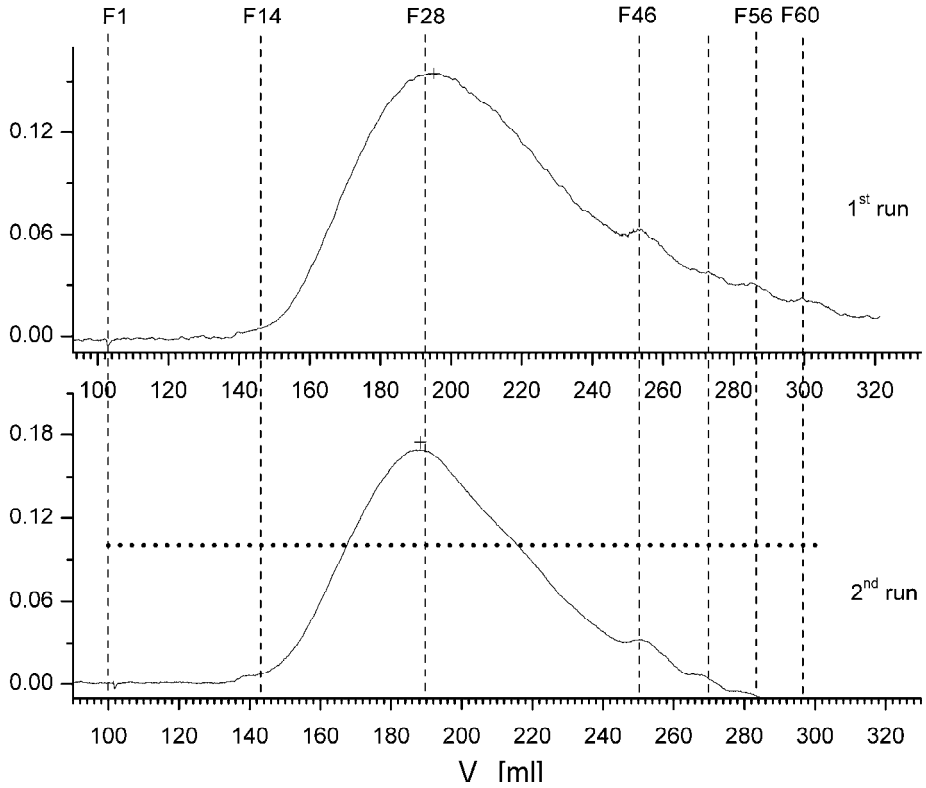

Figure 10-2: Traces of fraction by preparative GPC (Eluent: TCM).

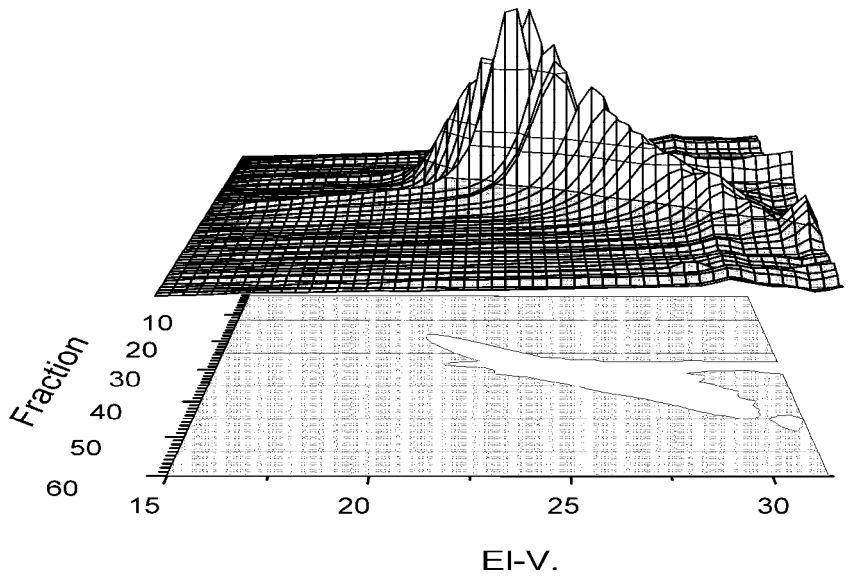

Figure 10-1: Fractionation, 2nd run: GPC traces of fractions.

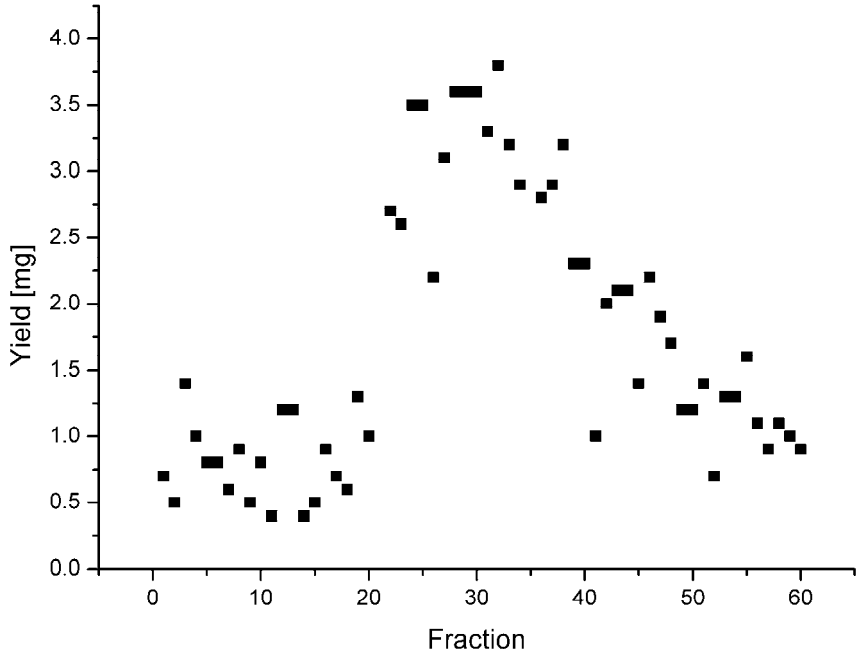

Figure 10-3: Fractionation, 2nd run: Yield against number of fraction.

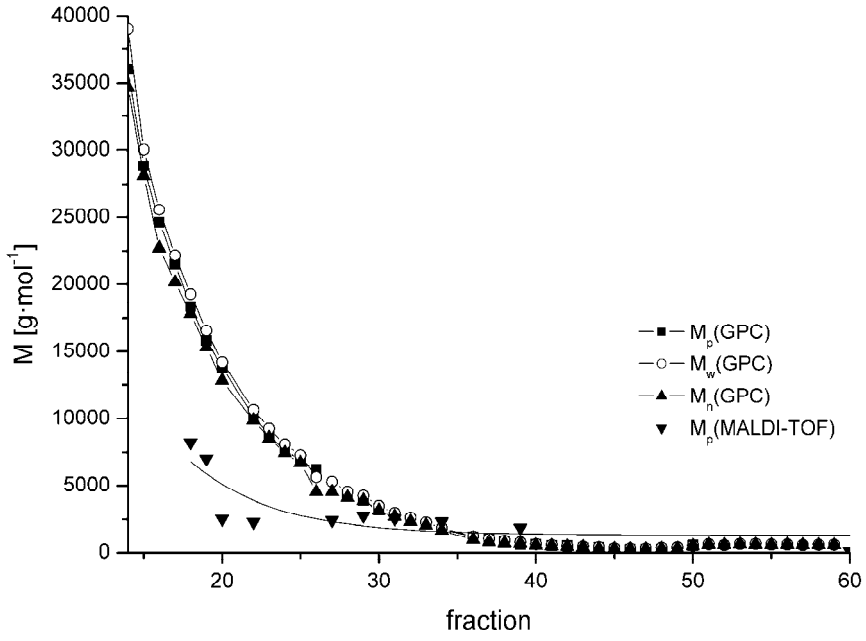

Figure 10-4: Fractionation, 2nd run: Molecular weights plotted against number of fraction.

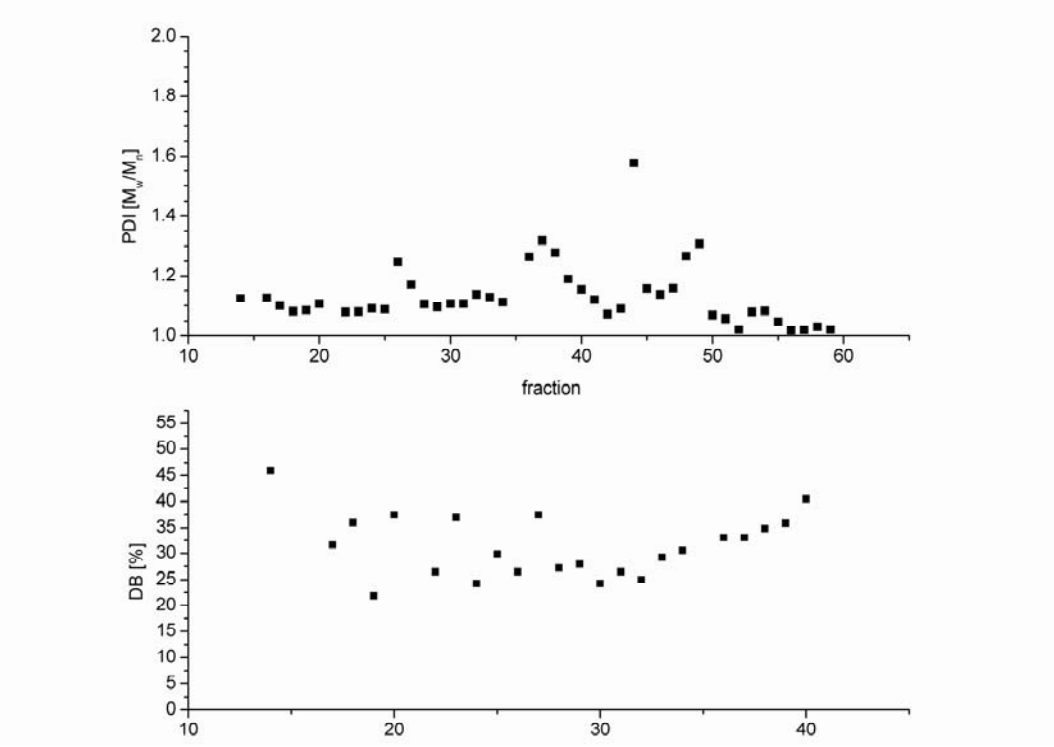

Figure 10-5: Fractionation, 2nd run: PDI, DB against fraction. 2nd run: PDI, DB against fraction.

10.2 Chapter 5: Polymer Networks – Dynamic Mechanical Analysis

Sample: PHEMA

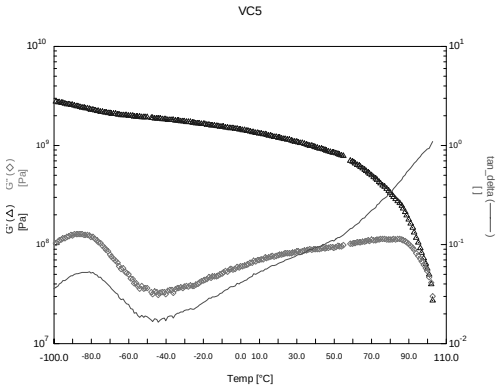

Sample: NW-14-20

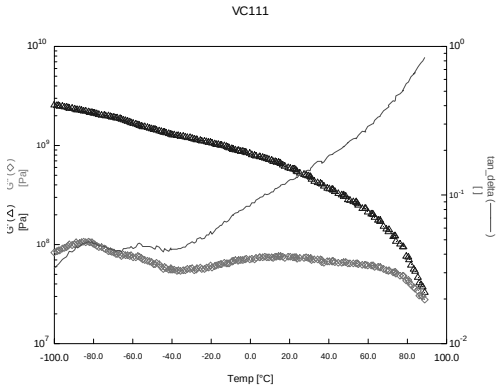

Sample: NW-14-40

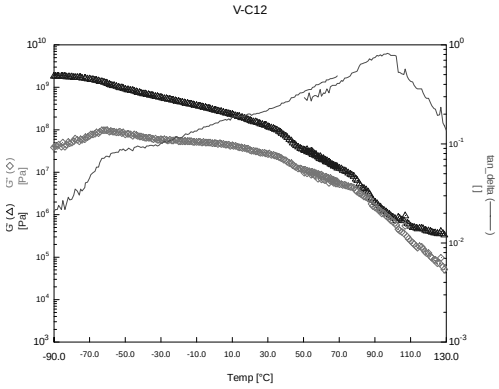

Sample: NW-14-60

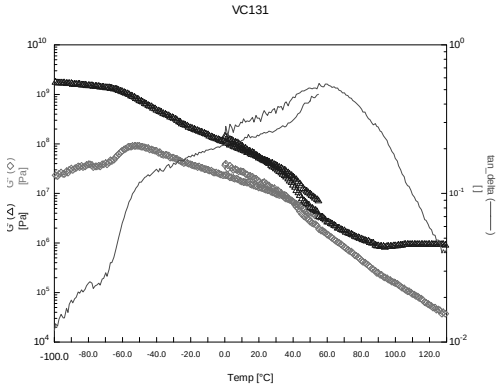

Sample: NW-22-20

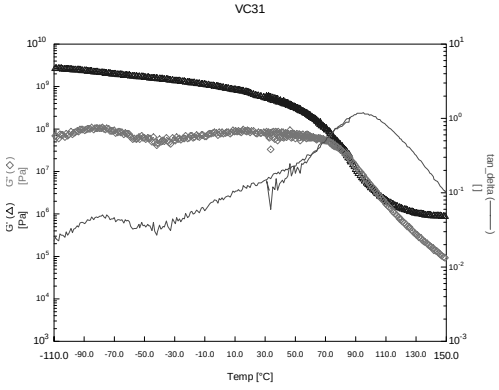

Sample: NW-22-40

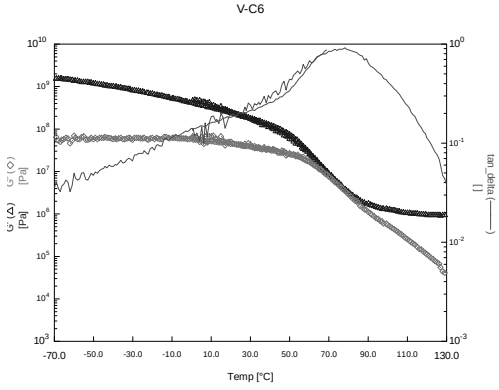

Sample: NW-22-60

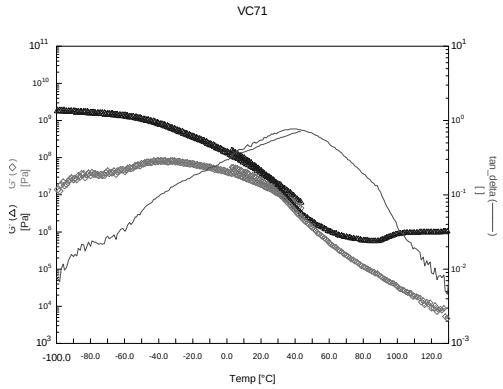

Sample: NW-41-20

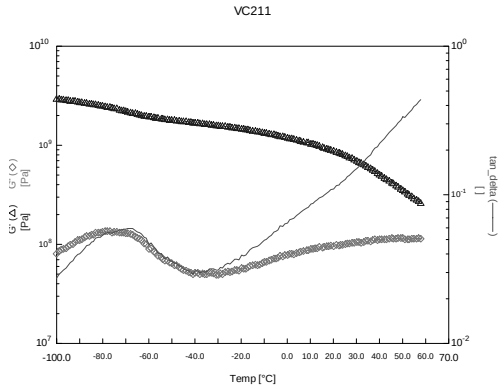

Sample: NW-41-40

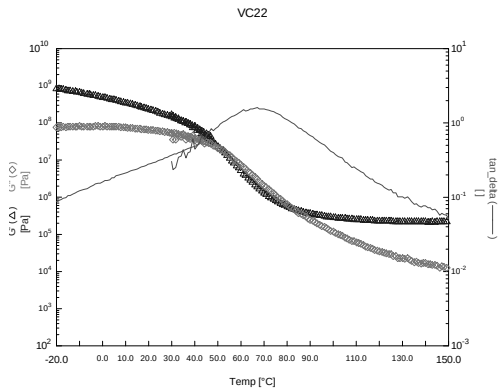

Sample: NW-41-60

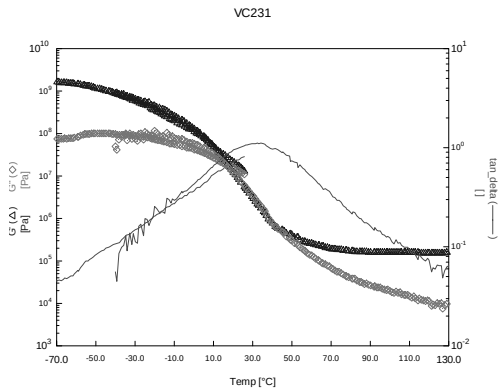

10.3 Chapter 5: Polymer Networks – Tensile Tests

Sample: PHEMA

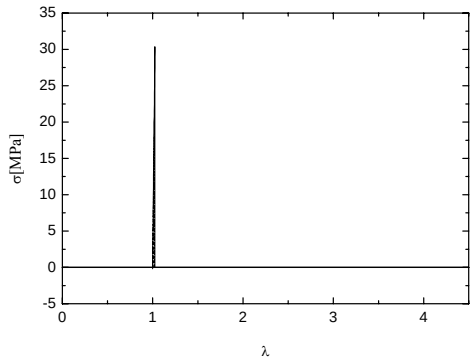

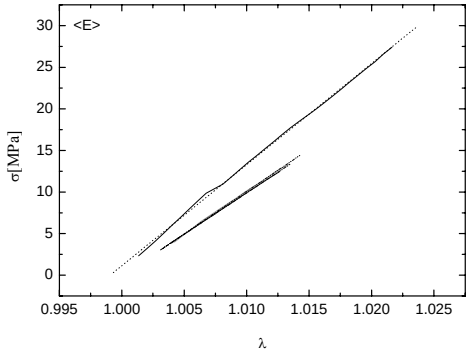

Sample: NW-14-40

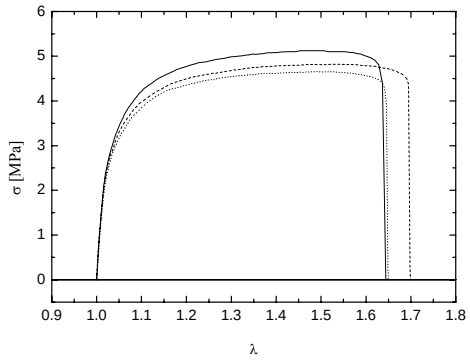

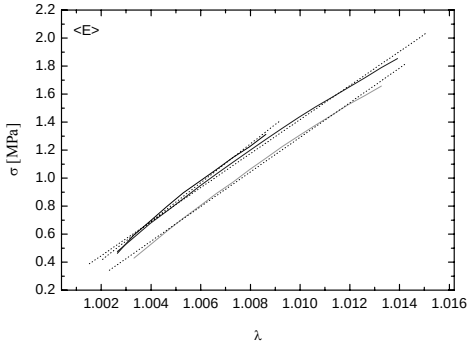

Sample: NW-14-60

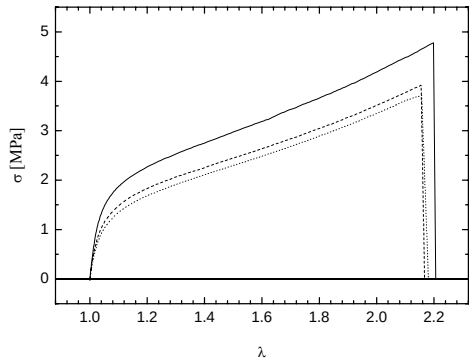

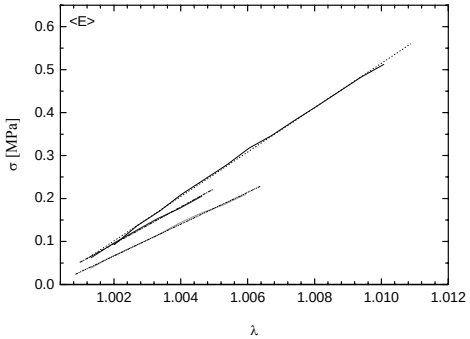

Sample: NW-22-40

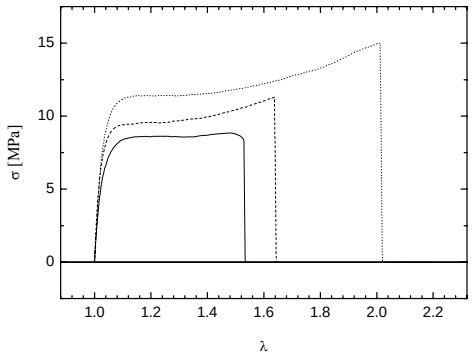

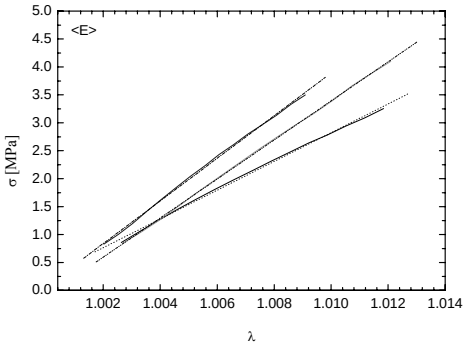

Sample: NW-22-60

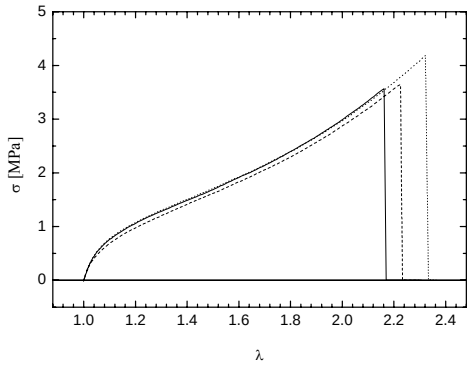

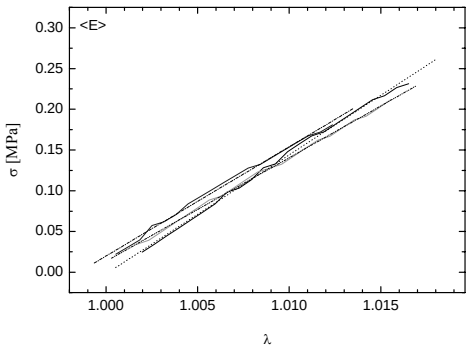

Sample: NW-41-40

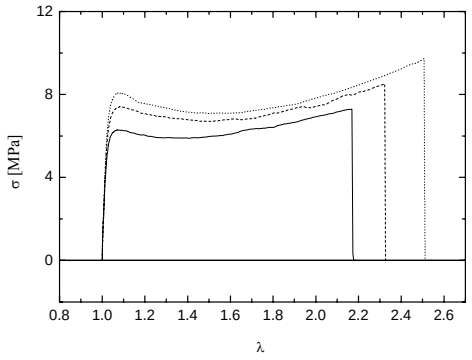

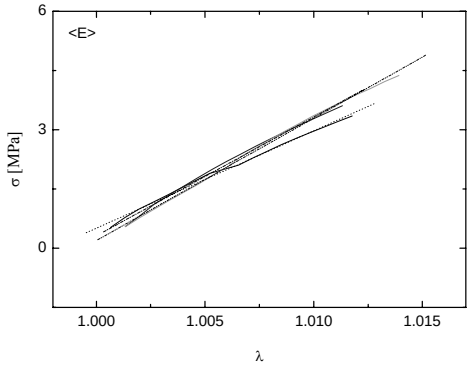

Sample: NW-41-60

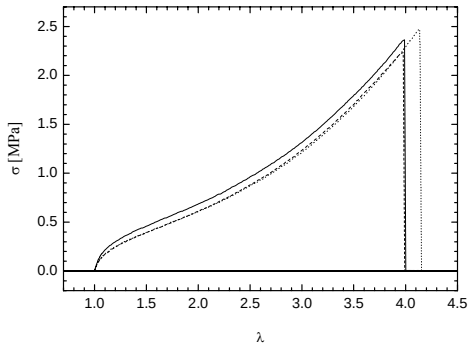

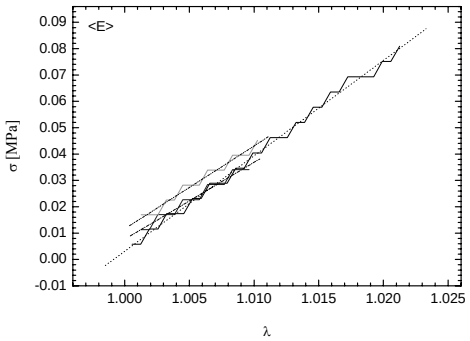

straight line: 1st sample
dashed line: 2nd sample
dotted line: 3rd sample.